Development of neutralizing and non-neutralizing antibodies targeting known and novel epitopes on *Clostridioides difficile* Toxin B

Von der Fakultät für Lebenswissenschaften

der Technischen Universität Carolo-Wilhelmina zu Braunschweig

zur Erlangung des Grades einer

Doktorin der Naturwissenschaften

(Dr. rer. nat.)

genehmigte

D i s s e r t a t i o n

von Viola Führner
aus Rheine

1. Referent:	Prof. Dr. Michael Hust
2. Referent:	Prof. Dr. Stefan Dübel
eingereicht am:	17.12.2018
mündliche Prüfung (Disputation) am:	05.04.2019
Druckjahr	2020

Vorveröffentlichungen der Dissertation

Teilergebnisse aus dieser Arbeit wurden mit Genehmigung der Fakultät für Lebenswissenschaften, vertreten durch den Mentor der Arbeit, in folgenden Beiträgen vorab veröffentlicht:

Publikationen:

- Fühner, V., Heine, P.A., Zilkens, K.J.C., Meier, D., Roth, K.D.R., Moreira, G.M.S.G., Hust, M. and Russo, G. (2018). Epitope Mapping via Phage Display from single gene libraries. *Methods Molecular Biology*

- Fühner, V., Heine, P.A., Helmsing, S., Goy, S., Heidepriem, J., Loeffler, F.F., Dübel, S., Gerhard, R. and Hust, M. (2018) Development of Neutralizing and Non-neutralizing Antibodies Targeting Known and Novel Epitopes of TcdB of *Clostridioides difficile*. *Frontiers in Microbiology* 9: 2908

- Chung, S.Y., Schöttelndreier, D., Tatge, H., Fühner, V., Hust, M., Beer, L.A. and Gerhard, R. (2018). The conserved Cys-2232 in Clostridioides difficile toxin B modulates oligomerization and receptor binding. *Frontiers in Microbiology* 9: 2314

- Beer, L.A., Tatge, H., Schneider, C., Ruschig, M., Hust, M., Barton, J., Thiemann, S., Fühner, V., Russo, G. and Gerhard, R. (2018). The binary toxin CDT of Clostridium difficile as tool for intracellular delivery of bacterial glucosyltransferase domains. *Toxins* 10: 225

- Moreira, G.M.S.G., Fühner, V. and Hust, M. (2018). Epitope Mapping by Phage Display. Phage display, Ed: Lim, T.S. and Hust, M., *Methods Molecular Biology* 1701: 497-518

Posterbeiträge:

- PEGS Lissabon 11 2017: Development of neutralizing antibodies targeting TcdB of *C. difficile;* Viola Fühner, Sebastian Goy, Saskia Helmsing, Stefan Dübel, Matthias Lochner, Ralf Gerhard, Michael Hust

- Pharm Tox Summit 2017: Development of an oligoclonal Antibody-Cocktail targeting TcdA and TcdB of *C. difficile*; Viola Fühner, Sebastian Goy, Stefan Dübel, Matthias Lochner, Ralf Gerhard, Michael Hust

- DGHM 2016: Development of an oligoclonal Antibody-Cocktail targeting TcdA and TcdB of *C. difficile;* Viola Fühner, Sebastian Goy, Stefan Dübel, Matthias Lochner, Ralf Gerhard, Michael Hust

- CLOSTPATH 9: DEVELPOMENT OF ANTIBODIES TARGETING TcdA AND TcdB OF *Clostiridium difficile*; Viola Fühner, Sebastian Goy, Stefan Dübel, Ralf Gerhard, Michael Hust

- ICDS: DEVELPOMENT OF ANTIBODIES TARGETING TcdA AND TcdB OF *Clostiridium difficile;* Viola Fühner, Sebastian Goy, Ralf Gerhard, Michael Hust, Stefan Dübel

Abstract

In this study, antibody phage display technology was used to generate a broad panel of fully human monoclonal antibodies that target TcdB, one of the main virulence factors of *Clostridioides difficile* and target of new therapeutic approaches.

TcdB has a complex domain structure and intoxicates cells via a multistep mechanism, thus offering several weak points which can be addressed with antibodies.

Applying different panning strategies against either full TcdB, truncated variants or single domains, 36 unique scFvs were generated of which 31 were further characterized after conversion into the bivalent scFv-Fc format. ELISA and Immunoblot analysis proved TcdB binding and domain specificity of these 31 antibodies analyzed, and confirmed the selection of antibodies with diverse binding characteristics.

Using a cell-based in vitro assay, all antibodies were screened for neutralization of TcdB induced cell rounding. Here two antibodies efficiently neutralized TcdB.

To test whether in vitro neutralization could be further improved by targeting different domains of TcdB at the same time, antibody combinations were tested in in vitro neutralization of TcdB induced cell rounding. Unfortunately, for the combinations tested in this study, the improvement of neutralization observed was rather of additive than synergistic nature.

To gain more information about the binding sites of the antibodies two independent approaches of epitope mapping were followed. With the combination of Peptide array and TcdB-fragment phage display, novel and already described epitopes on TcdB could be identified. By correlating these epitopes with the in vitro neutralization efficacy, a new epitope within the glucosyltransferase domain of TcdB was identified which conveys neutralization.

Thus, this study provides valuable information for further development of therapeutics against TcdB. Also, the two potent neutralizing antibodies might be candidates for further preclinical development. Future therapeutic use of these antibodies, preferably as antibody combination with antibodies targeting different domains or epitopes, is easily conceivable due to the human origin of these antibodies.

Table of contents

List of Tables

List of Figures

List of Abbreviations

Abbreviations	
°C	Grad Celsius
xg	Multiple times acceleration of gravity (9,81 m/s2)
α	Anti
µg	Microgram
µL	Microliter
µM	Micromolar
A	Ampere
A_X	Absorption at a wavelength of x nm
AP	Alkaline phosphatase
APS	Ammoniumperoxodisulfate
BCIP	5-Brom-4-chlor-3-indoxylphosphat
bla	ß-lactamase-gene
bp	Base pairs
BSA	Bovine serum albumin
CDiff	*Clostridioides difficile*
CDAD	*Clostridioides difficile* associated disease
CDR	Complementary determining region
cfu	Colony forming units
CH	Constant region of heavy chain
CIP	Calf intestinal alkaline Phosphatase
CL	Constant region of light chain
CPD	Cysteine protease domain
CROPs	Combined repetitive oligopeptides
dH2O	Deionized water
DNA	Deoxyribonucleic acid
dNTP	Deoxynucleotide triphosphate
E. coli	Escherichia coli
EDTA	Ethylenediaminetetraacetate
e.g.	Example given
ELISA	Enzyme-linked immunosorbent assay
EtBr	Ethidium bromide
EtOH	Ethanol
Fab	Fragment antigen binding
Fc	Fragment crystallizable
FCS	Fetal calf sera
Fv	Fragment variable

Abbreviations	
g	Gram
GTD	Glucosyltransferase domain
h	Hour
HEK	Human embryonic kidney
HF	High-fidelity
His	Histidin
HRP	Horseradish peroxidase
HVR	Hypervariable region
Ig	Immunoglobulin
IPTG	Isopropyl-β-D-thiogalactopyranoside
kb	Kilobase pairs
kDa	Kilodalton
kV	Kilovolt
L	Liter
M	Molar
mA	Milliampere
mAb	monoclonal antibody
min	Minute
MOI	Multiplicity of infection
mL	Milliliter
mM	Millimolar
MPBST	PBST with 2% milk powder
MTP	Micro titer plate
NBT	Nitro blue tetrazolium chloride
ng	Nanogram
nm	Nanometer
nM	Nanomolar
OD	Optical density
o.n.	Overnight
PBS	Phosphate buffered saline
PBST	Phosphate buffered saline with Tween-20
PCR	Polymerase chain reaction
PEI	Polyethyleneimine
pH	Pondus Hydrogenii
PVDF	polyvinylidene fluoride
rpm	Rotations per minute
RT	Room temperature
s	Seconds
scFv	Single chain variable Fragment
scFv-Fc	Single chain variable Fragment fused to human IgG1 Fc

Abbreviations	
SDS-PAGE	Sodium dodecyl sulfate polyacrylamide gel electrophoresis
SOC	Super optimal broth
TAE	Tris-Acetate-EDTA-buffer
TLD	Translocation domain
TMB	Tetramethylbenzidine
TN1	Tryptone N1
TRIS	TRIS-(hydroxymethyl)-aminomethane
V	Volt
v/v	Volume per volume
v/w	Volume per weight
VH	Variable Region of heavy chain
VL	Variable region of light chain
YT-Medium	Yeast extract- tryptone Medium

1 Introduction

1.1 Antibodies

Antibodies, also called immunoglobulins (Ig), are key molecules of the humoral adaptive immune response of gnathostomata. In a highly specific manner, they bind structures which are recognized as foreign or potentially dangerous e.g. viruses, bacteria, and parasites as well as molecules which are secreted by these pathogens. To render their target structures harmless, antibodies use three different mechanisms. Firstly, binding of the antibody can result in neutralization (of toxins, bacteria etc.) e.g. by inhibition of receptor binding. Secondly, opsonization triggers ingestion and elimination of pathogens by phagocytes and thirdly activation of the complement system starts a proteolytic cascade which leads to the destruction of the pathogen by the membrane attack complex (Murphy and Weaver, 2018).

With these diverse assignments, antibodies act as a link between humoral and cellular as well as adaptive and native immune response. The complex function of an antibody is also reflected in its structural features: to specifically bind to very heterogeneous antigens, antibodies need a region with high variability, but to interact with other components of the immune system a constant part is also required (Murphy and Weaver, 2018).

1.1.1 Antibody structure and recombinant antibody formats

Antibodies consist of four polypeptide chains, two identical heavy chains (50 kDa for IgG) and two identical light chains (25 kDa). Depending on the chromosomal origin of the light chain they can be divided in lambda (λ) and kappa (κ) light chains. In humans the ratio between λ-and κ antibodies is 2:1 (Murphy and Weaver, 2018).

The heavy chains are coupled to each other via disulfide bounds and each heavy chain is additionally linked to one light chain, again by a disulfide bond, which leads to a Y-shaped structure of the molecule (Murphy and Weaver, 2018).

Referring to the structure and the originating gene locus of the heavy chain, human antibodies can be classified into IgM-, IgD-, IgG-, IgE- and IgA isotypes. These structural differences facilitate specialized functions for all five antibody classes, e.g. in primary immune response (IgM) or in the defense of antigens on mucous membranes (IgA) (Woof and Kerr, 2006; Woof and Russell, 2011) . The most abundant antibody in human sera is the IgG antibody (Natvig and Kunkel, 1973).

The heavy and light chain of the IgG are composed of several ß-barrel immunoglobulin domains, designated as V_H, C_{H1}, C_{H2}, C_{H3} and V_L and C_L, respectively, where V stands for variable and C for constant or crystallizable (Edelman et al., 1969).

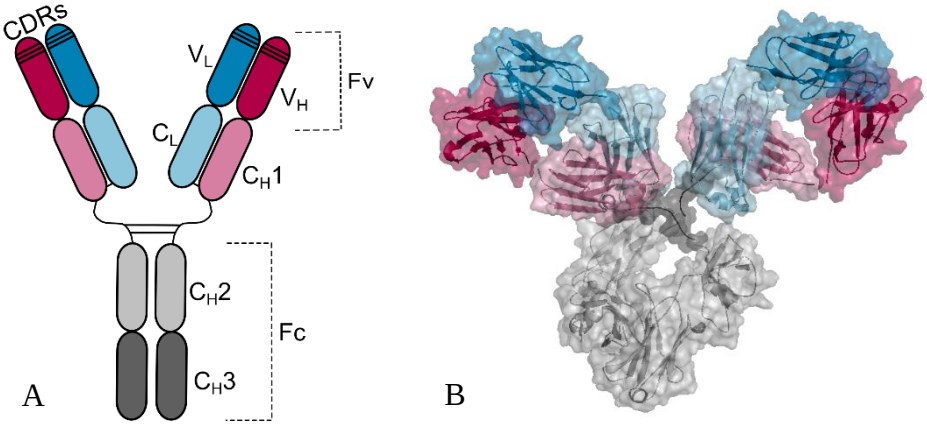

Figure 1-1: Structure of an IgG molecule

A) Schematic representation of an IgG and its domains. The heavy chain (red and grey) is composed of four domains (V_H, C_{H1}, C_{H2}, C_{H3}), the light chain (turquoise) consists of two domains (V_L and C_L). The polypeptide chains are connected covalently via disulfide bonds. V_H and V_L together build the Fragment variable (Fv), the Fragment crystallizable (Fc, grey) consists of C_{H2} and C_{H3}.

B) 3D structure of a crystallized IgG (Protein Data Bank 1IGY) visualized in cartoon style with transparent surface. The colors match to the schematic representation.

The V domains of both, heavy and light chain, harbor 3 highly variable loops, so-called complementary determining regions, which are stabilized by the more conserved *framework* regions. These loops are involved in antigen binding and define the antibody's specificity. Together with neighboring amino acids of the frameworks, they form the paratope, the interaction face between antibody and antigen (Murphy and Weaver, 2018; Sela-Culang et al., 2013). The variable antibody portion, built up by V_H and V_L, is also designated as *fragment variable*. Adding C_{H1} and C_L generates a so called *Fragment antigen binding* (Fab) (Edelman et al., 1969; Gitlin and Merler, 1961; Porter, 1959). In case of IgG, IgA and IgD, the Fab is coupled to C_{H2} and C_{H3} via a hinge region, which is a flexible linker connecting C_{H1} and C_{H2}. For IgG, IgA and IgD the hinge also harbors Cysteines which are necessary for dimerization of the molecule. CH_2 and CH_3 (in case of IgM and IgE also CH_4) form the *Fragment crystallizable* or *Fragment constant* (Fc), the constant part of the antibody. The antibody's Fc part fulfills various mediator functions of the immune response, like binding to and thereby activating of the complement system (via C1q), thus triggering native immune response (complement dependent cytotoxicity, CDC) as well as binding to Fc specific cell surface

receptors like FcγRI, FcγRIIa, FcγRIII, FcαRI and FcεRI which modulates the cellular immune response (Kapur et al., 2014; Mkaddem et al., 2014; Sutton and Davies, 2015)

Structural and sequential differences between antibody classes and subclasses within the CH_2 and CH_3 domains result in variations in the mediation of the immune response, mainly due to differences in affinity to the respective Fc receptors on the different cell types (Sun, 2014).

Since the late 1980th, with the establishment of recombinant DNA methods, ca. 100 different antibodies formats have been designed meeting the various requirements for its diverse applications (Brinkmann and Kontermann, 2017; Carter, 2006; Spiess et al., 2015)

For use in research, diagnostics and therapy, when no effector function is required, V_H and V_L can be covalently coupled via a short (often 15 AA) peptide linker to obtain a single chain fragment variable (scFv) (Figure 1-2). With a molecular weight of only 25-30 kDa this recombinant antibody fragment still completely replicates both, affinity and specificity of its parent antibody (Bird et al., 1988; Huston et al., 1988). Due to its small size it can penetrate tissue more easily than larger antibody fragments, but it is also less stable and has a reduced serum half-life (Röthlisberger et al., 2005; Thiel et al., 2002; Unverdorben et al., 2015).

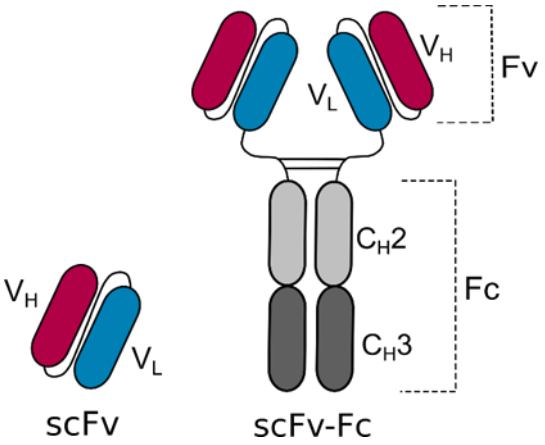

Figure 1-2: Recombinant antibody formats used in this study

In the scFv V_H and V_L are coupled via a peptide linker. In an scFv-Fc the scFv is connected to the domains of the Fc part via a hinge region

In an scFv-Fc, the scFv is coupled to the IgG C_H2 and C_H3 domains via the hinge region. Due to dimerization mediated by the hinge region and because of the Fc domain, which conciliates effector functions, the scFv-Fc has IgG like properties (Powers et al., 2001) (Figure 1-2).

Furthermore, this format is easily producible in mammalian cell culture, which makes it an attractive format for initial antibody development (Frenzel et al., 2013).

1.1.2 Antibody generation

Already in the end of the 19th century, when antibodies had not even been discovered yet, Emil von Behring and Shibasaburo Kitasato developed a way to immunize animals for production of polyclonal antibody sera for diphtheria and tetanus therapy (von Behring and Kitasato, 1890). Despite the fact that the development of the antisera therapy was an enormous progress in former times, it has some crucial drawbacks, especially lot to lot inconsistencies and adverse effects like serum sickness (Pirquet, 1905).

In 1975, Köhler and Milstein developed the so called hybridoma technology, a procedure which enables the generation and persistent production of monoclonal antibodies in hybridoma cells, thus overcoming the reproducibility issues of antibody sera. To obtain hybridoma cells, mice are immunized and B- lymphocytes are isolated from the spleen for subsequent fusion with immortal myeloma cells. After selection of successfully fused cells, single hybridoma clones are screened for secretion of an antibody with the desired properties (Köhler and Milstein, 1975). However, also hybridoma technology has some disadvantages, like limited number of candidates, inability to provide antibodies against highly conserved antigens as well as possible instability of the cell lines. (Bradbury et al., 2018; Kromenaker and Srienc, 1994). Furthermore, a recent study revealed that out of 126 hybridoma clones analyzed, 31.9 % contained one or more additional productive heavy or light chain which leads to issues with specificity and complicates cloning of the ‘right’ genes for the heavy and light chain (Bradbury et al., 2018).

1.1.2.1 Generation of monoclonal antibodies by phage display

In 1990, antibody phage display has been developed, allowing the presentation of antibody fragments on phage particles and consequently, the selection of antibody-phage on the basis of antigen binding (Barbas et al., 1991; Breitling et al., 1991; McCafferty et al., 1990). Most common is the fusion of the antibody to the pIII protein of a filamentous phage (, but also fusions to pVII and pIX have been described (Gao et al., 2002; Kwaśnikowski et al., 2005).

By PCR, V_H and V_L gene segments are amplified from peripheral blood mononuclear cells (PBMCs) and randomly combined by a two-step cloning. This process leads to a stochastic combination of heavy and light chains, allowing the construction of antibody libraries with more than 10^{10} different antibodies (Kügler et al., 2015). The V_H and V_L genes can be either directly inserted into the phage genome, or into a specialized vector for phage display, called

phagemid. A packaging signal on the phagemid confers its packaging into the phage particle, which leads to coupling of genotype and phenotype (Breitling et al., 1991).

Phage, which present antibodies that bind to an antigen of interest, are separated from non-binding antibody phage via a procedure that is called panning. A panning round comprises the following conceptual steps (Figure 1-3):

i) coincubation of antibody phage library and antigen
ii) removing of unbound phage
iii) elution of bound phage
iv) amplification of antibody phage using *E. coli.*

Normally, three rounds of panning are sufficient for a significant enrichment of antigen binding phage. To identify monoclonal antibodies with the desired properties, *E. coli* clones, infected with phage from the last panning round, are screened (Russo et al., 2018a).

In case the scFv-pIII fusion is encoded on a phagemid, an infection with a so called helperphage is necessary for phage amplification. The helperphage provides the missing genetic information for the remaining phage proteins necessary for phage production; furthermore, it carries a mutated M13 ori, therefore the phagemid is preferentially packaged into the phage particles during phage amplification instead of the helperphage genome (Vieira and Messing, 1987).

When the M13K07 phage is used to package the phagemids, statistically only one out of ten phage particles will carry a scFv-pIII fusion protein on its surface. This is due to a competition of wt pIII, encoded on the genome of M13K07 and the fusion-protein pIII which is encoded on the phagemid. If a polyvalent display is needed, a so called Hyperphage can be used instead. This phage carries a partial deletion of gIII, therefore the sole source of a functional gIII is the phagemid. Especially for the first panning round the use of a polyvalent display is advantageous and leads to an enhanced enrichment of target specific antibodies. (Rondot et al., 2001)

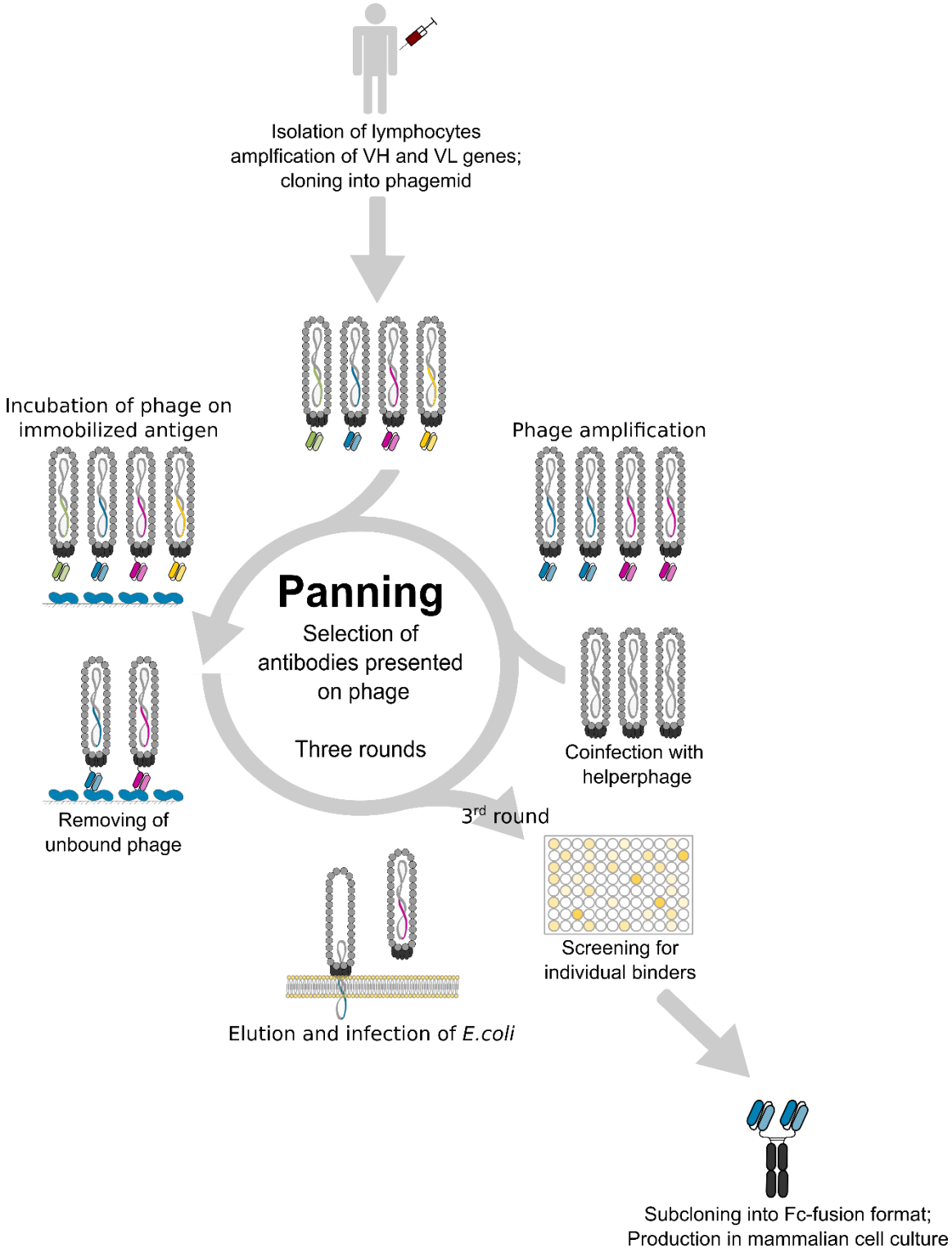

Figure 1-3: Schematic representation of the panning procedure

A panning consists of the following steps: coincubation of antibody phage library and antigen; removing of unbound phage, elution of bound phage and amplification of antibody phage in E. coli after coinfection with a helperphage. In the third panning round eluted phage are used for infection and infected E. coli cells are separated on agar plates. Subsequently single clones are screened for production of specific scFvs.

There are several important advantages of antibody-display methods in comparison to hybridoma technology: i) even self-antigens or toxic antigens can easily be used as targets, since antibody display circumvents the limitations of the in vivo immune response, ii) due to a tight control of the panning conditions, antibodies can directly be selected according to their binding properties, like epitope, domain, or even conformation specificity, iii) due to the size of the antibody libraries ($>10^{10}$), more antibody candidates can be included in the selection and screening process, iv) antibody phage display does not require animal immunization. Therefore phage display became the most widely used *in vitro* technology for antibody generation (Frenzel et al., 2016).

Instead of antibody fragments other proteins or peptides can be fused to the pIII protein and displayed on the phage surface (Smith, 1985), therefore this method can also be used to study protein-protein or protein-DNA interactions, to identify immunogenic proteins as potential biomarkers or to identify epitopes of antibodies (Becker et al., 2015; Cariccio et al., 2016; Kügler et al., 2008; Rebar et al., 1996; Scott and Smith, 1990; Zantow et al., 2016)

1.2 Clostridioides difficile and Clostridioides difficile associated disease

Clostridioides difficile (CDiff) is an anaerobic, rod shaped, gram positive, spore forming, toxicogenic, ubiquitous bacterium (see Figure 1-4) that can be detected in soil and water, as well as in stool samples of animals and humans (al Saif and Brazier, 1996).

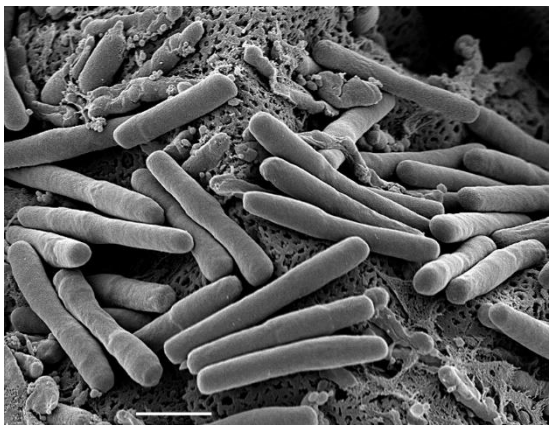

Figure 1-4: electron microscopy of Clostridioides difficile;

Scale bar ≙ 2µm. Source: Norbert Bannert, Kazimierz Madela/ Robert Koch Institute

CDiff was firstly described in the 1930ies by Ivan Hall and Elizabeth O'Toole as part of the normal gut flora of neonates. Referring to the difficult cultivation under strict anaerobic conditions they named it *Bacillus difficile* (Hall and O'Toole, 1935). In the end of the 1970ies *CDiff* was identified as the causative pathogen of antibiotic treatment associated diarrhea (Bartlett et al., 1978), also called *Clostridioides difficile* associated diarrhea (CDAD). Since then, the number of *CDiff* infections (CDI) has been increasing and in the last two decades *CDiff* even caused epidemic outbreaks (DePestel and Aronoff, 2013; Rupnik et al., 2009). Nowadays, the incidence of CDAD in Germany has risen to 5-20 cases per 100.000 per year (Burckhardt et al., 2008; Lübbert et al., 2014). Due to its association with antibiotic treatment and the resulting high potential for development of antibiotic resistance, the US Centers for Disease Control and Prevention (CDC) classifies *CDiff* as an urgent threat (Centers of Disease Control and Prevention, 2013).

Main risk factors for development of CDAD are hospitalization, advanced age and an impaired physiology of the intestine, particularly after antibiotic treatment with Clindamycin, Ampicillin or Cephalosporin, or due to other intestinal diseases or surgeries (reviewed in Elliott et al., 2007). Furthermore, patients treated with proton pump inhibitors, or non-steroidal anti-inflammatories have an increased risk for CDAD (Permpalung et al., 2016; Yearsley et

al., 2006). Another important factor is the state of the immune system: patients with immunodeficiency or under immune suppression are more likely to develop CDAD due to an impaired humoral immunity (Collini et al., 2012; Lübbert et al., 2013). But recently also more and more cases of community acquired CDI have been reported in younger patients without the obvious risk factors (Kuijper and van Dissel, 2008).

Development of CDI is a three step process i) uptake of spores via the fecal oral route ii) germination to a vegetative cell and colonization of the intestine iii) amplification and toxin production (Rineh et al., 2014)

The symptoms developed upon CDI cover a broad range of severity and include watery, sometimes bloody diarrhea, abdominal pain, fever, leukocytosis, hypalbuminemia, pseudomembranous colitis, toxic mega colon, intestinal perforation and sepsis (Robert Koch-Institut, 2009). The lethality ranges from 2%- 17%, mainly depending on the patients age, and the causing *Clostridioides difficile* strain (Pépin et al., 2005).

Disease and typical symptoms are only caused by toxigenic strains that carry a pathogenicity locus (PaLoc) on their genome (Natarajan et al., 2013). These strains express at least Toxin B (TcdB), but most strains express Toxin A (TcdA) and TcdB and some even in combination with the binary toxin CDT. Today there are 34 different toxinotypes described that vary in gene/protein sequence and/or gene expression (Rupnik et al., 2009; Rupnik and Janezic, 2016). In the last two decades the incidence of so called hypervirulent *CDiff* strains, most of which are classified as ribotype 027 strains, has increased. These strains carry mutations within the PaLoc, more exactly in the toxin repressor gene tcdc, which may lead to higher toxin expression levels and therefore more severe disease (Joost et al., 2009; Razavi et al., 2007).

1.2.1 TcdB, a major virulence factor of *Clostridioides difficile*

Together with the binary toxin (CDT), TcdA and TcdB are the main virulence factors of *CDiff*. All three toxins are secreted by the pathogen and are mainly responsible for the symptoms attributed to CDAD like destruction of the gut epithelium, leading to watery diarrhea and pseudomembranous colitis (Chandrasekaran and Lacy, 2017; Gerding et al., 2014; Just et al., 1995a, 1995b; Rupnik et al., 2009).

TcdA and TcdB are huge single-chain multidomain proteins consisting of the following functional domains: glucosyltransferase domain (GTD), cysteine protease domain (CPD),

translocation domain (TLD) and **C**ombined **R**epetitive **O**ligo **P**eptides (CROPS)-domain. A schematic representation of TcdB is given in Figure 1-5.

The N- terminal glucosyltransferase domain (TcdB AA1-543) is the actual toxic cargo, that acts on small Rho-GTPases within the cytosol of the host's cells. It transfers a glucose moiety from a uridine-diphosphate to threonine (Thr) 37 or Thr 35 in the switch I region of small Rho-GTPases like RhoA, RhoB, RhoC, RhoG, Rac1-3, Cdc42, and TC10 (Busch et al., 1998; Just et al., 1995a). Due to the glucosylation, the GTPases are trapped in an inactive state, which inhibits multiple signaling events in the host cell. One consequence that is easily observable is the breakdown of the actin cytoskeleton, leading to cell rounding (Just et al., 1995a).

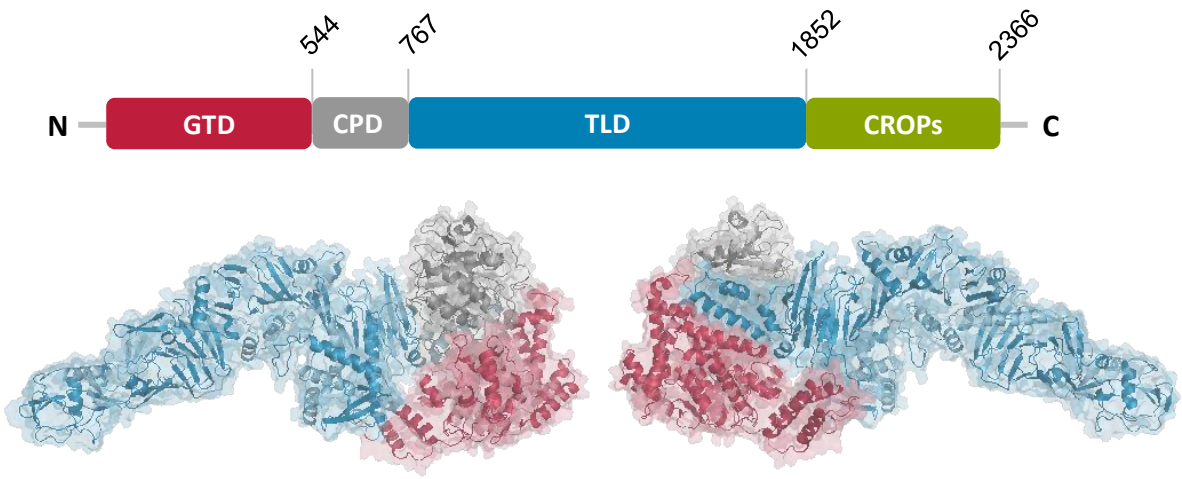

Figure 1-5: Schematic representation of TcdB:

A) Domain organization of TcdB: GTD= glucosyltransferase domain; CPD= cysteine protease domain; TLD= translocation domain and CROPs = combined repetitive oligo peptides

B) 3D model of TcdB without the CROPs based on a X-ray crystallography 3D structure of TcdA generated using swiss model. The colors are matching the schematic representation.

Amino acids 543-767 build up a cysteine protease domain that catalyzes the proteolytic auto-processing, that releases the GTD into the cytosol upon translocation. To prevent premature cleavage of the GTD, the cysteine protease domain requires activation induced by allosteric binding of cytosolic Inositol-hexakisphosphate ($InsP_6$) (Egerer et al., 2007, 2009).

The domain C-terminal of the cysteine protease is designated as the translocation domain (AA768-1852). It is the largest segment of TcdB and comprises almost 50% of the toxin. Nevertheless, exact information about the function and the molecular mechanisms involving this huge domain are still elusive, although notably progress had been made during the last

years. The TLD includes a stretch of amino acids (AA 830-990) which are proposed to be involved in pore formation for translocation of the N-terminal portion of the toxin across the endosome membrane upon acidification (Genisyuerek et al., 2011). Recently, three putative receptor binding regions of TcdB have been identified that are located within this domain. These interact with chondroitin sulfate proteoglycan 4 (PSPG4), polio virus receptor like 3 (PVRL3) or members of the frizzled protein family. The relevance of each single receptor in the course of the disease is still object of discussion (Chen et al., 2018; Gupta et al., 2017; LaFrance et al., 2015; Tao et al., 2016; Yuan et al., 2015).

The C-terminus of TcdA and TcdB is composed of repetitive elements, where long and short repeats are combined in so called **C**ombined **R**epetitive **O**ligo **P**eptides (CROPS). In case of TcdA the CROPs interact with carbohydrate structures [α-Gal-(1,3)-β-Gal-(1,4)-β-GlcNAc] on the cell surface of the target cells, mediating a first contact between toxin and target cell (Greco et al., 2006) and, furthermore, prevent premature auto-proteolytic cleavage of the toxin, by stabilization of its conformation (Olling et al., 2014). For TcdB the role of the CROPS is less defined, but due to the homology of the two toxins similar functions can be assumed. For both toxins it had been shown, that toxicity is at least partially preserved in CROP deletion mutants (Frisch et al., 2003; Manse and Baldwin, 2015; Olling et al., 2011). This finding stresses the importance of the receptor binding regions located within the TLD.

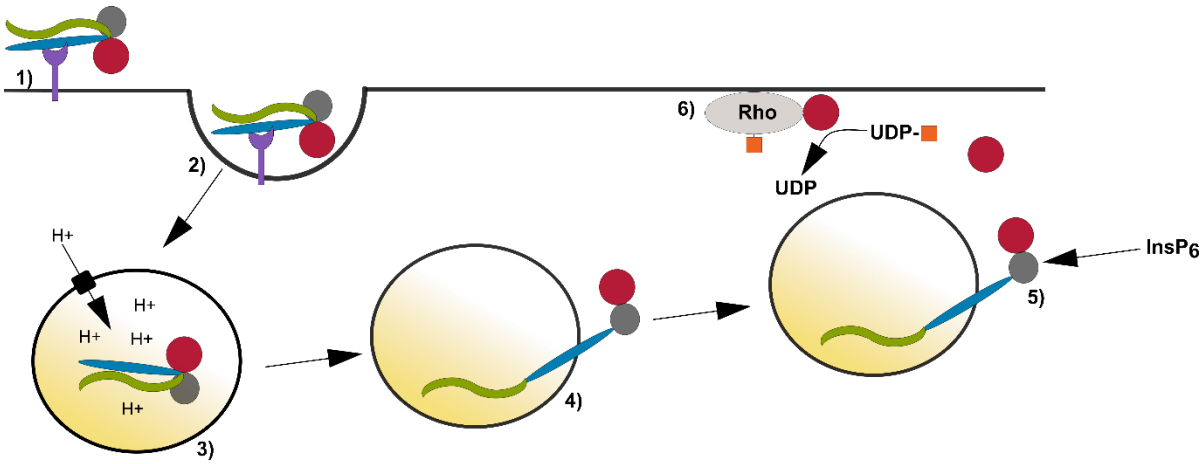

Figure 1-6: Schematic representation of the multistep intoxication mechanism by TcdB

1)Binding to several cell surface receptors (violet) via the CROPs (green) and the TLD (blue); 2) receptor mediated endocytosis; 3) acidification of endosomes; 4) conformational change and translocation of GTD (red) and CPD (grey) through the translocation pore 5) inositol hexakisphosphate induced autoproteolysis and 6) transfer of glucose moieties (orange) from UDP-glucose to small GTPases (beige). Figure adapted from Chandrasekaran and Lacy, 2017

Taken together, the functions of the single domains allow the conclusion of an intoxication with a multistep mechanism (Figure 1-6), involving the following steps: (1) cell/receptor binding, (2) endocytosis, (3) conformational change upon acidification of the endosome, (4) pore formation and translocation across the endosomal membrane, (5) auto processing and release of the enzymatic domain into the cytosol, (6) glucosylation of host GTPases. (Chandrasekaran and Lacy, 2017)

1.2.2 Current therapies for clostridium difficile associated disease

CDI is treated in an evidence based manner, depending on the severity of infection and symptoms. (Lübbert et al., 2014). Standard therapy for mild to moderate CDI provides, that treatment with the causative antibiotic is interrupted (when possible) and *CDiff* is directly targeted with the more specific antibiotics metronidazole, vancomycin or fidaxomicin (Bolton and Culshaw, 1986; Goldstein et al., 2012; Tedesco et al., 1978). However, antibiotic therapy presumably further disrupts the gut microbiota that confers colonization resistance against *CDiff*. Hence, in 20% -30% of CDI cases antibiotic therapy is not successful, or amelioration is only of temporary nature. These patients develop recurrences of CDI within two to six weeks after completion of antibiotic treatment (Pépin et al., 2006). Another concern about antibiotic therapy is the high potential of *CDiff* to evolve resistances (Centers of Disease Control and Prevention, 2013; Gao and Huang, 2015), therefore alternative therapy approaches are urgently needed.

One such alternative is stool transplantation or microbiome transfer. Up to now this form of therapy is still regarded as experimental, even though it gained particular attention because of the promising response rate of 89% in patients with recurrent CDI (Lübbert et al., 2014). However, long term risks of stool transplantations are still unknown, since there are numerous studies that indicate a linkage between the state of the intestinal microbiome and the development of diverse diseases e.g. autoimmune diseases, diabetes mellitus and obesity (Barlow et al., 2015; Hong et al., 2010; Karczewski et al., 2014; Rogers, 2015) therefore this therapy is only applicable to patients with multiple relapses (Lübbert et al., 2014).

Since the severe damage of the gut mucosa is mainly caused by TcdA and TcdB further therapy approaches directly target the toxins, either one or both. One example is Tolevamer, a non-antibiotic, toxin binding anionic polymer (>400 kDa) that binds to TcdA and TcdB in a non-covalent manner. But even though Tolevamer was able to neutralize TcdA and TcdB in an *in vitro* assay and prevented CDI in a hamster model, the clinical success of Tolevamer was

inferior to both metronidazole and vancomycin in two multinational randomized Phase III trials (Johnson et al., 2014; Kurtz et al., 2001).

The two toxins have also been exploited for vaccine development in several studies. Active immunization with toxoids, toxin fragments or chimeric toxins fragments induces a protective immune response in animal models (mouse and hamster) (Kim et al., 1987; Leuzzi et al., 2013; Wang et al., 2012). Toxoids of TcdA and TcdB have also already been proven to elicit toxin neutralizing serum antibody responses in humans (Kotloff et al., 2001). Furthermore, vaccination with toxoids led to resolution of recurrent CDAD in three patients with a history of 7-22 month of recurrent CDAD episodes (Sougioultzis et al., 2005). To date a placebo-controlled, randomized, observer-blinded clinical phase three study using a toxoid based vaccine is ongoing (Clostridium Difficile Vaccine Efficacy Trial - ClinicalTrials.gov). However, up to date there is no *CDiff* toxin based vaccine approved yet and furthermore, due to immunosenescence in elderly people, active immunization might be less efficient in the part of the population that is at particular risk of developing CDI upon hospitalization and antibiotic therapy (Pera et al., 2015).

Alternatively, passive immunization strategies might be used to prevent recurrence or even development of CDAD. Indeed, in October 2016 the monoclonal human antibody, Bezlotoxumab, has been approved for therapy of recurrent CDAD by the U.S. Food and Drug Administration (FDA). Bezlotoxumab is directed against the N-terminal portion of the CROPs of TcdB and blocks binding of TcdB to the target cells either by inhibition of binding to the cell surface carbohydrate structures, or by inhibition of binding to CSPG4 receptor (Babcock et al., 2006; Gupta et al., 2017; Orth et al., 2014). In two double-blind, randomized, placebo-controlled, phase 3 trials, MODIFY I and MODIFY II, combining antibiotic therapy with administration of Bezlotoxumab reduced the recurrence rate from 28% to 17% (MODIFY I) and from 26% to 16% (MODIFY II) (Wilcox et al., 2017). Nevertheless, due to the increasing number of toxinotypes (Rupnik and Janezic, 2016) that might not all be vulnerable to Bezlotoxumab as well as the limited efficacy, there is still room for improvement. Improvement could be achieved using defined combinations of antibodies, targeting different epitopes of TcdB at the same time. Also a better understanding of the toxins function and epitopes that might convey neutralization is needed for a more rational antibody generation strategy and/or vaccine design.

1.3 Objectives

Aim of the work was to use an antibody phage display approach to generate a panel of monoclonal human antibodies against TcdB. After conversion into scFv-Fc format, the binding properties and epitopes of the antibody candidates as well as the neutralization potential should be determined. By correlating the neutralization efficacy with the epitopes found for the respective antibodies, this work will provide valuable knowledge for future development of therapeutic antibodies against TcdB and rational vaccine development strategies.

2 Materials and Methods

2.1 Materials

2.1.1 Consumables

The consumables used in this study are listed in Table 2-1.

Table 2-1: Consumables

Consumables	**Manufacturer**
24 well Polypropylene Plate	Sarstedt, Nürmbrecht
Air-o-Seal hydrophobic Gas permeable seal	4titude, Dorking, UK
Amicon Ultra Centrifugal filters 30K	Merck Millipore KGaA, Burlington, USA
Blotting paper (550 g/m2)	Sartorius, Göttingen
Cannula	B. Braun International GmbH, Melsungen
Costar Microtiter-plate 96 well polystyrene	Corning Inc., New York, USA
Cryo tube vials (2 mL)	Nunc/ Thermo Scientific
Disposable Cuvettes	Brand, Wertheim
Disposable spatula (L-shape)	VWR, Darmstadt
Electroporation cuvettes, GenePulser 0.1 cm	Bio-Rad Laboratories, München
Filter (0,45 µm, 0,2 µm)	Sartorius, Göttingen
Filter paper (3mm)	Bio-Rad, München
Inoculation loops	VWR, Darmstadt
MabSelect SuRe Protein A affinity matrix	GE Healthcare, Freiburg
Microtiter-polypropylene plate 96 well, U-shape	Greiner Bio-one, Frickenhausen
Multiply-µStrip Pro 8-strip	Sarstedt, Nümbrecht
Parafilm	American National Can, Chicago, USA
Pasteur pipettes (3 mL)	Hartenstein, Würzburg
PCR- Reaction-tube	Greiner Bio-one, Frickenhausen
Petridishes 70x20 mm; 150x20 mm	Greiner Bio-one, Frickenhausen
Pipette Tips (10 µL, 200 µL, 1000 µL, 5000 µL)	Sarstedt, Nürmbrecht
Pipette tips, filtered (10 µL, 200 µL, 1000 µL)	Sarstedt, Nürmbrecht
Polypropylene centrifugation tubes (15 mL, 50 mL)	Corning Inc., New York, USA
Polystyrene tissue culture flask T75, canted neck, vented cap	Corning Inc., New York, USA
Polystyrene tissue culture plate 96x wells CELLSTAR	Greiner Bio-one, Frickenhausen
PVDF membrane	Carl Roth, Karlsruhe
Reaction tubes (1,5 mL, 2 mL)	Sarstedt, Nürmbrecht
Serological pipets (2 mL, 5 mL, 10 mL, 25 mL)	Sarstedt, Nümbrecht
Screw lid micro caps 2 mL	Sarstedt, Nümbrecht

Consumables	Manufacturer
Syringe Inject	B. Braun International GmbH, Melsungen
Unifilter (10 mL)	GE Healthcare, Freiburg
Uniplate PP (10 mL)	GE Healthcare, Freiburg
Whatman filter paper	GE Healthcare, Freiburg
Whatman syringe filter, 0.45 µm	GE Healthcare, Freiburg
Zeba™ Spin Desalting Columns, 89892	Thermo Fisher Scientific Inc., Waltham, USA.

2.1.2 Technical devices

The technical devices used in this study are listed in Table 2-2.

Table 2-2: Technical devices

Device	Model	Manufacturer
Blot-Apparatus	TransBlot Turbo; Semi-Dry Transfer Cell	BioRad, München
Centrifuges	5415D, 5804R and 5810R	Eppendorf, Hamburg
	Multifuge 3 S-R	Heraeus, Hanau
	Sorvall RC5	Thermo Fisher Scientific Inc., Waltham, USA
	Sorvall RC5B Plus	Thermo Fisher Scientific Inc., Waltham, USA.
Electrophorese-chamber (Agarose gels)	PerfectBlue Mini S	PeqLab, Erlangen
Electrophorese-chamber (SDS gels)	Mini Protean III cell	BioRad, München
Electroporation device	Micro Pulser™	BioRad, München
ELISA-readers	Tecan Sunrise	Tecan, Crailsheim
	Epoch	BioTek, Bad Friedrichshall
ELISA-washers	Columbus, Hydro-Speed	Tecan, Crailsheim
	Columbus, Pro	Tecan, Crailsheim
	Columbus, Plus	Tecan, Crailsheim
Gel documentation	ChemiDoc MP	BioRad, München
Incubators	BE400	Memmert, Schwabach
	Certomat® BS-1	Sartorius, Göttigen
	Infors Multitron HT, Minitron HT	Infors HT, Einsbach
	Hera Cell	Heraeus, Hanau
Laminar flow bench	MSC-Advantage	Thermo Fisher Scientific Inc., Waltham, USA.

Device	Model	Manufacturer
Laminar flow bench	Herasafe	Heraeus, Hanau
Microscopes	Eclipse TS100	Nikon, Minato, Japan
	Axiovert 200	Carl Zeiss, Oberkochen
Mixing device	Vortex Genie 2	Scientific Industries, New York, USA
MTP-shake incubator	Vortemp56	Labnet International, Inc, Edison, USA
pH-Meter	CG810	Schott, Mainz
Photometer	Libra S11	Biochrom, Berlin
Pipettes	Research	Eppendorf, Hamburg
	Biohit eLine	Sartorius, Göttingen
Pipettor, multichannel	Acu-Jet	Brand, Wertheim
Power supply	Electrophoresis Power Supply 301	Amersham Bioscience, Freiburg,
	Electrophoresis Power Supply 601	Amersham Bioscience, Freiburg,
Protein purification system	Profinia	BioRad, München
Spectrophotometer	ND1000	PeqLab, Erlangen
Thermocycler	DNA Engine MJ research PTC-200 Minicycler™	BioRad, München
Thermomixer	Thermomixer comfort, Thermomixer compact	BioRad, München
	Mixing block MB-102	Bioer, Hangzhou, China
Scale	Laboratory LC 2200 S, E 1200 S, A120 S	Sartorius, Göttingen
Sonicator	Bioruptor® Pico	Diagenode, Denville, USA
Waterbath	Waterbath GFL	Laborbedarf, Braunschweig
Water purification system	Arium 611	Sartorius, Göttingen

2.1.3 Chemicals

All chemicals used in this project were purchased from following suppliers: ApplChem GmbH (Darmstadt, Germany), Carl Roth GmbH (Karlsruhe, Germany), Merck KGaA (Darmstadt, Germany), Roche Diagnostics GmbH (Penzberg, Germany), SERVA Electrophoresis GmbH (Heidelberg, Germany) and Sigma-Aldrich Chemie GmbH (Steinheim, Germany)

2.1.4 Bacteria strains, phage and cell lines

All bacteria strains, phage and cell lines used in this study are listed in Table 2-3.

Table 2-3: Bacteria strains, phage and cell lines

Strain	Genotype/ description	Application	Source
E. coli TG1	K-12 supE thi-1 _(lac-proAB) _(mcrB-hsdSM)5, (rK-mK-) F' [traD36 proAB+ lacIq lacZ_M15]	Panning	GE Healthcare, Freiburg
E. coli XL1 blue MRF'	Δ(mcrA)183 Δ(mcrCBhsdSMR-mrr) 173 endA1 supE44 thi-1 recA1 gyrA96 relA1 lac [F′ proAB lacIqZΔM15 Tn10 (Tetr)]	Panning and cloning	Stratagene, LA Jolla, USA
E. coli TOP10F'	F'[lacIq Tn10(tetR)] mcrA Δ(mrr-hsdRMS-mcrBC) φ80lacZΔM15 ΔlacX74 deoR nupG recA1 araD139 Δ(ara-leu)7697 galU galK rpsL(StrR) endA1 λ-	Cloning of Antigen library	Invitrogen, Carlsbad, CA, USA
M13K07	wt	Phage production	(Vieira and Messing, 1987)
Hyperperphage	M13K07ΔgIII	Phage production	(Rondot et al., 2001)
Vero Cells	African green monkey kidney epithelial cell line, adherent	Cell rounding assay	MHH Hannover, Inst. f. Toxikologie
HEK293-6E	Human embryo kidney cell line, growth in suspension, expresses Epstein-Barr-Virus-Nuclear-Antigen 1	Antibody production	(Durocher et al., 2002)
Expi293F™ Cells	Derived from HEK293-6E cells, optimized for growth in higher densities	Antibody production	Thermo Fisher Scientific Inc., Waltham, USA

2.1.5 Plasmids

The plasmids used in this study are listed in Table 2-4.

Table 2-4: Plasmids

Plasmid	Description	Reference
pHAL30	Phagemid, coding for scFv:pIII fusion proteins; library Vector for HAL9/10 naïve human antibody libraries	(Kügler et al., 2015, 9)
pHORF3	Phagemid, coding for oligopeptide:pIII fusion proteins, library vector for ORFeome or single gene –fragment display libraries	(Kügler et al., 2008)
pCSE2.6-hIgG1-Fc	Plasmid for scFv-Fc production in mammalian cell culture	(Beer et al., 2018; Russo et al., 2018b)

2.1.6 Kits

Kits were used for DNA purification from PCR mixes or *E. coli* cultures. An overview of the kits used in this study is given in Table 2-5.

Table 2-5: Molecular-biological kits

Kit	Application	Manufacturer
Hi Yield® Gel/PCR DNA Fragment Extraction Kit,	DNA Purification	SLG; Süd-Laborbedarf Gauting
Fast DNA End Repair Kit	Generation of blunt ends after DNA sonication	Thermo Fisher Scientific Inc., Waltham, USA
NucleoSpin® Gel and PCR Clean-up	DNA Purification	Macherey-Nagel, Düren
NucleoSpin® Plasmid	Plasmid extraction	Macherey-Nagel, Düren
NucleoBond Xtra Midi,	Plasmid extraction	Macherey-Nagel, Düren

2.1.7 Antibodies

In ELISA, Immunoblots or peptide arrays, enzyme or fluorochrome coupled antibodies were used as detection system. A list of antibodies used is given in Table 2-6

Table 2-6: Antibodies

Antibody	Description	Manufacturer
A0168	Goat anti-mouse IgG (Fc specific) HRP conjugated	Sigma Aldrich, München
A0170	Goat anti-human IgG (Fc specific) HRP conjugated	Sigma Aldrich, München
9E10	Mouse anti-c-myc-tag	AG Dübel, Braunschweig
A80-304D6	Anti-human IgG-Fc Fragment; cross-adsorbed DyLight® 680 conjugated	Bethyl Laboratories Inc. Montgomery, USA
12CA5	Anti-HA Peptide ReadyTag Mouse IgG2b	Bio X Cell, West Lebanon, USA
5470S	Polyclonal anti-Mouse IgG (H+L) DyLight® 680 conjugated	Cell signaling technology, Denvers, USA

2.1.8 Oligonucleotides

Oligonucleotides were used as primers for DNA amplification in colony PCR as well as standard PCRs. All oligonucleotides use this work are listed in the following Table 2-7.

Table 2-7: Oligonucleotides

Name	ID	Sequence (5'-3')	Application
MHgIII-r	11	CTAAAGTTTTGTCGTCTTTCC	Colony PCR on pHAL30, pHORF3, sequencing
MHLacZ-Pro-f	125	GGCTCGTATGTTGTGTGG	Colony PCR on pHAL30, pHORF3
ToR-pCMV-mIgG01-FC-seq-f	410	CACTTTGCCTTTCTCTCC	Colony PCR on pCSE2.6-hIgG1-Fc-XP

Name	ID	Sequence (5'-3')	Application
ToR-pCMV-mIgG01-Fc-seq-r	411	CAGATGGCTGGCAACTAG	Colony PCR on pCSE2.6-hIgG1-Fc-XP
ToR-pCMV-Seq-f	728	TGGTAGCAACAGCTACAG	Sequencing
CM2-f	886	CGCAAATGGGCGGTAGGCGTG	Sequencing
ViF218-TcdB-for	3081	ATGAGTTTAGTTAATAGAAAACAGTTAGAAAAAATGG	Amplification of tcdB gene from genomic DNA
ViF218-TcdB-rev	3082	CTATTCACTAATCACTAATTGAGCTGTATCAGG	Amplification of tcdB gene from genomic DNA

2.1.9 Enzymes

Enzymes (polymerases, restriction enzymes, proteases and ligases) used in this study are listed in Table 2-8.

Table 2-8: Enzymes

Name	Application	Manufacturer
GoTaq® DNA-Polymerase	Colony PCR	Promega (Mannheim, DE)
NcoI HF	restriction of DNA	New England Biolabs (Frankfurt a. M., DE)
NotI HF	restriction of DNA	New England Biolabs (Frankfurt a. M., DE)
PmeI HF	digestion of pHORF3 Vector	New England Biolabs (Frankfurt a. M., DE)
Phusion DNA-Polymerase	Amplification of tcdB gene	New England Biolabs (Frankfurt a. M., DE)
T4 DNA Ligase	Ligation of inserts into vector backbones	Promega (Mannheim, DE)
Trypsin	Elution of phage	Sigma-Aldrich (Taufkirchen, DE)
Trypsin/EDTA	Cell passaging	Biochrom

2.1.10 Media, Supplements and Buffers

The media and supplements used for cultivation of mammalian cells or *E. coli* are listed in Table 2-9, Table 2-10 and Table 2-11.

Table 2-9: Media and solutions for cultivation of mammalian cells

Media/Solution	Application	Manufacturer
RPMI1640	cultivation of Vero cells	Merck Biochrom GmbH, Berlin
L-Glutamine	media supplement for cultivation of Vero cells (2 mM),HEK293-6E and Expi293F cells (8 mM)	Merck Biochrom GmbH, Berlin
FBS superior (Fetal bovine serum)	cultivation of Vero cells	Merck Biochrom GmbH, Berlin
TRYPSIN/EDTA (0,05 %/0,02 %) in PBS, w/o Ca2+, Mg2+	detachment of Vero cells for passaging	Merck Biochrom GmbH, Berlin
FreeStyle™ F17 Expression Medium	HEK293-6E production media	Thermo Fisher Scientific Inc., Waltham, USA
Pluronic-F68	anti-foam agent	PAN-Biotech GmbH, Aidenbach
TN1 (Tryptone N1)	supplement for boosting yields of human cell cultures	Merck Biochrom GmbH, Berlin
HEK TF	Expi293F production media	XELL AG, Bielefeld
HEK FS	supplement for boosting yields of human cell cultures	XELL AG, Bielefeld

Table 2-10: Media used for E. coli cultivation

Basic Media	Composition	
2x YT Media	1 % (w/v)	Bacto-Yeast Extract
	1.6 % (w/v)	Bacto-Tryptone
	0.5 % (w/v)	NaCl
SOC Media	0.5 % (w/v)	Bacto-Yeast Extract
	2.0 % (w/v)	Bacto-Tryptone
	0.05 % (w/v)	NaCl
	1.8 % (w/v)	Glucose

Table 2-11: Supplemented media used for E. coli cultivation and selection

Supplemented Media	Supplements
2x YT- A	100 µg/mL ampicillin
2x YT- GA	100 mM glucose, 100 µg/mL ampicillin
2x YT- AK	100 µg/mL ampicillin, 50 µg/mL kanamycin
2x YT- T	20 µg/mL tetracycline

In Table 2-12 the compositions of buffers and solutions used are listed.

Table 2-12: Composition of buffers and solutions

Application	Description	Composition		
DNA gel electrophoresis	TAE buffer (pH 8.0)	40 20 2	mM mM mM	Tris Acetic acid Ethylenediaminetetraacetic acid
	Agarose gel	1 5	% (w/v) µg L^{-1}	TAE buffer (solvent) Agarose Ethidium bromide
SDS PAGE and staining	5x Laemmli buffer (reducing)	10 50 25 0.2	% (w/v) % (w/v) % (v/v) % (w/v)	Sodium dodecyl sulfate Glycerol β-Mercaptoethanol Bromophenol blue
	SDS-PAGE buffer (pH 8.3)	25 192 0.1	mM mM % (w/v)	Tris Glycine Sodium dodecyl sulfate
	Coomassie staining solution	0.5 10 2.5	% (w/v) % (v/v) % (v/v)	Coomassie Brilliant Blue R250 Acetic acid 2-Propanol
	Stopping solution	12 50	% (v/v) % (v/v)	Acetic acid Methanol
	Silver solution	0.2 0.075	% (w/v) % (v/v)	$AgNO_3$ 37% Formaldehyde
	Fixation solution	0.05	% (v/v)	Stopping solution (solvent) 37% Formaldehyde
	Developer	6.0 0.05 2	% (w/v) % (v/v) % (v/v)	Stopping solution (solvent) Na_2CO_3 37% Formaldehyde 10 mg $Na_2S_2O_3$ x $5H_2O$ ad 50 mL H_2O
Western blotting and immunostaining	Blotting buffer (pH 8.3)	25 192	mM mM	Tris Glycin
	NBT	30 70	g L^{-1} %(v/v)	Nitro blue tetrazolium chloride N,N-Dimethylformamide
	BCIP	15 70	g L^{-1} %(v/v)	5-Bromo-4-chloro-3-indolyl phosphate (di-sodium-salt) N,N-Dimethylformamide
	AP substrate buffer	100 0.5	mM mM	Tris $MgCl_2$
ELISA, panning, immunostaining, peptide array	PBS (phosphate buffered saline, pH 7.4)	140 2,7 10 1,8	mM mM mM mM	NaCl KCl Na_2HPO_4 x $2H_2O$ KH_2PO_4
	PBST	0.05	% (v/v)	PBS (solvent) Tween20
	MPBST	2	% (w/v)	PBST (solvent) Milk powder
ELISA	TMB A (pH 4.1)	30 50	mM mM	KCl Citric acid

Application	Description	Composition		
		90	% (v/v)	Ethanol
		10	% (v/v)	Acetone
		0.3	% (v/v)	H_2O_2
	TMB B	1	mM	3,3',5,5'-Tetramethylbenzidine
				PBS (solvent)
Cell counting	Trypan blue	0.1	% (w/v)	Trypan blue
	Phage precipitation buffer	20	% (v/v)	Polyethylene glycol (~M_w 6000)
		2.5	M	NaCl
Packaging of phage display libraries	Phage dilution buffer (pH 7.5)	10	mM	Tris
		20	mM	NaCl
		2	mM	Ethylenediaminetetraacetic acid
Peptide array	Fluorescent blocking buffer	purchased from Rockland, Limerick, USA		

If not mentioned otherwise, water was used as solvent and the pH was adjusted with 1 M HCl and 1 M NaOH.

2.1.11 Software

The software used is listed in Table 2-13.

Table 2-13: Software

Software	Application	Reference
Image Lab	ChemiDoc MP image processing	Bio-Rad
VBase2	Analysis of antibody sequences	(Mollova et al., 2010)
ImageJ	Cell counting	Wayne Rasband (NIH)
PyMol v1.3	visualization of protein 3D structures	The PyMOL Molecular Graphics System, Schrödinger, LLC.
PepSlide®	Analysis of the peptide array	Sicasys software GmbH
SWISS-MODEL	Protein structure homology modelling	(Waterhouse et al., 2018)
NCBI	Literature, Protein- and Gene-sequences	http://www.ncbi.uhm.nih.gov
Microsoft office	Text and Data editing	https://de.libreoffice.org
Inkscape 0.91	Figures	https://inkscape.org/
Geneious 4.8.5	*In silico* cloning, sequence analysis	https://www.geneious.com

2.2 Methods

2.2.1 Molecular biological methods

2.2.1.1 DNA preparation

Plasmid DNA was isolated from *E. coli* overnight cultures with commercial plasmid DNA preparation kits (NucleoBond Xtra plasmid Midiprep or NucleoSpin Plasmid Miniprep Kit Macherey&Nagel) according to their manuals.

PCR-products or products of enzymatic plasmid digestion were either purified directly from the reaction mix or from agarose gels after electrophoresis with a commercial PCR clean up and gel extraction kits (NucleoSpin Gel and PCR clean-up, Macherey&Nagel or Hi Yield® Gel/PCR DNA Fragment Extraction Kit, SLG). The DNA was eluted or solubilized with ddH_2O and stored at -20 °C.

2.2.1.2 Photospectrometric determination of DNA concentration

To determine the concentration of DNA preparations the absorbance at $\lambda = 260$ nm was measured using a spectrophotometer. The following formula was applied to calculate the concentration: $A_{260} = 1 \triangleq 1$ ng μL^{-1}.

2.2.1.3 Agarose gel electrophoresis

A 1% Agarose gel was placed inside an electrophoresis chamber and the chamber was filled with 1x TAE buffer. DNA samples were mixed with 6x loading dye and loaded onto the gel. After separation of DNA fragments at 110 V for 25-30 min. The gel was documented using UV radiation in the ChemiDoc™ (BioRad) imaging system.

2.2.1.4 DNA sequencing

To control cloning, analyze clones obtained from phage display or characterize the TcdB-gene-fragment library Sanger sequencing was performed.

Sequencing of purified plasmids or PCR products was carried out by Seqlab Sequence Laboratories GmbH (Göttingen, Germany).

2.2.1.5 Polymerase chain reaction

The DNA amplification by PCR was performed to control cloning success, to analyze clones after panning or to amplify genes from genomic DNA of *Clostridioides difficile*.

2.2.1.6 Colony PCR

Colony PCR was performed either after panning to verify that obtained *E. coli* clones contain pHAL30 plasmids with complete scFv genes (V_H and V_L inserts), or to control cloning success after transformation of ligated plasmids into *E. coli*. DNA was amplified using primers flanking the cloning sites of the vectors (Primers 11 and 125 for pHAL30 or pHORF3 and primers 410 and 411 for pCSE2.6 vectors). A small amount of *E. coli* cells was added as DNA template to the reaction mix. The reaction mix (Table 2-14) was incubated in a thermocycler with the appropriate temperature program (Table 2-15). After the PCR, the reaction mix was analyzed by agarose gel electrophoresis.

Table 2-14: Reaction mix for colony PCR

Stock solution	**Volumes [µL] per 10 µL reaction mix**
5x Green GoTag Reaction Buffer	2.0
25 mM $MgCl_2$	0.4
10 mM dNTP mix	0.2
10 mM forward primer	0.5
10 mM reverse primer	0.5
5 U μL^{-1} GoTag DNA Polymerase	0.05
Water	6.35

Table 2-15: Temperature program for colony PCR

Step	**Temperature [°C]**	**Time [s]**	**Repeats**
1. Initial denaturation	94	180	x1
2. Denaturation	94	40	x25
3. Annealing	52	20	
4. Elongation	72	30/kb	
5. Final Elongation	72	600	x1
6. Store	16	forever	

2.2.1.8 Amplification of tcdB gene

For generation of a TcdB gene fragment library, the tcdB gene had to be amplified from genomic DNA isolated from *Clostridioides difficile* strain 630 by PCR, as described in Table 2-16 and Table 2-17. To avoid mutations in the gene the Phusion DNA polymerase which has a lower error rate of $4.4x10^{-7}$ was used.

Table 2-16: Reaction mix for PCR

Component	Volume [µL]
5x Phusion Buffer	20
10 µM Primer ViF218-TcdB-for	5
10 µM Primer ViF218-TcdB-rev	5
dNTPs 10mM	3
Phusion polymerase 2U /µL	1
Genomic DNA	1,34 (≙ 250 ng)
dH2O	64,66

DNA was amplified in 25 temperature cycles using the following program.

Table 2-17: Temperature program for PCR

Step	Temperature [°C]	Time [s]	Repeats
1	98	30	1x
2	98	10	25x
3	64 / 67	20	
4	72	285	
5	72	300	1x
6	16	For ever	1x

Success of DNA amplification was verified by Agarose gel electrophoresis

2.2.1.9 DNA cloning

2.2.1.9.1 Cloning of scFv DNA fragments from pHAL30 to pCSE2.6

For production of antibodies as scFv-Fcs in mammalian cells the scFv-coding DNA segment had to be cloned into the pCSE2.6-hIgG1 –XP vector. For this purpose, 1 µg scFv containing pHAL30 was digested with NcoI and NotI (20 U each) for 90 min at 37 °C according to manufacturer's instructions. After the separation of the DNA fragments by agarose gel electrophoresis, the scFv-DNA was extracted from the gel and purified as described in 2.2.1.1 The pCSE2.6-hIgG1-Fc-XP vector backbone was NcoI and NotI digested, too and directly purified. Concentration of vector backbone and insert DNA was determined. A threefold molar excess of scFv-DNA was ligated into the vector using 1 U T4 ligase (Promega) according to manufacturer's instructions. Ligation mix was heat inactivated and 2 µL were used for heat

shock transformation of *E. coli*. Success of cloning was verified by colony PCR (see 2.2.1.6) and DNA sequencing (see 2.2.1.4)

2.2.1.9.2 Cloning of tcdB single gene library using pHORF3

For cloning of tcdB single gene library the tcdB gene was amplified from genomic DNA as described in 2.2.1.7. Success of PCR was confirmed by agarose gel electrophoresis and PCR product was purified from the gel as described in 2.2.1.1. The PCR product (1,25 µg) was diluted in 100 µL ddH_2O and fragmented using Bioruptor® Pico sonicator (Diagenode) using following settings: 45 cycles, 30 s sonication at low intensity, 30 s pause. Sample was chilled in a 4 °C waterbath throughout fragmentation process. Fragmented DNA was concentrated using Amicon Ultra Centrifugal filters (30K; Millipore). Blunt ends were generated using the Fast DNA End Repair Kit (Thermo Fisher Scientific Inc., Waltham, USA) according to manufacturer's instructions. DNA product was purified as described in 2.2.1.1. Afterwards, a 10-fold molar excess of gene fragments were ligated into PmeI digested and CIP treated pHORF3 (see also Table 2-18). The ligation mix was incubated at 16 °C overnight.

Table 2-18: composition of ligation mix

Component	**Volume**
pHORF3 cut pmeI/CIP	3,5 µl (≙ 1000 ng)
Fragmented tcdB	7,6 µl (≙ 360 ng)
Ligase Buffer (10x)	10 µl
Promega T4 DNA Ligase (3 U/µl)	3,33 (≙ 10U)
dH2O	75,5

To get rid of salts interfering with *E. coli* transformation by electroporation, ligation mix buffer was exchanged to H_2O using Amicon Ultra Centrifugal filters (30K von Millipore).

Electro competent TOP10F' cells were thawed on ice. Twenty-five µL of cells were mixed with 175 ng ligated DNA in 5µL ddH_20 and transferred into a pre-chilled (4 °C) electroporation cuvette. Electroporation was performed using a 1,8 kV pulse in the Micro Pulser™ device. One mL prewarmed (37 °C) SOC media was immediately added and the cells were transferred into reaction tubes. After an incubation at 650 rpm and 37 °C for 1 hour cells were plated on 2xYT-GA-agar in a square dish. After incubation at 37 °C overnight 25 mL of 2x YT media was added to the plates and the colonies were scraped off using a glass spatula. 20 % (v/v) glycerol was added to the bacteria suspension. After transferring to screw lid tubes the library was shock frozen in liquid nitrogen and stored at -80 °C.

2.2.2 Bacterial cultivation techniques

2.2.2.1 Sterilization

All materials, media and solutions used for sterile work, were autoclaved at 121 °C for 20 min. Heat sensitive substances were sterilized by filtration through 0,2 µm pore filters.

2.2.2.2 Storage of E. coli

For long term conservation, aliquots of *E. coli* overnight cultures, or dense *E. coli* cultures were supplemented with 20% glycerol (v/v) and stored at -80 °C.

Liquid cultures or colonies on agar plates were stored at 4 °C for shorter time periods of up to one week.

2.2.2.3 E. coli transformation

For transformation of *E. coli* two different techniques were used. For simple cloning of inserts from one vector backbone to another heat shock transformation was performed. For cloning of libraries, transformation rates normally obtained by heat shock transformation are not sufficient, therefore electroporation was used for this purpose (see 2.2.1.9.2).

2.2.2.3.1 Transformation by heat shock

25 µL of chemically competent cells were slowly thawed on wet ice. The cells were mixed with 2 µL of heat inactivated ligation mix and incubated on ice for 15 min. After a 42 °C heat shock for 1 min. cells were directly placed back into the ice bath for another two min. Prewarmed SOC media (250 µL) was added and the cells were incubated at 37 °C and 650 rpm for 30 min. The cell suspension was plated on prewarmed 2xYT-G-agar, supplemented with the proper antibiotic and incubated overnight at 37 °C.

2.2.2.4 Production of soluble scFv in E. coli in MTP

The cavities of a U-shape 96 well polypropylene plate were filled with 150 µL 2xYT-GA media. Each well (except of one negative control well) was inoculated with an *E. coli* clone containing a pHAL30 plasmid with an scFv insert. *E. coli* clones were incubated overnight at 37 °C at 800 rpm in a Vortemp56 incubator. This plate is referred to as the master plate.

The cavities of a new U-shape 96 well polypropylene plate were filled with 150 µL 2xYT-GA media and each well was inoculated with 10 µL of the overnight culture from the corresponding well of the master plate. The fresh cultures were incubated for ~1,5 h at 37 °C and 800 rpm until an $O.D._{600\ nm}$ of 0,5 was reached. The cells were pelleted by centrifugation

and the old media was removed. The cell pellets were resuspended in 150 µL 2xYT-A media containing 50 µM Isopropyl-β-D-thiogalactopyranosid (IPTG) to induce the LacZ promoter and start the scFv production. After overnight incubation at 30 °C and 800 rpm the cells were pelleted and the scFv containing supernatant was harvested.

2.2.3 Phage handling

2.2.3.1 Packaging of peptide libraries with Hyperphage

For ORF enrichment and to package the pHORF3-TcdB-gene fragment library into phage particles with polyvalent display, Hyperphage was used for infection.

An aliquot of the TcdB-single gene library was used to inoculate 400 mL of 2xYT media to an $O.D._{600\ nm}$ of 0,1. Cells were incubated at 37 °C and 250 rpm in an Infors Multitron HT incubator until an $O.D._{600\ nm}$ 0,5 was reached.

Since the cells still lack the genetic information for the phage coat proteins, infection with M13K07ΔgIII "Hyperphage" was performed: 25 mL of the cell suspension were transferred to a 50 mL Falcon tube, mixed with 20 multiplicity of infection (MOI) Hyperphage (M13K07ΔgIII) and incubated 30 min at 37 °C without shaking. After 30 min of incubation at 37 °C at 250 rpm to express the kanamycin resistance, cells were pelleted 10 min at 3220 xg and transferred to 400 mL of 2xYT-AK media. TcdB-Fragment-phage were produced >20h at 30 °C and 250 rpm in an Infors Multitron HT incubator.

The phage particles were harvested from the cultivation slurry by a two-step precipitation. Therefore, the bacteria were pelleted by centrifugation at 10.000 xg for 30 min in a pre-chilled centrifuge and the supernatant was transferred into a fresh vessel. The phage particles were precipitated at 4 °C overnight by adding 1/5 volume phage precipitation buffer (PEG-NaCl). The precipitated phage particles were pelleted by 1h centrifugation at 12.000 xg and 4 °C (Sorval Centrifuge RC5B Plus, Rotor F9S) and resuspended in 10 mL phage dilution buffer (PDB). To increase purity, the phage were filtered (Whatman syringe filter, 0.45 µm) and again 1/5 volume of phage precipitation buffer was added for the 2nd phage precipitation (2h on ice). Phage were pelleted for 30 min at 20.000 xg and 4 °C (Sorval Centrifuge RC5B Plus, Rotor SS34) and resuspended in 1 mL of PDB. Remaining *E. coli* cells were pelleted for 2 min at 16,100 xg and TcdB-fragment phage libraries were collected and stored at 4 °C.

2.2.3.2 Production of monoclonal phage in MTP

The cavities of a U-shape 96 well polypropylene plate were filled with 150 µL 2xYT-GA media. Each well (except of one negative control well) was inoculated with an *E. coli* clone containing a pHORF3 plasmid with a tcdB gene fragment insert. *E. coli* clones were incubated overnight at 37 °C at 800 rpm in a Vortemp56 incubator. This plate is referred to as the master plate.

The cavities of a new U-shape 96 well polypropylene plate were filled with 150 µL 2xYT-GA media and each well was inoculated with 10 µL of the overnight culture from the corresponding well of the master plate. The fresh cultures were incubated for ~1,5 h at 37 °C and 800 rpm until an $O.D._{600}$ was reached. To each well Hyperphage particles with a MOI of 20 was added. The infection took place within 30 min at 37 °C. After that the cells were incubated another 30 min at 37 °C with shaking (800 rpm in a Vortemp56 incubator). To induce phage production a media change had to be performed, therefore the cells were pelleted for 10 min in a centrifuge at 3220 xg and the media was discarded. The pellet was resuspended in 150 µL 2xYT-AK media and monoclonal phage were produced overnight at 30 °C and 800 rpm.

2.2.3.3 Titer determination

For titer determination after phage production or elution, phage particles were serially diluted in PBS. Ten µL of each phage dilution were used to infect 50 µL of *E. coli* culture at an $O.D._{600\ nm}$ of 0,5 (exponential growth phase). After infection for 30 min at 37 °C, *E. coli* was plated on 2xYT-GA agar and incubated at 37 °C overnight. The colonies were counted and the titer was calculated.

2.2.3.4 Panning for antibody selection

To generate antibodies against various TcdB domains three rounds of panning were performed using the naïve human scFv-libraries HAL9 and HAL10 (Kügler et al., 2015).

For this purpose, a cavity of a 96 well Costar MTP was either first coated with 5 µg of an antigen used for library preclearance and then blocked with panning block, or directly blocked. $5x10^{10}$ phage particles, derived from HAL9 and HAL10 were diluted in 150 µL panning block transferred to the preclearance well and incubated for one hour.

In a next step the phage incubated in the actual panning well. Beforehand, this well had been coated with 5/2/1 µg (1^{st} /2^{nd} /3^{rd} panning round, respectively) of antigen in 100 µl PBS for 1h at RT or overnight at 4 °C and blocked with 2% MPBST.

After two hours non-bound phage were removed by stringent washing with PBST (10 x / 20 x / 30 x, depending on panning round). The remaining phage were eluted by proteolytic cleavage using trypsin (150 µL; 10 µg /mL trypsin in PBS;) for 30 min at 37 °C. Ten µL of eluted phage were used for titer determination as described in 2.2.3.3. The colonies obtained during titer determination can be used to screen single *E. coli* clones as described in 2.2.6.2.

For the next panning round the remaining phage were amplified. For this purpose, they were mixed with 150 µL of an *E. coli* TG1 culture at $O.D._{600\ nm}$ 0.5 and incubated 30 min at 37 °C. Cells were pelleted for ten min at 3220 xg, resuspended in 1 mL 2xYT-GA media and cultivated in a VorTemp™ 56 incubator at 37 °C and 600 rpm until $O.D._{600\ nm}$ 0.5 was reached. Twenty MOI M13K07 phage were added for coinfection to enable subsequent phage production. After incubation at 37 °C, 30 min w/o shaking and 30 min with shaking, cells were pelleted as described above and media was exchanged to 2xYT-AK media. Phage were produced during overnight cultivation at 30 °C and 600 rpm. *E. coli* cells were pelleted by centrifugation at 3220xg for 10 min and scFv-phage containing supernatant was collected, 50 µL were directly used for the next panning round.

2.2.3.5 Panning for epitope identification

Preclearance of library from sticky phage

A cavity of a 96 well Costar MTP was coated with 1 µg of an unrelated scFv-Fc in 100 µL of PBS. The antibody solution was discarded and the well was completely blocked with panning block (1% BSA, 1% milk powder in PBST). Per each panning at least $1x10^9$ TcdB-fragment phage particles were diluted in 150 µL of panning block and incubated in the preclearance well.

Selection of epitope presenting phage

To isolate TcdB-fragment phage, that present an epitope containing TcdB fragment as a pIII fusion protein an adapted panning protocol with double competition and three successive peptide-phage - antibody interaction steps was used. For this purpose, three wells were coated with 1 µg scFv-hFc of interest. Afterwards the wells were blocked with 2% MPBST. The precleared phage were transferred to the first of the three panning wells and 1 µg of the anti ErbB4 antibody was added in solution as competitor. Every hour the unbound phage were transferred to the consecutive panning well. To prevent the previous wells from drying and to diminish sticky phage 1µg of an unrelated antibody in 150 µL PBST was added. When

incubation in the third well was completed, weakly bound phage were removed by washing with PBST in a Tecan Columbus ELISA washer using the following programs: well one- 10x harsh bottom washing; well two- 9x normal washing; well three- 3x normal washing. Remaining phage were eluted using 150 µL 10 µg/mL trypsin during an incubation for 30 min at 37 °C. Eluted phage were collected and 10 µL were used for titer determination as described in 2.2.3.3.

2.2.4 Biochemical methods

2.2.4.1 Protein A purification of Fc-fusion Proteins

Recombinantly produced antibodies were purified by affinity purification with the protein A MabSelect™ System (GE Healthcare) in a 24 deep well vacuum filtration plate. The column material was equilibrated by 3x washing with PBS. Up to 9 mL of cell free production supernatant were filled into the wells and allowed to pass the column material by gravity flow. After 5 min of incubation vacuum was applied to remove remaining supernatant. For larger production scales the loading step was repeated. The protein A matrix was washed three times with PBS to remove unbound impurities. Afterwards antibodies were eluted at pH3 in three steps. First 500 µL of protein A elution buffer was added to the matrix and incubated for 5 min, vacuum was applied. The second and third elution were performed with 750 µL elution buffer. To neutralize pH, the eluted antibodies were directly mixed with 220 µL of 1 M Tris. Afterwards the buffer of the eluate was exchanged to PBS either by use of Zeba™ Desalt Spin column or by dialysis. Antibody concentration was determined via UV/VIS spectrometry using Nanodrop ND1000. Purified antibodies were stored at -80 °C.

2.2.4.2 Discontinuous SDS PAGE

Produced proteins were analyzed by discontinuous SDS-PAGE as described by Laemmli (Laemmli, 1970) with a stacking gel to focus the proteins and a separation gel. The compositions are given in the following tables (Table 2-19, Table 2-20).

Table 2-19:composition stacking gel

Stock solution	**Volume per gel**
Water	1.0 mL
30 % (w/v) Acrylamide/Bis	260 µL
1 M Tris-HCl, pH 6.8	200 µL
10 % (w/v) SDS	15 µL
10 % APS (Ammonium persulfate in H_2O)	15 µL
Tetramethylethylendiamin	2 µL

Table 2-20: composition separation gel

Stock solution	**Volume per 12% gel**
Water	1.3 mL
30 % (w/v) Acrylamide/Bis	1.6 mL
1.5 M Tris-HCl, pH 8.8	1.0 mL
10 % (w/v) SDS	40 µL
10 % APS (Ammonium persulfate in H_2O)	40 µL
Tetramethylethylendiamin	2 µL

Laemmli buffer was added to the protein samples and after denaturation for 10 min at 96 °C samples were loaded to the gel. The samples were separated at 25mA /gel for 45-55 min.

2.2.4.3 Coomassie staining of SDS gels

The polyacrylamide gel was placed in a glass dish, covered with Coomassie staining solution and heated shortly in a microwave. Afterwards the gel was incubated on a rocker until the staining was complete. The gel was rinsed with water and destained using acetic acid (10 v/v). When the protein bands became clearly visible and the background staining was fainted the gel was documented.

2.2.4.4 Silver stain of SDS gels

The polyacrylamide gel was submerged in fresh fixation solution and incubated for 1 hour at room temperature on a rocker. Afterwards, it was dehydrated by three subsequent incubations in 50 % (v/v) ethanol of 15 min. The gel was incubated 1 min in 0.13 mg mL^{-1} $Na_2S_2O_3$ and was washed three times 20 s with water. Next, it was incubated for 20 min in staining solution and washed two times 20 s with water. After adding of developer solution protein bands became visible within a few min. The gel was washed two times 2 min with water and staining was stopped by incubation in stopping solution. The gel was stored in water and documented.

2.2.6 Immunological assays

2.2.6.1 Western blot and immunostaining

For specific detection of proteins in a sample, or for antibody characterization, western blotting with subsequent immunostaining was performed.

Proteins were transferred from an SDS-Gel to a PVDF membrane by semi dry blotting using the Trans-Blot® Turbo™ transfer system (Biorad). The blotting sandwich was built up in the blotting cassette according to manufacturer's instructions. According to the size of the target proteins a Bio-Rad optimized protocol was chosen. Large proteins (>150 kDa; TcdB and fragments) were blotted for ten min, with constant current of 1.3 A and up to 25 V, smaller proteins for 30 min, with up to 1.0 A and constant voltage of 25 V. After blotting the PVDF membrane was blocked by incubation in 2 %MPBST for 1h at room temperature on a rocker.

The blot was submerged in a dilution of primary antibody in 2 % MPBST and incubated at least 1 h at room temperature or 4 °C overnight. Afterwards the blot was washed three times using PBST and incubated with the AP- conjugated secondary antibody diluted in MPBST for 45 min at room temperature on a rocker.

After another washing step (three times with PBST) the blot was developed with NBT BCIP (100 µL each in 10 mL of AP substrate buffer) until bands became visible. The membrane was thoroughly washed with water and dried between paper towels.

2.2.6.2 Indirect antigen ELISA for scFv screening

Supernatants from soluble scFv production in MTP (see 2.2.2.4) were screened for specific binding by indirect antigen ELISA. Therefore, each cavity of a Costar 96 well ELISA plate was coated with 100 ng antigen in 100 µL PBS, either overnight at 4 °C or 1,5 h at RT. All cavities were blocked with MPBST. Afterwards, as well as after each of the following incubation steps, plates were washed three times with ddH2O- 0,05% Tween, all antibodies were diluted in MPBST. ScFv containing *E. coli* supernatants were transferred to the assay plate in a 1:2 dilution and incubated 1,5 h. After washing anti c-Myc antibody 9E10 was added to the wells and incubated 1 h. Bound 9E10 antibody was detected with HRP conjugated anti-mouse antibody in a 1:40.000 dilution (A0168, Fcγ specific). After final washing ELISA was developed with freshly prepared TMB substrate solution for up to 30 min. Colorimetric reaction was stopped by addition of an equal volume of stop solution and signals were detected in an ELISA reader (signal at 450 nm, reference at 620 nm).

2.2.6.3 Indirect antigen ELISA for scFv-Fc characterization

To determine binding specifity of produced scFv -Fc antibodies as well as to map the binding region of the antibodies, indirect antigen ELISAs were performed. For this purpose, each cavity of a Costar 96 well ELISA plate was coated with 100 ng antigen in 100 µL PBS, either overnight at 4 °C or 1.5 h at RT. All cavities were blocked with MPBST by incubation for 1 h at RT. Afterwards, as well as after each of the following incubation steps, plates were washed three times with ddH2O- 0,05 % Tween using the BioTek HydroSpeed ELISA washer. Generated scFv-Fc were used as primary antibodies, diluted in MPBST and transferred to the ELISA plate. After incubation of 1 h and subsequent washing, bound scFv-Fc were detected using an HRP-conjugated goat anti-human IgG (Fc specific) antibody (A0170; Sigma-Aldrich) in a 1:70,000 dilution. The ELISA was developed using TMB substrate and colorimetric reaction was stop with H_2SO_4. Intensity of staining was measured in an ELISA reader (signal at 450 nm, reference at 620 nm) and correlates to the amount of scFv-Fc bound to the antigen.

2.2.6.4 Monoclonal phage capture ELISA

After panning for epitope identification, monoclonal TcdB-fragment-phage from phage production in MTP (see 2.2.3.2) were screened for specific binding to selected scFv-Fc antibodies. Therefore, the scFv-Fc antibody was diluted in PBS and 100 ng were coated in each cavity of a Costar 96 well ELISA plate overnight at 4 °C. The solution was discarded and all cavities were completely saturated with 2 % MPBST for one hour. Afterwards, as well as after each of the following incubation steps, plates were washed three times with ddH2O-0,05 % Tween using the BioTek HydroSpeed ELISA washer.

Twenty-five µL TcdB-fragment-phage containing *E. coli* supernatants were transferred to the assay plate, mixed with 75 µL MPBST and incubated 1.5 h. Bound Phage were detected using HRP conjugated mouse anti-M13 antibody (pVIII specific GE healthcare) in a 1:40,000 dilution. After 45 min of incubation and washing the ELISA was developed by adding 100 µL TMB substrate solution per well. Colorimetric reaction was stopped with an equal volume of stop solution and signals were detected (signal at 450 nm, reference at 620 nm).

2.2.6.5 Peptide array

The peptide arrays were purchased from PEPperPRINT GmbH (Heidelberg). The array was hydrated at RT with PBST for 15 min on an orbital shaker. Afterwards the array was blocked with fluorescent blocking buffer (Rockland). After washing with PBST monoclonal scFv-Fc antibodies diluted in staining buffer were incubated on the arrays overnight at 4 °C and 200 rpm. The array was washed 3 x (few secs) with PBS-T. Anti-Human IgG-Fc Fragment cross-adsorbed DyLight 680 conjugated antibody (Biomol) was diluted 1:200 in staining buffer and incubated on the array (30 min, RT, 200 rpm). The array was washed three times with PBST, dipped in 1 mM TrisHCl pH7.4 and air dried. Fluorescence signals at 700 nm was scanned. Afterwards the HA-tag control peptides were stained, using Anti-HA Peptide Ready Tag Mouse IgG2b (BioXcell) in a 1:5000 dilution in staining buffer as a primary, and Anti-Mouse IgG (H+L) DyLight 680 conjugated antibody (Cell Signaling Technology) 1:5000 in staining buffer as a secondary antibody. Incubation with both antibodies was 30 min at RT and 200 rpm followed by three times washing with PBST. After staining was completed, arrays were dipped in 1mM TrisHCl pH7.4, air dried and used for a second scan.

Analysis of the scans was performed using the software Pep Slide Analyzer.

2.2.7 Cell biological methods

2.2.7.1 Storage of mammalian cells

For longer time periods mammalian cells were stored in the vapor phase over liquid nitrogen in freezing media containing DMSO (% of DMSO depends on the cell line) as cryoprotectant.

2.2.7.2 Thawing of Vero cells

An aliquot of ~3x10^6 Vero cells was removed from the nitrogen tank and directly placed into a water bath, tempered at 37 °C. As soon as the cell suspension was melted it was diluted in 5 mL prewarmed cultivation media (RPMI 1640 supplemented with 10% (v/v) FCS and 2 mM stable L-Glutamine). To remove the DMSO, cells were carefully pelleted at 130 xg for five min., supernatant was discarded and cells were transferred to a 75T flask containing 20 mL cultivation media already pH equilibrated by incubation at 37 °C in 5% CO_2. Cells were incubated at 37 °C and 5% CO_2 and monitored daily after thawing.

2.2.7.3 Cultivation and passaging of Vero cells

Vero cells were passaged two to three times weekly, when cell density was exceeding 90% confluency. For this purpose, old media was discarded and cells were washed with PBS to remove dead cells and residual media. Trypsin EDTA was added in a way that the cultivation area was slightly covered. Cells were incubated at 37 °C for 5-10 min until cell shape changed to a spherical shape. Dissociation was stopped by rinsing the full cultivation area with 2,5 volumes of complete growth media (RPMI 1640 with 10% FBS and 2 mM Glutamine). By rinsing and pipetting up and down, cells were detached from the surface and cell aggregates were dissociated. 1/20 - 1/5 of cell suspension was seeded into a fresh cultivation vessel filled with prewarmed complete growth media.

2.2.7.4 Freezing of Vero cells

Vero cells were frozen according to information provided by ATCC®. Vero cells were detached from T75 flasks by trypsinization as described in 2.2.7.3. Cell suspension was transferred into a 15 mL Falcon tube and an aliquot was used for cell counting in a Neubauer chamber. Cells were pelleted at 130 xg for 5 min. The supernatant was discarded and the pellet was resuspended in ice cold growth media supplemented with 5% DMSO. The cell density was set to > 3x10^6 cells 1.8 mL^{-1}. Cell suspension was aliquoted à 1.8 mL into cryo- screw lid tubes. For a controlled freezing process tubes were placed into a pre-chilled (4 °C) freezing

container (Mr. Frosty, Nalgene®) filled with isopropanol and transferred to -80 °C. For long term storage the cells were moved to a liquid nitrogen tank.

2.2.7.5 Vero cell intoxication assay with TcdB

10.000 cells were seeded into each cavity of a 96 well polystyrene plate and cultivated in 100 µL of complete growth media (RPMI1640 supplemented with 10% (v/v) FBS and 2mM L-glutamine) at 37 °C and 5% CO_2. The next day TcdB and scFv-Fc antibodies were melted on ice, diluted in pre-warmed complete growth media and mixed in a cavity of a 96 well polystyrene plate. For all assay plates the following controls were prepared: TcdB only, TcdB + isotype control antibody and media only. After incubation of 30 min at RT the cultivation media in the Vero cell growth plate was replaced with the TcdB-antibody mixture. Cells were monitored for morphological changes. After 4-6 hours, when ~70% of cells in the TcdB – isotype control wells were rounded off, pictures of all wells were collected. The percentage of round cells in each well was determined by counting, using ImageJ software.

2.2.7.6 Cultivation of HEK293-6E / Expi293F™ cells

HEK293-6E and Expi293F™ cells were cultivated in serum free F17 media supplemented with 8mM L-glutamine and 0,1 % (w/v) Pluronic-F68 at 37 °C, 5% CO_2 and 110 rpm in polycarbonate flasks with ventilated caps. Cells were passaged every 2-3 days and seeded to a cell density of 0.2 $x10^6$ cells mL^{-1}.

2.2.7.7 Transfection of HEK293-6E/ Expi293F™ cells

For transient production of scFv-Fcs in mammalian cells PEI mediated transfection of HEK293-6E or Expi293F™ cells was performed.

Per mL of cell culture volume, 1 µg DNA and 5 µg PEI were each diluted in 50 µL F17 media (supplemented with 8 mM L-glutamine and 0,1 % (w/v) Pluronic-F68), and then mixed in a cavity of a polystyrene plate. After 25 min when the DNA-PEI complex was formed the transfection mix was added to HEK293-6E or Expi293F™ cells in exponential growth phase (1.5- 1.8 x 10^6 cells/mL). Cells were cultivated at 37 °C and 5% CO_2 in an InforsHT Minitron incubator (RPM depended on the cultivation vessel). Two days after transfection cells were fed with 1 volume of complete F17 media plus 1/5 volume of TN1 (HEK293-6E cells) or 1 volume HEK TF (+8 mM L-Glu) plus 1/5 volume HEK FS (Expi293F cells). Production was continued for 5 more days, then the cells were pelleted by centrifugation (10 min at 1500 xg) and the supernatant was collected to purify the produced scFv-Fc antibodies as described in 2.2.4.1.

3 Results

3.1 TcdB variants for antibody generation and characterization

In this study, a phage display approach was used to generate antibodies against various domains and regions of TcdB. For the panning, as well as for subsequent antibody characterization and neutralization assays, recombinant TcdB, as well as domains and fragments thereof, were used. A schematic representation of the antigen and antigen fragments is given in Figure 3-1.

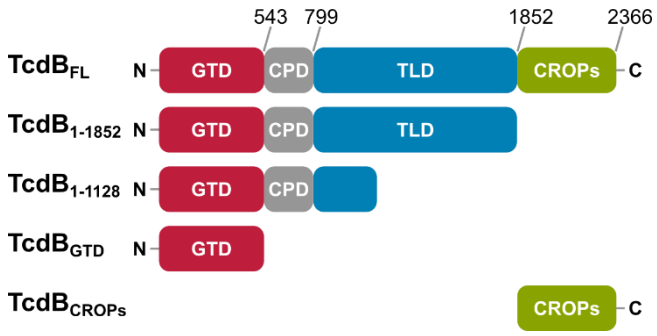

Figure 3-1: Schematic representation of TcdB Fragments

TcdB fragments used in this study. All Fragments derived from TcdB of C. difficile strain VPI10463. TcdB$_{FL}$: wild type (wt) TcdB; TcdB$_{1-1852}$: wt TcdB missing the CROP domain; TcdB$_{1-1128}$: N-terminal 1128 aa of wt TcdB; TcdB$_{GTD}$: enzymatically inactive mutant (D286/288N) of TcdB glucosyltransferase domain; TcdB$_{CROPs}$ combined repetitive oligopeptides, missing the first short repeat

The antigens were produced with a C-terminal 6 x His-tag in a *B. megaterium* expression system, and purified via Ni^{2+}-affinity chromatography, except of TcdB$_{CROPs}$, which was produced as GST-fusion protein in *E. coli* and purified via Glutathione-sepharose chromatography. TcdB$_{CROPs}$ was cleaved from the GST-tag by thrombin cleavage.

The aa sequence of the TcdB fragments used corresponds to *C. difficile* strain VPI10463, a *C. difficile* reference strain. TcdB$_{GTD}$ was produced as a glucosyltransferase-deficient mutant (D286/288N) for higher yields and purity of the protein.

All TcdB variants used were kindly provided by Ralf Gerhard, Sebastian Goy and Helma Tagte (Hannover Medical School, Institute for Toxicology).

3.2 Antibody generation

3.2.1 Panning and sequence analysis

To generate antibodies against the various domains of *Clostridioides difficile* Toxin B (TcdB), a phage display approach was used. Phage display was performed using the two naïve human scFv-libraries HAL9 and HAL10 (Kügler et al., 2015).

To gain a broader antibody diversity and to cover a broader range of epitopes, a total of six pannings was performed on either $TcdB_{1-1852}$, $TcdB_{CROPs}$ or the full-length toxin ($TcdB_{FL}$). An overview over the panning strategies and the success of the pannings is given in Table 3-1.

Table 3-1 Panning strategies and outcome

Panning	TcdB Fragment	°C	negative selection	Clones screened	Clones analyzed	Unique	characterized as Fc-Fusion
ViF087	$TcdB_{1-1852}$	RT	$TcdB_{1-1128}$	92	19	11	10
ViF088	$TcdB_{1-1852}$	RT	no	92	13	3	3
ViF090	$TcdB_{1-1852}$	37	$TcdB_{1-1128}$	92	17	2	2
ViF091	$TcdB_{1-1852}$	37	no	92	11	1	1
ViF137	$TcdB_{CROPs}$	RT	no	92	24	12	8
SH1429*	$TcdB_{FL}$	RT	no	92	12	7	7
Σ human antibodies				**552**	**96**	**36**	**31**
*Panning was performed by Saskia Helmsing							

For two pannings on $TcdB_{1-1852}$, a negative preselection on the N-terminal fraction of TcdB ($TcdB_{1-1128}$) was performed to direct the selection pressure towards antibodies that bind within the translocation domain (TLD) more exactly, between aa 1128 and aa 1852.

Since the toxins conformation might be temperature dependent, the panning on $TcdB_{1-1852}$ was performed at room temperature and at 37 °C. The pannings on $TcdB_{CROPs}$ or $TcdB_{FL}$ were only performed at room temperature, since panning at 37 °C seemed to decrease antibody diversity, as only two and one unique clones could be generated in the pannings at 37 °C on $TcdB_{1-1852}$ (ViF090 and ViF091).

For each panning three rounds of antibody enrichment were performed. Afterwards a total of 552 clones was screened for production of TcdB specific scFv in an antigen ELISA. As antigen in the ELISA the TcdB variant used in the respective panning was immobilized in MTP plates. As an example, the result of the screening ELISA after panning on $TcdB_{1-1852}$ at room temperature with negative selection on $TcdB_{1-1128}$ (panning ViF087) is given in Figure 3-2.

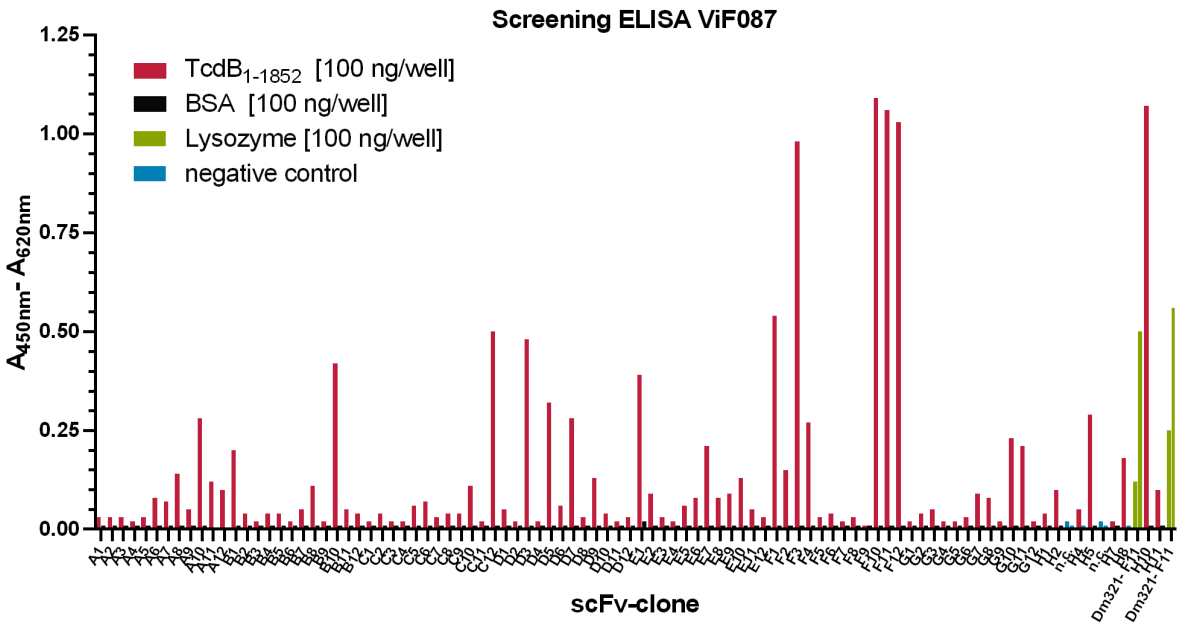

Figure 3-2: Screening ELISA

Exemplary shown for the screening after panning on $TcdB_{1-1852}$ with negative selection on $TcdB_{1-1128}$. Ninety-two clones were screened production of scFv binding to TcdB1-1852. BSA was used as a negative control antigen to prove specificity of selected antibodies. As negative control to determine assay background cultivation media was used. The positive control was an anti-lysozyme antibody Dm321-F11 on 100 ng coated lysozyme.

On basis of the signal intensity and the signal to noise ratio in the screening ELISA, a total of 96 antibody clones were further analyzed. Sequencing with subsequent V-gene analysis and CDR comparison using the VBASE2 tool (Mollova et al., 2010), revealed the isolation of 36 unique scFvs /monoclonal antibodies (mAbs) (Table 3-2).

The distribution of the V genes used, as well as the ratio of lambda and kappa antibodies was determined: Of the 36 antibodies 15 (41 %) are IGHV1, 18 (50 %) IGHV3, two (5,5 %) IGHV5 and one IGHV6. No IGHV2, IGHV4 or IGHV7 antibodies were isolated. Even though the lambda- and kappa antibody libraries HAL9 and HAL10 were used in equal amounts in a pooled approach, the majority (29) of the isolated antibodies contain a lambda light chain (9x IGLV1, 10x IGLV2, 8x IGLV3, 2x IGLV6) and only 7 antibodies (18,9 %) a kappa light chain (2x IGKV1, 5x IGKV3).

Table 3-2 Germline distribution of selected scFvs

#	mAb name	V VH	D VH	J VH	V VL	J VL
1	ViF087_A10	IGHV1-18*01	IGHD3-3*01	IGHJ4*02	IGLV1-44*01	IGLJ3*02
2	ViF087_B1	IGHV3-30*04	IGHD3-10*01inv	IGHJ6*02	IGLV1-47*01	IGLJ3*02
3	ViF087_B10	IGHV1-46*03	not found	IGHJ6*02	IGKV3-20*01	IGKJ4*01
4	ViF087_E1	IGHV1-69*01	IGHD2-2*01	IGHJ4*02	IGKV3-15*01	IGKJ1*01
5	ViF087_E7	IGHV1-18*01	IGHD1-26*01	IGHJ3*02	IGKV1-12*02	IGKJ4*01
6	ViF087_F1	IGHV3-33*01	IGHD4-17*01	IGHJ2*01	IGLV3-19*01	IGLJ3*01
7	ViF087_F3	IGHV1-3*01	IGHD5-12*01	IGHJ5*02	IGLV2-18*02	IGLJ3*02
8	ViF087_G10	IGHV1-69*01	IGHD3-22*01	IGHJ5*02	IGLV1-47*01	IGLJ3*02
9	ViF087_G11	IGHV3-30*01	IGHD4-17*01	IGHJ4*02	IGLV3-19*01	IGLJ3*01
10	ViF087_H5	IGHV1-46*03	IGHD4-17*01	IGHJ4*02	IGLV2-14*01	IGLJ3*02
11	ViF088_C5	IGHV3-13*01	IGHD3-16*01	IGHJ4*02	IGLV6-57*01	IGLJ3*01
12	ViF088_E10	IGHV3-30*18	IGHD6-13*01inv	IGHJ6*03	IGLV3-19*01	IGLJ3*02
13	ViF088_H10	IGHV3-33*01	IGHD3-10*01	IGHJ3*02	IGLV1-51*01	IGLJ3*02
14	ViF090_A6	IGHV1-69*01	IGHD2-15*01	IGHJ4*02	IGLV6-57*01	IGLJ3*02
15	ViF090_G5	IGHV1-3*01	IGHD5-12*01	IGHJ5*02	IGLV2-14*01	IGLJ3*01
16	ViF091_B10	IGHV1-69*06	IGHD2-21*01	IGHJ5*02	IGLV1-44*01	IGLJ3*02
17	ViF137_A3	IGHV3-23*04	IGHD6-19*01	IGHJ3*02	IGKV3-20*01	IGKJ4*01
18	ViF137_A6	IGHV3-7*01	IGHD6-13*01	IGHJ4*02	IGLV3-21*02	IGLJ3*01
19	ViF137_A9	IGHV5-51*01	IGHD1-14*01	IGHJ3*02	IGLV2-8*01	IGLJ3*02
20	ViF137_C1	IGHV3-23*04	IGHD5-5*01	IGHJ6*02	IGLV2-8*01	IGLJ3*01
21	ViF137_C2	IGHV3-23*01	IGHD5-18*01	IGHJ4*02	IGLV1-47*01	IGLJ3*02
22	ViF137_C3	IGHV1-69*01	IGHD6-13*01	IGHJ5*02	IGLV2-8*01	IGLJ3*01
23	ViF137_E4	IGHV3-21*01	IGHD6-19*01	IGHJ6*02	IGLV2-11*01	IGLJ3*02
24	ViF137_E7	IGHV5-51*01	IGHD1-1*01	IGHJ3*02	IGLV2-14*01	IGLJ3*02
25	SH1429_B1	IGHV1-3*01	IGHD5-12*01	IGHJ5*02	IGLV2-14*04	IGLJ1*01
26	SH1429_B10	IGHV3	IGHD2-8*02inv	IGHJ3*02	IGKV3-20*01	IGKJ2*01
27	SH1429_C10	IGHV3	IGHD2-15*01	IGHJ6*02	IGLV2-8*01	IGLJ3*02
28	SH1429_D6	IGHV6	IGHD2-2*03inv	IGHJ3*02	IGLV3-19*01	IGLJ1*01
29	SH1429_G1	IGHV3	IGHD2-2*02inv	IGHJ3*02	IGKV3-20*01	IGKJ4*01
30	SH1429_G6	IGHV1-18*01	IGHD3-3*01	IGHJ4*02	IGLV1-40*01	IGLJ3*02
31	SH1429_H7	IGHV3	IGHD6-19*01	IGHJ4*02	IGLV1-47*01	IGLJ3*01
32	ViF087_C12	IGHV3-48*03	IGHD3-3*01	IGHJ3*02	IGLV3-19*01	IGLJ3*02
33	ViF137_A1	IGHV1-2*02	IGHD4-17*01	IGHJ5*02	IGLV1-51*01	IGLJ3*01
34	ViF137_A5	IGHV3-30*04	IGHD5-12*01	IGHJ4*02	IGLV3-19*01	IGLJ3*01
35	ViF137_D1	IGHV1-2*02	IGHD6-13*01	IGHJ4*02	IGKV1-5*01	IGKJ1*01
36	ViF137_D4	IGHV3-23*04	IGHD4-23*01	IGHJ4*02	IGLV3-19*01	IGLJ3*01
Antibodies not included in further characterization						

Compared to the small scFv format that is well suitable for phage display and production in *E. coli*, the scFv-Fc format has some advantages for antibody characterization. First it has a higher apparent affinity, second it can be easily purified by Protein A affinity chromatography from mammalian cell culture production supernatant. To enable the production of monoclonal antibodies in HEK293-6E cells in an scFv-Fc format with a human IgG1 Fc part, the scFv genes were cloned into the mammalian expression vector pCSE2.6-hIgG1-Fc-XP. The success of cloning was verified by colony PCR and sanger sequencing (data not shown).

The plasmid DNA was transfected into HEK293-6E cells or Expi293F™ cells for transient production for a time period of seven days in suspension culture. The antibodies were purified from the culture supernatant by protein A affinity chromatography.

The purity and integrity of the scFv-Fc preparations was controlled by reducing SDS-PAGE with subsequent Coomassie staining (representative example given in Figure 3-3Figure 3-3: Coomassie stained SDS PAGE of purified scFv-Fc antibodies). As expected, all antibodies had an apparent molecular weight of ~ 60 kDa. They run in the SDS-PAGE as multiple bands, which is due to glycosylation. Since there were no visible impurities or breakdown products of the scFv-Fcs, the degree of purity of the antibody preparations was above 95 %.

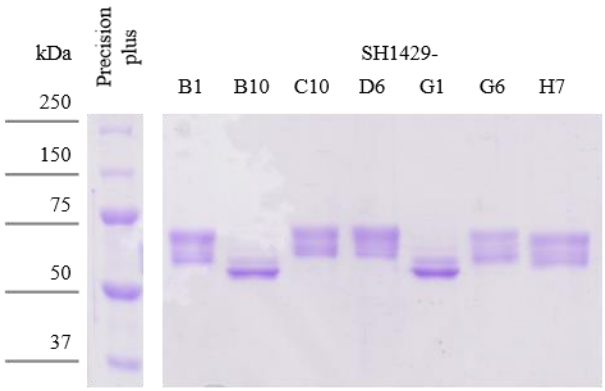

Figure 3-3: Coomassie stained SDS PAGE of purified scFv-Fc antibodies

Antibodies from panning on TcdBFL (Panning SH1429) were produced in HEK293-6E cells in 5 mL scale as scFv-hIgG1-Fc. Antibodies were purified from the supernatant by protein A affinity chromatography. 0,5 µg of the respective antibody was applied to a 12% polyacrylamide gel under reducing conditions. After electrophoresis proteins were stained using Coomassie blue staining solution.

The produced scFv-Fc antibodies were used in further experiments to characterize the antibody antigen interaction and functional cell-based assays to test antigen neutralization.

3.2.2 Validation of antigen binding and domain mapping

Thirty-one of the 36 generated mAbs were successfully produced in scFv-Fc format and further analyzed by titration ELISA. This ELISA was designed to verify that format change from scFv to the bivalent scFv-Fc did not impair antigen recognition, second, to analyze $TcdB_{FL}$ binding of antibodies that were generated on TcdB fragments, third, to validate antibody specificity and fourth, to determine the binding domains or regions of the respective mAbs. Therefore, the binding to four different TcdB variants ($TcdB_{FL}$, $TcdB_{1-1852}$, $TcdB_{GTD}$ and $TcdB_{CROPs}$) as immobilized antigens was addressed in this ELISA (Figure 3-4, Table 3-5).

In this ELISA setup, all mAbs bound to their respective panning TcdB variant in a concentration dependent manner: The mAbs derived from the panning on $TcdB_{1-1852}$ (ViF087, ViF088, ViF090 and ViF091) also bound $TcdB_{1-1852}$ after format change. For the antibodies generated on $TcdB_{CROPs}$ (ViF137), the binding to the CROPs domain was validated and the antibodies originating from the panning on $TcdB_{FL}$ still bound to full-length toxin. However, the antibodiesViF137_C3 (Figure 3-4 H) and SH1429_B10 (Figure 3-4 I) showed a very weak binding in ELISA.

The antibodies were also tested on $TcdB_{FL}$ as antigen, since epitopes that might be accessible in TcdB fragments might be shielded by parts of the protein in $TcdB_{FL}$. Also, the overall folding of different TcdB variants might be different. Interestingly, almost no binding to $TcdB_{FL}$ was detected for some mAbs [ViF087_G11, ViF087_H5 (Figure 3-4 A), ViF088_C5, ViF088_E10 and ViF137_C2 (Figure 3-4 E)] despite of binding to the panning antigen. For further antibodies [ViF087_A10, ViF087_B1, ViF087_B10, ViF087_F1 (Figure 3-4 A), ViF091_B10, ViF137A9 and ViF137_C1 (Figure 3-4 E)] the binding to $TcdB_{FL}$ was notably reduced (≤50% signal intensity at highest concentration) compared to the respective panning TcdB variant.

To validate domain specificity, the antibodies derived from pannings on the N-terminal fraction of TcdB were tested for binding on the C-terminal CROPs domain and vice versa. As expected, there was no binding to $TcdB_{1-1852}$ or $TcdB_{GTD}$ of mAbs that were generated by panning against $TcdB_{CROPs}$ [mAbs ViF137 (Figure 3-4 F, G)] and no binding to $TcdB_{CROPs}$ of mAbs that were generated by panning against $TcdB_{1-1852}$ [mAbs ViF087, ViF088, ViF090 and ViF091_B10 (Figure 3-4 D, H)] proving domain specificity of the mAbs generated in this study.

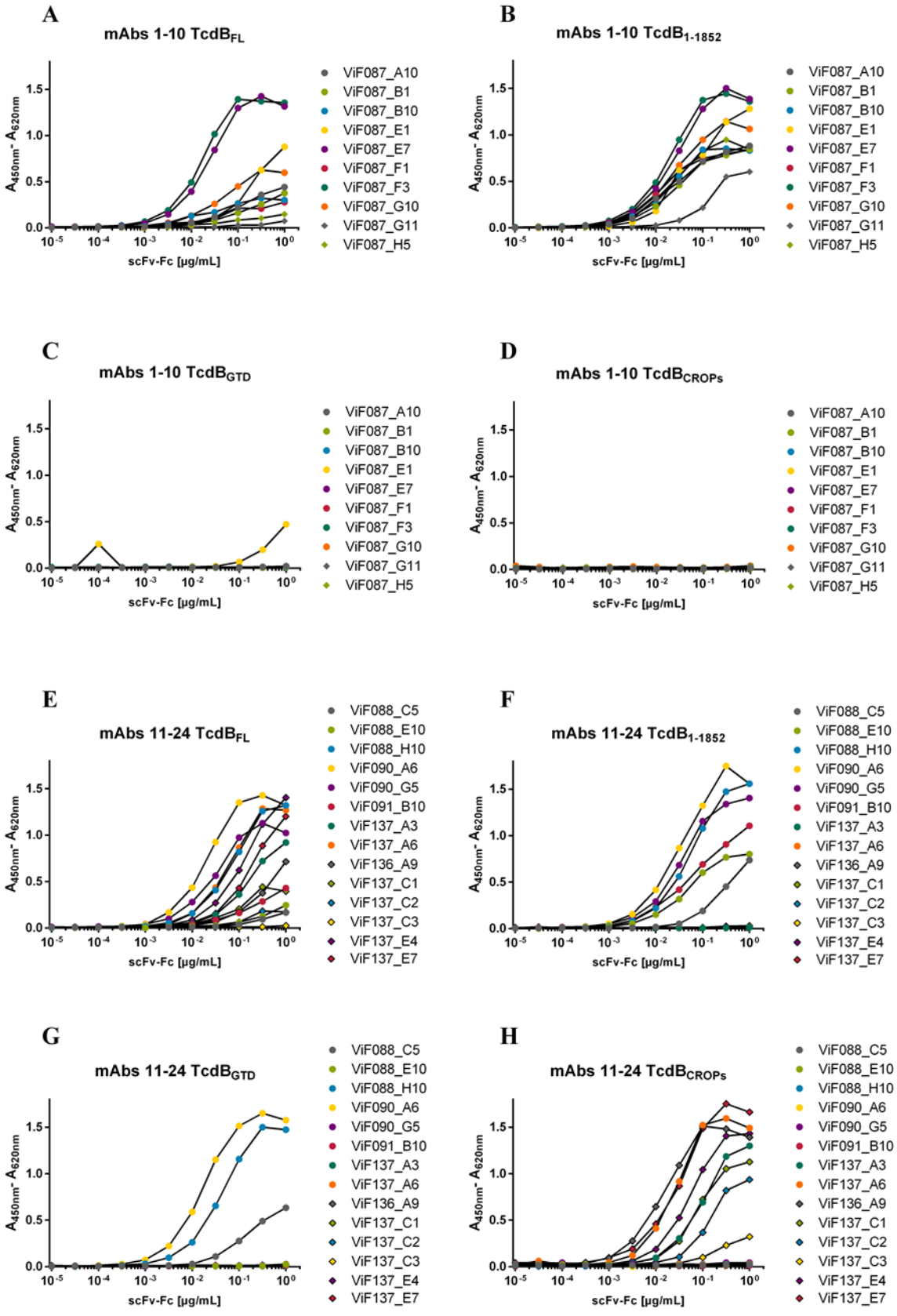
A
mAbs 1-10 TcdB$_{FL}$
B
mAbs 1-10 TcdB$_{1-1852}$
C
mAbs 1-10 TcdB$_{GTD}$
D
mAbs 1-10 TcdB$_{CROPs}$
E
mAbs 11-24 TcdB$_{FL}$
F
mAbs 11-24 TcdB$_{1-1852}$
G
mAbs 11-24 TcdB$_{GTD}$
H
mAbs 11-24 TcdB$_{CROPs}$
A$_{450nm}$- A$_{620nm}$
scFv-Fc [µg/mL]
ViF087_A10
ViF087_B1
ViF087_B10
ViF087_E1
ViF087_E7
ViF087_F1
ViF087_F3
ViF087_G10
ViF087_G11
ViF087_H5
ViF088_C5
ViF088_E10
ViF088_H10
ViF090_A6
ViF090_G5
ViF091_B10
ViF137_A3
ViF137_A6
ViF136_A9
ViF137_C1
ViF137_C2
ViF137_C3
ViF137_E4
ViF137_E7

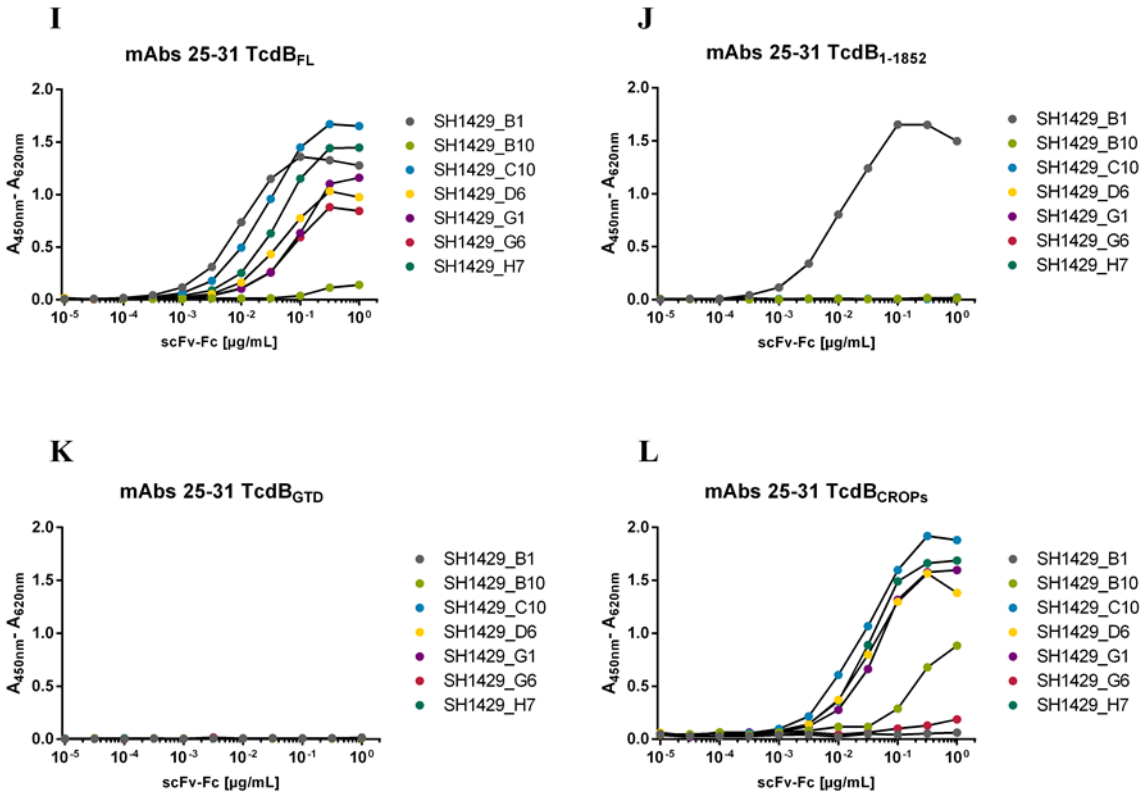

Figure 3-4: Titration ELISA on TcdB variants:

31 mAbs were tested for binding on 100 ng immobilized TcdB variants. Bound scFv-Fcs were detected using a HRP conjugated anti- human Fcγ antibody (Sigma Aldrich, A0170, 1: 70,000 in MPBST). ***A, E, I:*** *Titration on TcdB$_{FL}$;* ***B, F, J:*** *Titration on TcdB$_{1-1852}$;* ***C, G, K:*** *TcdB$_{GTD}$ was used as antigen;* ***D, H, L:*** *Titration on TcdB$_{CROPs}$*

Of the 31 mAbs tested in this assay, 14 bound to TcdBCROPs, among them all antibodies derived from the panning against TcdBCROPs [mAbs ViF137 (Figure 3-4 H)], as well as the majority of the antibodies derived from the panning against TcdBFL [SH1429_B10, SH1429_C10, SH1429_D6, SH1429_G1, SH1429_G6 (only very weak) and SH1429_H7 (Figure 3-4 L)].

Four mAbs [ViF087_E1, ViF088_C5, ViF088_H10 and ViF090_A6 (Figure 3-4 C, G)] bound to TcdB$_{GTD}$ in a concentration dependent manner indicating an epitope within the GTD domain of TcdB. The remaining 13 antibodies bound to immobilized TcdB$_{1-1852}$, but not to TcdB$_{GTD}$. Therefore, it is likely that these antibodies bind to epitopes between aa 543 and aa 1852, but due to possible differences in protein folding between the different TcdB variants, and the two amino acids exchanged in TcdB$_{GTD}$ compared to wt sequence used in TcdB$_{1-1852}$, a lack of TcdB$_{GTD}$ binding in this experiment is not sufficient to exclude an epitope within this domain.

3.3 *In vitro* neutralization

In this study 31 unique antibodies against TcdB were generated and binding validated by antigen ELISA. But mere antigen binding is not an indicator for TcdB neutralization. However, for possible further clinical development of the antibodies potent TcdB neutralization is required. Additionally, neutralizing and to some extend also non-neutralizing antibodies can be of great value to gain deeper understanding of the toxin's mode of action, especially when the respective epitopes or binding regions of the antibodies are known.

To address the neutralization capacity of the antibodies, they were tested for *in vitro* neutralization of TcdB. Therefore, a cell-based assay with Vero cells was used. This assay is based on the cell rounding induced by TcdB: Upon cellular uptake of TcdB and release of the glucosyltransferase domain to the cytosol, the glucosyltransferase domain glucosylates small Rho GTPases which impairs several cell-signaling pathways and consequently leads to a breakdown of the actin cytoskeleton. This effect includes morphological changes like the formation of retraction fibers and finally the typical TcdB induced-cell rounding (see Figure 3-5). The cell rounding was also used as read out for this assay.

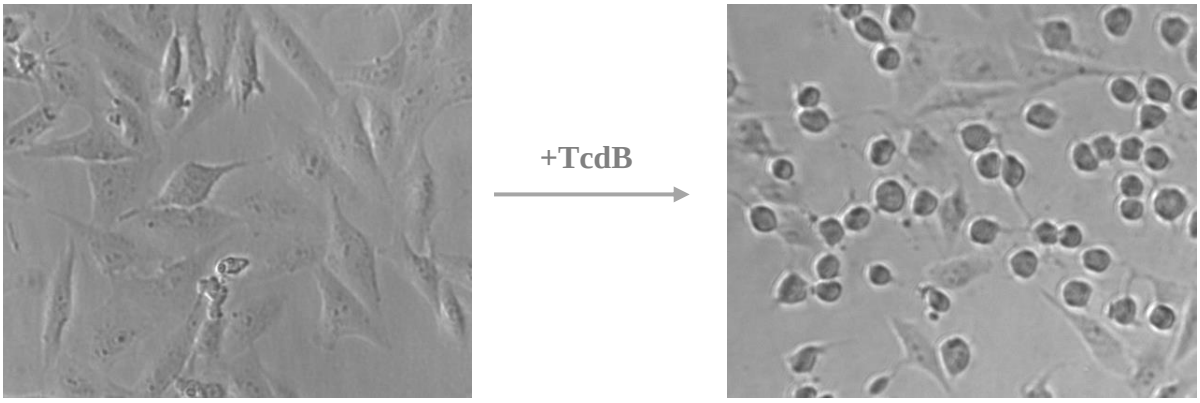

Figure 3-5: TcdB induced cell rounding of Vero cells

Left panel: Vero cells cultivated with supplemented RPMI medium. Right panel: Vero cell treated with 0,1 pM TcdB

Neutralization efficacy of an antibody was analyzed by comparing percentage of round cells in samples of cells treated with TcdB only to cells treated with TcdB preincubated with an antibody.

3.3.1 TcdB induces concentration dependent cell rounding of Vero cells

In a first test, the optimal working concentration of $TcdB_{FL}$ for this assay had to be determined. Therefore, a serial dilution of TcdB was prepared in culture media and applied to Vero cells. After 5 h of intoxication pictures of the cells were collected and the percentage of round cells was determined. Cell rounding was correlating with $TcdB_{FL}$ concentration (see Figure 3-6).

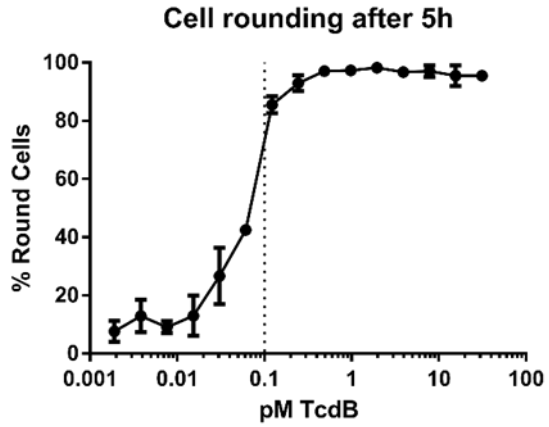

Figure 3-6: In vitro intoxication of Vero cells using a serial dilution of $TcdB_{FL}$

For following neutralization experiments a $TcdB_{FL}$ concentration of 0.1 pM (a concentration corresponding to ~ 80% cell rounding) was used. To be able to also notice slight neutralization effects mediated by the antibodies a concentration of TcdB that is beyond saturation was chosen.

3.3.2 Antibody mediated inhibition of TcdB induced cell rounding

To test if the antibodies generated in this study confer *in vitro* neutralization of TcdB, 0.1 pM of the active full-length toxin was coincubated with 100 nM mAb in cultivation media. After preincubation to give time to establish an antibi antigen binding the mixture was transferred to Vero cells. When cell rounding in control wells (TcdB w/o antibody) was ~80% pictures of the cells were collected. To determine neutralization efficacy, the percentage of round cells was determined and normalized to the percentage of round cells in the control wells (Vero cells w/o $TcdB_{FL}$ and Vero cells with $TcdB_{FL}$ w/o mAb).

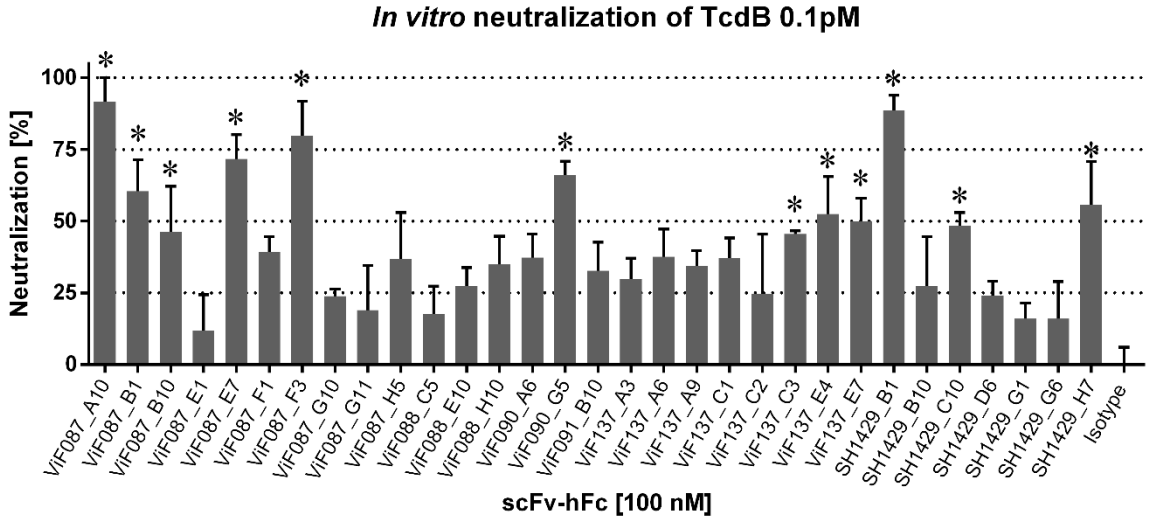

Figure 3-7: Screening for in vitro TcdB neutralization:

*Initial screening for neutralization using all 31 mAbs in a 10,000-fold molar excess. Bars represent technical triplicates with SD as error bars. A one-way ANOVA test was performed for each antibody against the isotype control TM43_E10 (Kügler et al., 2015). *: p <0.0001*

In a first screening for neutralization including all 31 antibodies that were further characterized in this study, all mAbs reduced the percentage of round cells after TcdB treatment to some extent, thus all antibodies had at least slight neutralizing effects. However, significant neutralization was achieved with 12 out of 31 mAbs ($p < 0.0001$) (Figure 3-7).

For five antibodies (ViF087_B1, ViF087_E7, ViF090_G5, ViF137_E4 and SH1429_H7) preincubation of TcdB with either one of them resulted in more than 50 % neutralization. Best *in vitro* neutralization of TcdB was achieved using ViF087_A10, ViF087_F3 and SH1429_B1 (>75 % reduction of cell rounding).

To validate the efficient $TcdB_{FL}$ neutralization of ViF087_A10 and SH1429_B1 and to be able to estimate IC_{50} values of these mAbs in this assay, a serial dilution was performed (Figure 3-8). ViF087_F3 was not included since it contains the same heavy chain as SH1429_B1 which suggests a neutralization via the same epitope. Furthermore, size exclusion chromatography revealed partial aggregation of ViF087_F3, which is not the case for SH1429_B1 (Supplementary Figure 7-1).

The dilution series confirmed the results of the neutralization screening. At the starting concentration of 100 nM ViF087_A10 and SH1429_B1 nearly completely inhibited the cell rounding induced by $TcdB_{FL}$ intoxication (Figure 3-8). However, the dilution series revealed that SH1429_B1 is roughly ten times more potent than ViF087_A10, since 0.1 nM SH1429_B1 were sufficient to reduce cell rounding by ~50% whereas 1 nM of ViF087_A10 was needed to achieve a comparable effect.

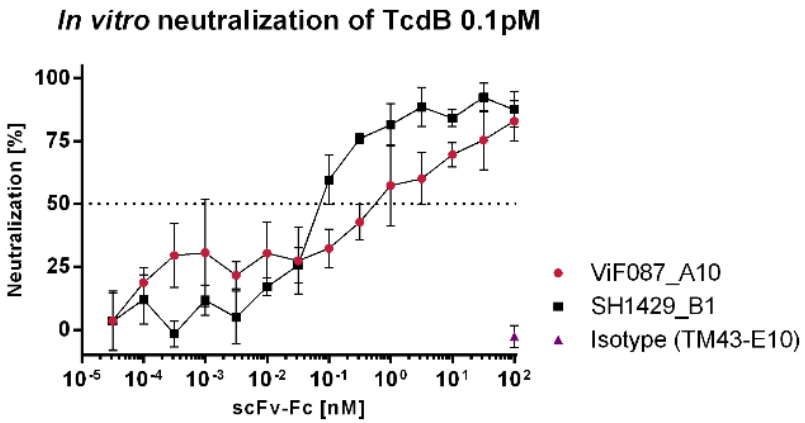

Figure 3-8:Validation of in vitro TcdB neutralization for ViF087_A10 and SH1429_B1

IC_{50} values of ViF087_A10 and SH1429_B1 were estimated with serial antibody dilutions.

In a next assay a combination of ViF087_A10 and SH1429_B1 was used to neutralize $TcdB_{FL}$ in an *in vitro* assay, but neutralization achieved with this combination was not stronger as for SH1429_B1 alone (data not shown).

3.3.3 Inhibition of TcdB induced cell rounding using antibody combinations

Unlike Bezlotoxumab, the human anti- TcdB antibody already approved by the FDA for therapy of recurrent CDI (Navalkele and Chopra, 2018), the two most potent neutralizing antibodies generated in this study (ViF087_A10 and SH1429_B1) bind to epitopes within $TcdB_{1-1852}$ (Figure 3-4 B, J). Bezlotoxumab binds to two epitopes within the CROPs which are involved in cell binding via carbohydrate structures (Orth et al., 2014) and or inhibition of binding to CSPG4 (Gupta et al., 2017), proving that neutralization via this repetitive domain is feasible. However, three cellular receptors of TcdB are described that bind to $TcdB_{TLD}$, with members of the frizzled family, which bind to $TcdB_{1285-1804}$ (aa 1285-1804 contain the FZD binding site, with amino acids between position 1430 and 1600 directly involved in protein-protein interaction) with an affinitiy of 13 nM (Chen et al., 2018; Gupta et al., 2017; LaFrance et al., 2015; Tao et al., 2016; Yuan et al., 2015). Hence, it might be possible that the anti-$TcdB_{CROPs}$ antibodies generated in this study reduce CROPs mediated binding of TcdB to the cell surface, but that TcdB induced cell rounding is not reduced, because of the numerous compensation mechanisms, mediated by the additional cell surface receptors. In this case a combination of the mAbs directed against $TcdB_{CROPs}$ with mAbs that bind to the N-terminal domains could lead to improved neutralization and synergistic effect. To test this hypothesis, combinations of either ViF087_A10 or SH1429_B1 with mAbs directed against $TcdB_{CROPs}$ were tested in an *in vitro* TcdB neutralization assay. Therefore 0,1 pM of TcdB was preincubated with 1 nM ViF087_A10 or 0,1 nM SH1429_B1 [the concentration needed for ~50% TcdB neutralization as determined by titration (Figure 3-8)] and 100 nM of either of the 14 anti- $TcdB_{CROPs}$ mAbs for 30 min at room temperature and then transferred to Vero cells. TcdB neutralization for each antibody combination was compared to neutralization achieved with ViF087_A10, or SH1429_B1 alone in the same assay, as well as with neutralization achieved in the first screening.

Neutralization mediated by 1 nM ViF087_A10 in this assay was 41%. Addition of a second mAb directed against $TcdB_{CROPs}$ in a concentration of 100 nM increased neutralization. The highest total neutralization for ViF087_A10 was in combination with ViF137_E4 (73%), SH1429_C10 (70%) and SH1429_H7 (66%) (Figure 3-9 A).

For SH1429_B1, 0,1 nM mAb reduced cell rounding by 49%. As for ViF087_A10, addition of 100 nM of an anti- $TcdB_{CROPs}$ mAb increased neutralization and best neutralizing with SH1429_B1 was achieved in combination with the same $TcdB_{CROPs}$ binders as for ViF087_A10, namely ViF137_E4 (79%), SH1429_C10 (78,9%) and SH1429_H7 (83,6%) (Figure 3-9 B).

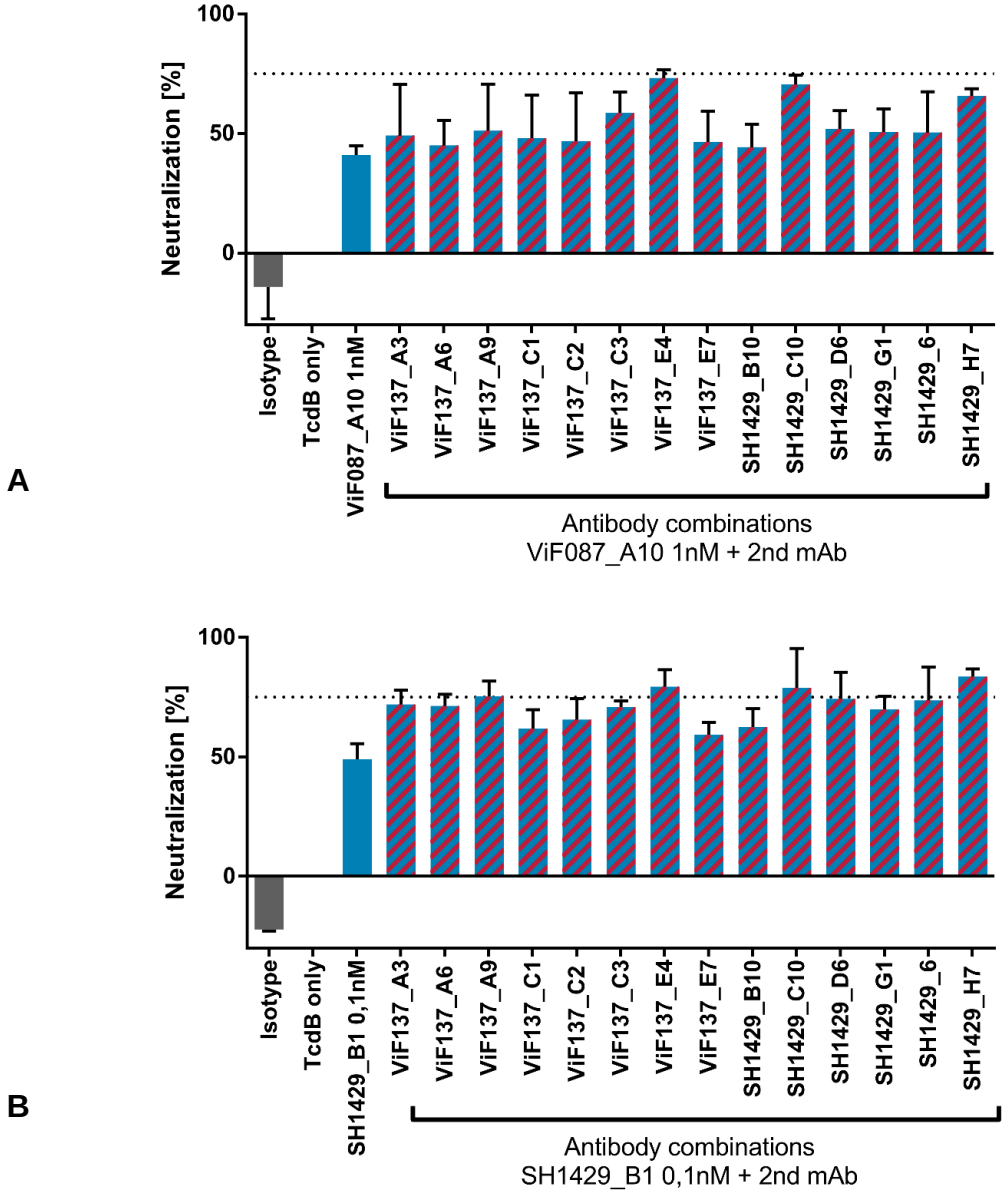

Figure 3-9: In vitro TcdB neutralization using antibody combinations

*In vitro neutralization assay of 0,1pM TcdB using antibody combinations. TcdB and either 1 nM of ViF087_A10 **(A)** or 0,1 nM SH1429_B1 **(B)** mAbs were coincubated in cultivation media with 100 nM of CROPs binding mAbs.*

Remarkably, the anti- $TcdB_{CROPs}$ mAbs leading to the highest increase of neutralization with either ViF087_A10 or SH1429_B1 in this assay were same mAbs that already showed best neutralization among $TcdB_{CROPs}$ binders in the initial screening as single antibodies (ViF137_E4 53%, SH1429_C10 48%, SH1429_H7 56%). Therefore, the increase of neutralization in this combinatory assay was based on additive- rather than synergistic effects.

3.4 Epitope mapping

For future rational development of toxin neutralizing antibodies as therapeutics for CDAD, or TcdB fragments as vaccines, more information about potential neutralizing epitopes is required. To identify the epitopes of ViF087_A10 and SH1429_B1 that elicit neutralization, as well as to gain more information about the binding sites of the remaining antibodies, three different assays were performed, that, taken together, provide deep information about the antibody-antigen interaction and the nature and location of the antibodies' epitopes.

3.4.1 Epitope characterization by test of antibodies in immunoblots

The first assay addressed the question what kind of epitopes the antibodies bind. In general, epitopes can be classified as linear or conformational epitopes. Linear epitopes consist of a continuous stretch of aa on the primary structure, therefore binding of the antibody to a linear epitope does not depend on protein folding. If the antibody binding to its epitope requires protein folding the epitope is designated conformational. Conformational epitopes can be either continuous or discontinuous, which refers to the positioning of the contributing amino acids on the primary structure. Upon protein folding, amino acids that are located far apart on the primary structure can come into close proximity and thus build discontinuous epitopes.

Upon heating in SDS and ß-Mercaptoethanol containing buffer, the proteins are denatured and therefore discontinuous epitopes as well as, at least partially, continuous conformational epitopes are destroyed. Hence, testing the antibody binding to denatured protein transferred to a PVDF membrane by western blotting can give valuable information about the nature of an antibody's epitope.

Hence, 5 µg of the TcdB variants were analyzed under denaturing and reducing conditions in SDS-PAGE followed by western blotting and immunostaining. An exemplary result of an immunostaining is given in Figure 3-10 and the overall results are summarized in Table 3-5.

Of the seventeen antibodies binding to $TcdB_{1\text{-}1852}$ only two ViF088_H10 and ViF090_A6 bound to denatured TcdB variants (see Figure 3-10). For eight mAbs mixed results were obtained, either the binding was very weak, or not all TcdB variants tested were bound. For another seven antibodies against $TcdB_{1\text{-}1852}$ there was no binding to denatured TcdB at all.

Of the 14 antibodies binding to $TcdB_{CROPs}$ only one did not bind to denatured TcdB whereas the remaining 13 did (data not shown).

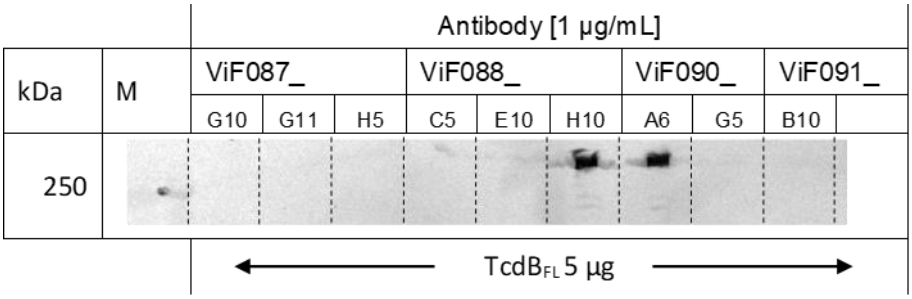

Figure 3-10: Immunoblot staining of $TcdB_{FL}$

SDS and ß Mercaptoethanol treated $TcdB_{FL}$ was applied to an SDS gel and after electrophoresis transferred to a PVDF membrane. Blotted protein was detected using various mAbs from this study as primary- and an AP conjugated anti-human Fc-antibody as secondary antibody. The immunoblot was developed using NBT/BCIP substrate. From the panel of mAbs shown here, ViF088_H10 and ViF090_A6 bound strongly to denatured $TcdB_{FL}$. There might also be very slight binding of ViF088_C5, but this is regarded as an unclear

Whilst most antibodies directed against the N-terminal fraction of TcdB seem to bind conformational epitopes, the antibodies against the C-terminal CROPs most likely bind to linear epitopes.

3.4.2 Epitope mapping by peptide array

As a first approach for epitope mapping, a peptide array was used, which enables parallelized epitope screening for a larger number of antibodies. Disadvantage of this method is that discontinuous epitopes cannot be mapped and also conformational epitopes can be problematic, because of the limited size of the peptides. For this study 15 mer peptides were used which at least allow the formation of α-helical structures. Also, due to very high local concentraions of the spotted peptides, the sensitivity of this assay might be higher than the immunoblot analysis.

The arrays were spotted with peptides of TcdB with an offset of two amino acids (example given in Table 3-3). The experiment was performed in collaboration with Jasmin Heidepriem and data evaluation with Dr. Felix Loeffler (Max Planck Institute of Colloids and Interfaces).

Table 3-3: Layout of the peptide array

Amino acids of TcdB	Row	column	Peptide Sequence
414- 428	8	14	LNPAISEDNDFNTTT------
416- 430	8	15	--PAISEDNDFNTTTNT----
418- 432	8	16	----ISEDNDFNTTTNTFI--
420- 434	8	17	------EDNDFNTTTNTFIDS

All antibodies were tested at a concentration of 1 µg/mL. For a significant number of antibodies signal intensity was very low with this concentration or there were no signals detectable at all. In these cases, incubation with primary and secondary antibody was repeated at a concentration of the primary antibody of 100 µg/mL. Unfortunately, this approach was not successful for most antibodies or results were difficult to interpret. One such example is mAb ViF087_B10. The 15 peptides that showed strongest binding include four neighboring peptides starting at aa positions 288, 290, 292 and 294, so this region was highly overrepresented in the top hits. Nevertheless, this antibody seemed to have a broader cross-specificity as the remaining 11 peptides originated from different regions of the toxin and didn`t have common features (see Supplementary Table 7-1).

Nevertheless, the two neutralizing antibodies ViF087_A10 and SH1429_B1 both specifically bound to five 15 mer peptides starting between aa 414 and 422. ViF087_A10 also interacted with two further peptides starting at aa 402 and 404 (Figure 3-11).

MAb ViF087_E1 strongly, but not exclusively, bound to a peptide that spans aa 522-537 (Supplementary Table 7-2).

Two antibodies (ViF137_A9 and ViF137_E7) reacted with three and four clusters of peptides within the CROP domain (aa 1858-1869, 2084-2095, 2216-2227 and aa 1860-1867, 2084-2093, 2218-2225, 2236-2249 respectively) (Figure 3-11). These clusters contain a common motif which probably reassembles the key amino acids necessary for antibody-antigen interaction [KYYF† († =D or N) and *KYYF† (*=I, S or D; † =D or N), respectively] (Supplementary Table 7-2).

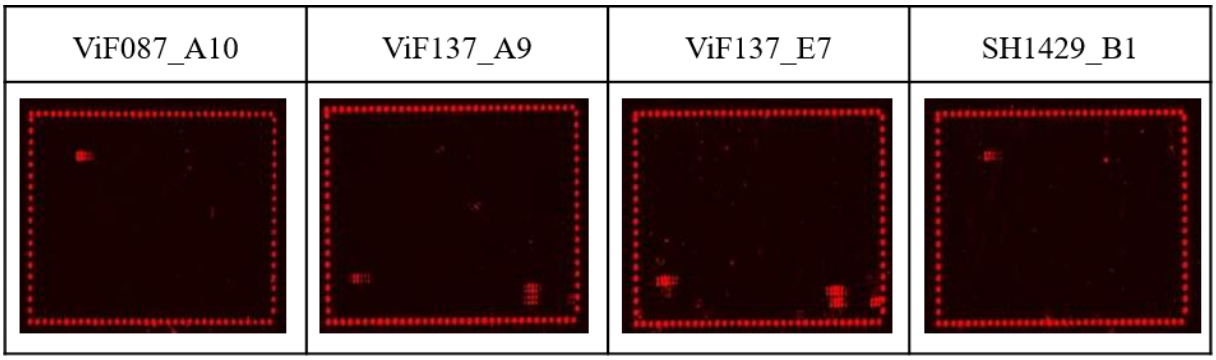

Figure 3-11: Exemplary results of the peptide array:

Result of the peptide array exemplary shown for four of the 31 antibodies tested. ViF087_A10 and SH1429_B1 react with a cluster of peptides within the GTD domain. ViF137_A9 and ViF137_E7 bind to three clusters of peptides within the CROPs

Further antibodies that, according to the ELISA, were directed against the CROPs, namely ViF137_A3, ViF137_A6, ViF137_C3, SH1429_C10, SH1429_D6 and SH1429_G1 reacted with peptides derived from the CROPs. But the result of the peptide array was difficult to interpret, since they did not exclusively bind to only one cluster of neighboring peptides but showed a higher degree of cross-specificity or tolerance of aa substitutions, therefore epitope identification only by peptide array was not feasible for these antibodies.

3.4.3 Epitope mapping by phage display

To confirm the epitopes regions found by peptide array and to identify further epitopes or at least binding regions of the remaining antibodies a second, independent approach was chosen for epitope mapping, namely TcdB-fragment phage-display. This approach has the advantage that also larger TcdB-fragments (>100 aa) can be displayed on the phage, therefore the chance to also map conformational or even discontinuous epitopes is higher.

To generate a TcdB-fragment phage display library, the tcdB-gene was amplified from genomic DNA of *C. difficile* strain 630 and the amplicon was fragmented. As analyzed by agarose gel electrophoresis, sonication led to DNA fragments of ~ 100- 400 bp in size (Figure 3-12).

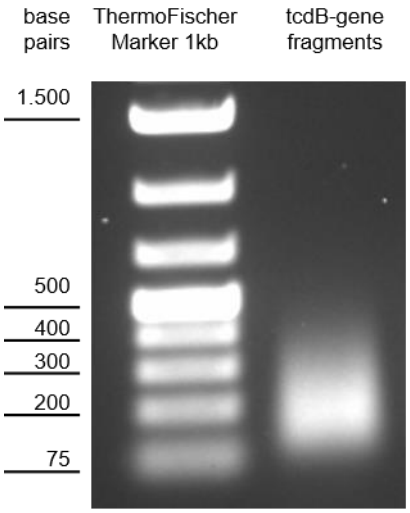

Figure 3-12: Analysis of DNA fragmentation after sonication

An aliquot of fragmented DNA was applied to a 2% Agarose gel. Fragmentation using the Bioruptor sonicator system led to tcdB fragments ranging from ~100 -400 bp in length.

After blunt end polishing, DNA fragments were ligated into pHORF3 vector that was subsequently used for transformation of electrocompetent *E. coli* (strain TOP10F'). Electroporation led to transformation of 1,9 x 10^7 independent clones.

Due to the undirected blunt end cloning and the random fragmentation of the amplified tcdB gene, in theory only 1 out of 18 clones obtained by electroporation would carry a tcdB-fragment- gIII fusion that leads to expression of a functional fusion protein [50% right orientation, 33% thereof correct reading frame of the insert, 33% thereof right insert length (3n+1) to get the signal sequence and gIII in the same reading frame].

Hence, the tcdB-gene fragment library was packaged with Hyperphage (M13K07ΔgIII), missing a functional gIII. Consequently, pHORF3 plasmids with a tcdB insert of 3n+1 nucleotides and without stop codons were the sole source of functional gIII, which led to an enrichment of correct open reading frames (Table 3-4).

After purification of TcdB-fragment phage, a test infection of an *E. coli* XL1 blue MRF' culture at an $O.D._{600\ nm}$ of 0,5 was performed. Infected *E. coli* clones were thinned out and 92 randomly picked single clones were sequenced to analyze insert size, ORF enrichment and TcdB coverage of the library after packaging into phage. A summary of the library characterization is given in Table 3-4. The library characterization was performed in collaboration with Philip Heine.

Table 3-4: Characterization of TcdB-fragment library

Library size (independent clones, before packaging)	1,9 x 10^7	
In frame insert rate after packaging	65%	
Mean insert length	39 aa	data of packaged library before panning
Shortest TcdB fragment found	13 aa	
Longest TcdB fragment found	73 aa	

Sequencing revealed, that ORF enrichment was successful: sixty out of the 92 clones (65%) carried correct inserts within the pHORF3 plasmids, allowing expression of functional TcdB-fragment-pIII fusions. Also the TcdB-protein coverage was addressed, therefore the translated DNA sequences of all 60 clones carrying functional TcdB-fragment pIII fusions were aligned to the TcdB aa sequence (see Supplementary Figure 7-2). A complete coverage was not achieved with this limited number of clones, but fragment distribution was rather even.

The TcdB-fragment library was used for pannings on immobilized mAbs and/or pannings in solution. The pannings were performed together with Philip Heine. For the pannings in solution, the TcdB-fragment phage bound to the respective mAb were separated from unbound phage by immunoprecipitation using protein A coupled magnetic beads.

The isolated phage were used to infect *E. coli* in logarithmic growth phase. Successfully infected *E. coli* clones were selected with the help of an ampicillin resistance mediated by the pHORF3 plasmid. *E. coli* clones, carrying tcdb-gene fragments coding for the potential epitope region were identified by monoclonal phage ELISA on immobilized mAbs.

For 18 out of 31 mAbs the screening ELISA resulted in the identification of monoclonal, TcdB- fragment presenting phage that specifically bound to the corresponding anti- TcdB-antibody but not to an irrelevant control antibody (exemplary shown for SH1429_C10 in Figure 3-13).

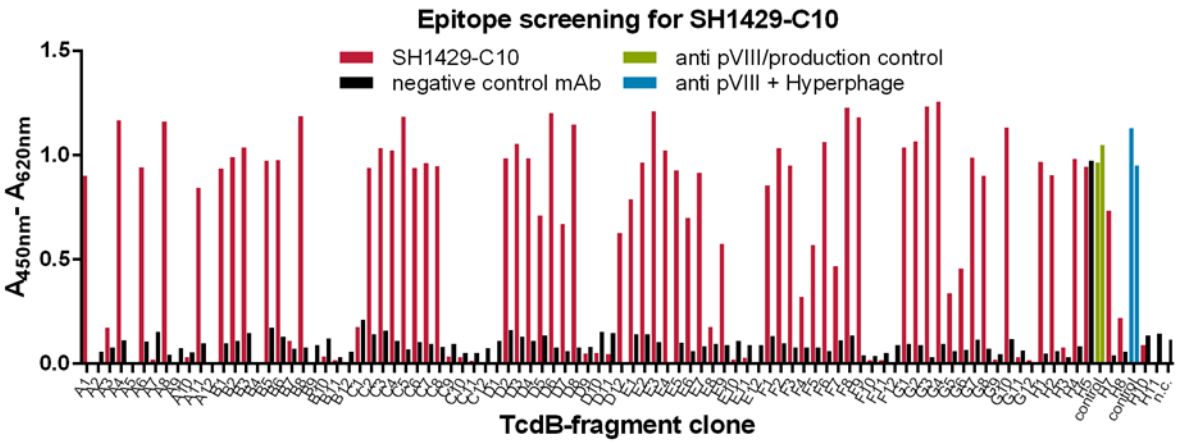

Figure 3-13: Screening ELISA after TcdB-fragment panning for SH1429_C10

93 clones were screened for production of TcdB-fragment phage specifically binding to SH1429_C10 (red) but not an unrelated isotype control antibody (black). Green bars: anti pIII antibody was coated as capture antibody to confirm production of a randomly chosen clone. Blue bars: anti pIII was coated and instead of produced monoclonal TcdB-fragment phage, Hyperphage was added afterwards as a control of the detection system. Columns 1-4 of the ELISA plate were incubated with TcdB-fragment phage originating from the first panning well, 5-8 from the second and 9-12 from the third well.

Based on the signal to noise ratio clones were selected for sequencing. Also clones yielding lower ELISA signals were included, since affinity of the antibodies to shorter TcdB-fragments (which might provide higher epitope resolution) might be comparably lower, thus leading to decreased binding and consequently lower signal intensity in ELISA.

The obtained sequences were translated into aa sequences and aligned to the TcdB sequence. For each mAb, the stretch of amino acids that was covered by all sequenced clones (excluding clear outliers) that carried correct inserts in the pHORF3 vector, is referred to as the minimal epitope region (MER) (Table 3-5). This region encompasses the core amino acids for antigen-antibody interaction, but not necessarily all amino acids that contribute to binding.

For two antibodies from pannings against $TcdB_{1-1852}$, ViF088_H10 and ViF090_A6, an almost identical MER in the N-terminal part of the GTD was identified, it comprised aa 24- 84 or aa 23-83, respectively. These amino acids make up three alpha helices that belong to an alpha helical bundle at the toxins N-terminus (Figure 3-14).

For ViF087_B10, TcdB-fragment phage screening resulted in identification of only one hit (aa 289-313). Nevertheless, together with the data of the peptide array an epitope region could be assigned (Figure 3-14).

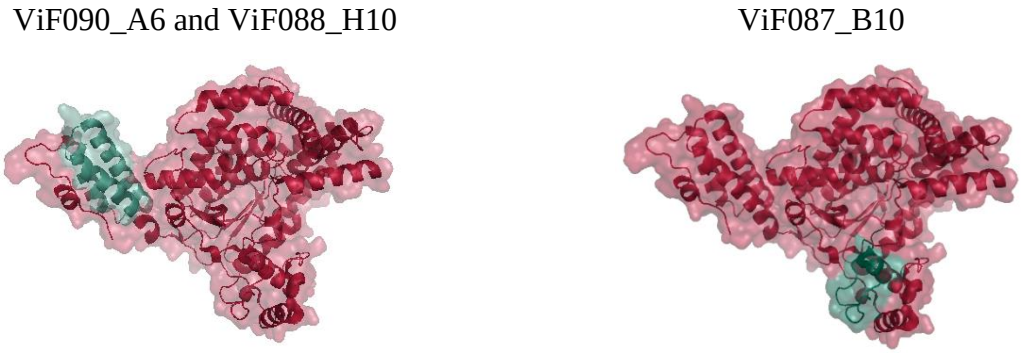

Figure 3-14: Epitope regions of ViF090_A6, ViF088_H10 and ViF087_B10

Combined data of peptide array and phage display: Epitope of ViF090_A6 and ViF088_H10 (left); epitope of ViF087_B10 (right) highlighted in green on the 3D model of TcdB GTD generated by X-Ray crystallography (PDB 2bvm)

The MER of the two best neutralizing mAbs generated in this study (ViF087_A10 and SH1429_B1) was also located in the GTD (aa 423-433). For ViF087_A10 the signal noise ratio of epitope presenting clones in screening ELISA was comparably low, nevertheless the MER was in accordance to the peptides bound in the peptide array for both mAbs.

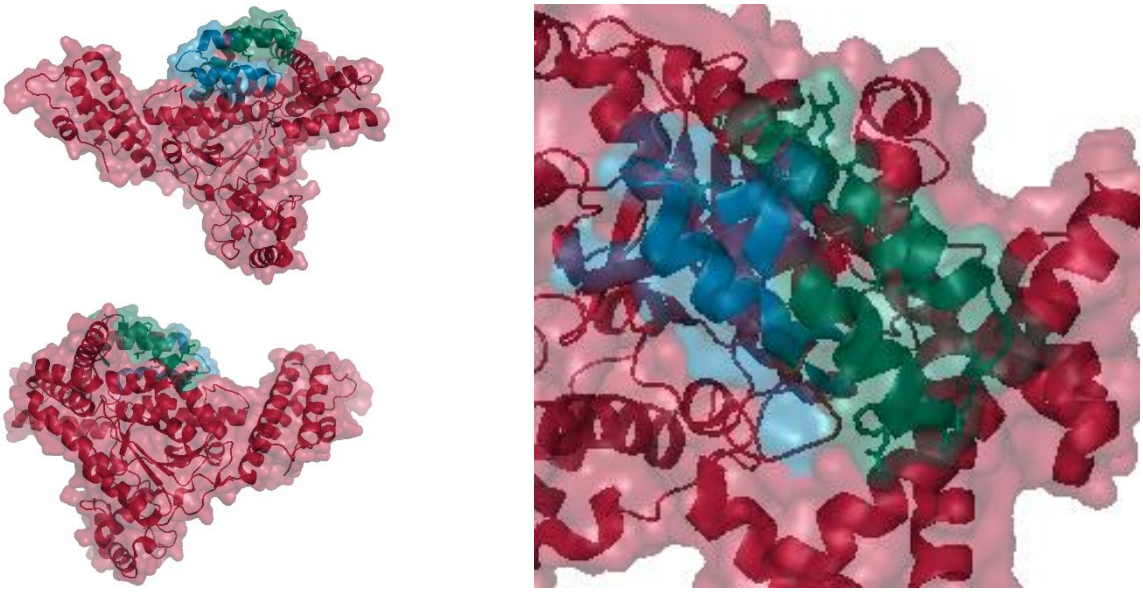

Figure 3-15: Epitope region of ViF087_A10

Combined data of Peptide array and phage display; the epitope region of ViF087_A10 is highlighted in green on the 3D model of TcdB GTD generated by X-Ray crystallography (PDB 2bvm); the two helices involved in substrate recognition are shown in blue.

As shown in Figure 3-15 for ViF087_A10, the MER is located directly next to the Rho-GTPase binding groove of TcdB.

For ViF087_E1 a MER between aa 528 and aa 543 was identified, which corresponds to the C-terminus of the GTD (Figure 3-16) and overlaps with the peptide that was strongly bound in the peptide array (aa 522-537).

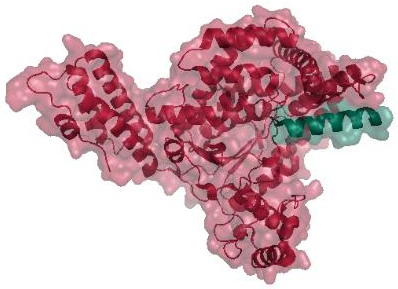

Figure 3-16: Epitope of ViF087_E1

The epitope of ViF087_E1, an α-helical structure at the C-terminus of the GTD is shown in green on the crystal structure of this domain (PDB 2bvm)

For ViF137_A9 and ViF137_E7 the MERs identified by phage display were in accordance with the results of the peptide array (Figure 3-17). Albeit, for both antibodies three cluster of peptides were identified by peptide array, for ViF137_A9 only one, and for ViF137_E7 two of the three clusters were confirmed by phage display.

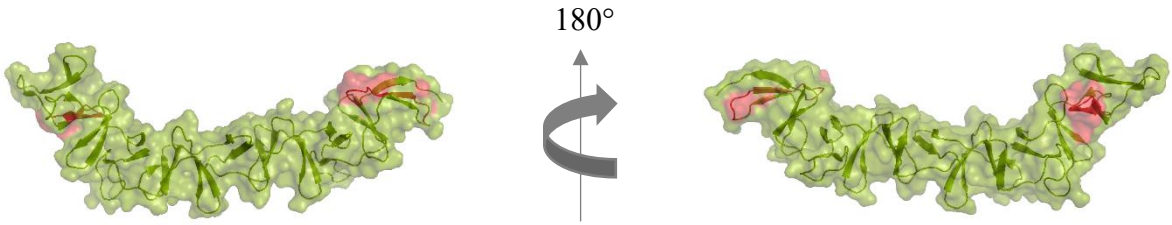

Figure 3-17: Epitopes 1 and 2 of ViF137_A9 and ViF137_E7

Epitopes (combined data of peptide array and phage display) are highlighted in red on the crystal structure of the CROPs (PDB 4np4)

The MER of ViF137_C3 was located in the N-terminal portion of the CROPs and spanned aa 1860-1992 (Figure 3-18). For SH1429_D6, the MER found spans a stretch of 118 amino acids in the middle of the CROPs (aa 2010- 2118) and the MER of SH1429_G6 aa 2228-2291.

The seven remaining mAbs ViF137_A3, ViF137_A6, ViF137_E4, SH1429_B10, SH1429_C10, SH1429_G1 and SH1429_H7 all bound to the C-terminal part of TcdB, the MERs of these epitopes resembled the last 70-130 aa of the CROPs domain.

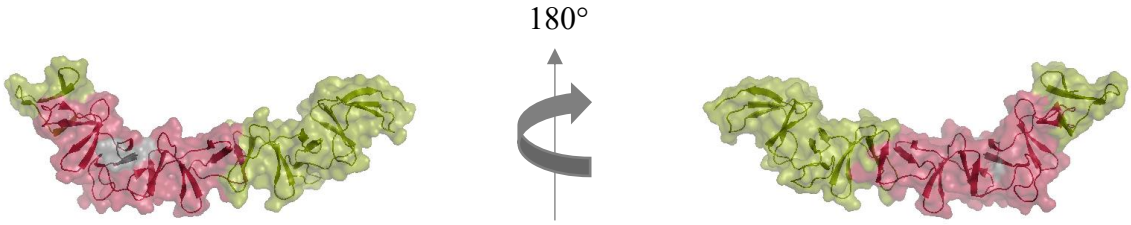

Figure 3-18: Epitope of ViF137_C3

Epitope of ViF137_C3 shown in red and residues protected from H/D exchange by Bezlotoxumab in grey (Orth et al. 2014)

For ViF137_A3, ViF137_A6, ViF137_C3, SH1429_C10, SH1429_D6 and SH1429_G1 a reevaluation of the results of the peptide array was done after identification of the MERs by phage display. In all cases peptide clusters were identified that were strongly bound by the respective antibodies and which were in accordance to the MERs identified by phage display (Table 3-5 and Supplementary Table 7-1 - Supplementary Table 7-5).

Taken together, the data generated by peptide array and phage display are in good agreement (Table 3-5) and give valuable information about the antibody-antigen interactions.

Figure 3-19: Positions of the epitopes on TcdB

Epitopes of the antibodies generated in this study (upper pane, the two best neutralizers are shown in red) and epitopes of neutralizing antibodies generated by others (lower panel). The numbers correspond to the numbers of the mAbs used in the tables.

A summary of the epitopes of the antibodies generated in this study, also in comparison with already published epitopes of neutralizing antibodies is given in Figure 3-19. Hence some epitopes overlap with already published epitopes, also a lot of novel epitopes were identified.

Table 3-5: Summary of antibody characterization

#	mAb name	Antigen (Panning)	TcdB variants bound in ELISA	WB	Peptide array (position of 1st aa of 15mer peptide)	Minimal epitope region (MER, Phage display)	No of clones included in MER
1	ViF087_A10	$TcdB_{1-1852}$	$TcdB_{FL,}$ (≤50%), $TcdB_{1-1852}$	-	aa 402-404 and aa 412-422	aa 423– 433	5 (low signal : noise ratio)
2	ViF087_B1	$TcdB_{1-1852}$	$TcdB_{FL,}$ (≤50%), $TcdB_{1-1852}$	+/-		no hits	-
3	ViF087_B10	$TcdB_{1-1852}$	$TcdB_{FL,}$ (≤50%), $TcdB_{1-1852}$	+/-	aa 288-294 (not exclusively)	aa 289-313	1
4	ViF087_E1	$TcdB_{1-1852}$	$TcdB_{FL}$, $TcdB_{1-1852}$, $TcdB_{GTD}$	+/-	aa 522	aa 528- 543	16
5	ViF087_E7	$TcdB_{1-1852}$	$TcdB_{FL}$, $TcdB_{1-1852}$,	+/-		no hits	-
6	ViF087_F1	$TcdB_{1-1852}$	$TcdB_{FL,}$ (≤50%), $TcdB_{1-1852}$,	-		no hits	-
7	ViF087_F3	$TcdB_{1-1852}$	$TcdB_{FL}$, $TcdB_{1-1852}$,	+/-		no hits	-
8	ViF087_G10	$TcdB_{1-1852}$	$TcdB_{FL}$, $TcdB_{1-1852}$,	-		no hits	-
9	ViF087_G11	$TcdB_{1-1852}$	$TcdB_{FL}$, $TcdB_{1-1852}$,	-		no hits	-
10	ViF087_H5	$TcdB_{1-1852}$	$TcdB_{FL}$, $TcdB_{1-1852}$,	+/-		no hits	-
11	ViF088_C5	$TcdB_{1-1852}$	$TcdB_{FL}$, $TcdB_{1-1852}$, $TcdB_{GTD}$	+/-		no hits	-
12	ViF088_E10	$TcdB_{1-1852}$	$TcdB_{FL}$, $TcdB_{1-1852}$,	-		no hits	-
13	ViF088_H10	$TcdB_{1-1852}$	$TcdB_{FL}$, $TcdB_{1-1852}$, $TcdB_{GTD}$	+		aa 24- 84	12
14	ViF090_A6	$TcdB_{1-1852}$	$TcdB_{FL}$, $TcdB_{1-1852}$, $TcdB_{GTD}$	+		aa 23- 83	4
15	ViF090_G5	$TcdB_{1-1852}$	$TcdB_{FL}$, $TcdB_{1-1852}$,	-		no hits	-
16	ViF091_B10	$TcdB_{1-1852}$	$TcdB_{FL,}$ (≤50%), $TcdB_{1-1852}$	-		no hits	-
17	ViF137_A3	$TcdB_{CROPs}$	$TcdB_{FL}$, $TcdB_{CROPs}$	+	aa 2342-2344 (not exclusively)	aa 2284- 2364	6
18	ViF137_A6	$TcdB_{CROPs}$	$TcdB_{FL}$, $TcdB_{CROPs}$	+	aa 2340- 2344	aa 2275- 2364	23
19	ViF137_A9	$TcdB_{CROPs}$	$TcdB_{FL}$ (≤50%), $TcdB_{CROPs}$	+	KYYF° (°=D or N) aa 1854-1862, 2080-2086 and 2212-2216	aa 1858- 1868	13
20	ViF137_C1	$TcdB_{CROPs}$	$TcdB_{FL}$ (≤50%), $TcdB_{CROPs}$	+		no hits	-
21	ViF137_C2	$TcdB_{CROPs}$	$TcdB_{FL}$ (-), $TcdB_{CROPs}$	+		no hits	-
22	ViF137_C3	$TcdB_{CROPs}$	$TcdB_{CROPs}$ (-)	+	aa 1922-1938	aa 1860– 1992	3
23	ViF137_E4	$TcdB_{CROPs}$	$TcdB_{FL}$, $TcdB_{CROPs}$	+	aa 2342-2344	aa 2292- 2364	18
24	ViF137_E7	$TcdB_{CROPs}$	$TcdB_{FL}$, $TcdB_{CROPs}$	+	*KYYF° (*=I, S or D; ° =D or N) aa 1852-1860, 2078-2084 and 2212-2216	2 epitopes, shared motif: DKYYFNP AA 1862-1868 and 2220- 2226	17+5
25	SH1429_B1	$TcdB_{FL}$	$TcdB_{FL}$, $TcdB_{1-1852}$	+/-	aa 414-424	aa 423- 432	8
26	SH1429_B10	$TcdB_{FL}$	$TcdB_{FL}$, $TcdB_{CROPs}$	-		aa 2267-2364	19

#	mAb name	Antigen (Panning)	TcdB variants bound in ELISA	WB	Peptide array (position of 1st aa of 15mer peptide)	Minimal epitope region (MER, Phage display)	No of clones included in MER
27	SH1429_C10	$TcdB_{FL}$	$TcdB_{FL}$, $TcdB_{CROPs}$	+	aa 2340-2342	aa 2333-2363	15
28	SH1429_D6	$TcdB_{FL}$	$TcdB_{FL}$, $TcdB_{CROPs}$	+	aa 2078 and 2084	aa 2010– 2118	6
29	SH1429_G1	$TcdB_{FL}$	$TcdB_{FL}$, $TcdB_{CROPs}$	+	aa 2316-2324	aa 2267– 2364	10
30	SH1429_G6	$TcdB_{FL}$	$TcdB_{FL}$, $TcdB_{CROPs}$ (-)	+		aa 2228 - 2291	4
31	SH1429_H7	$TcdB_{FL}$	$TcdB_{FL}$, $TcdB_{CROPs}$	+		aa 2276– 2364	11

4 Discussion

Clostridioides difficile is the causative agent of *Clostridioides difficile* associated diarrhea (CDAD) (Bartlett et al., 1978). During the last decades the incidence of CDAD in Germany has risen to 5-20 cases per 100.000 per year (Burckhardt et al., 2008; Lübbert et al., 2014). Due to its association with antibiotic treatment and the resulting high potential for development of antibiotic resistance, the US Centers for Disease Control and Prevention (CDC) classify *CDiff* as an urgent threat (Centers of Disease Control and Prevention, 2013). To fight this threat new therapeutic strategies are urgently needed.

The main virulence factors of *CDiff* are the two large clostridial toxins TcdA and TcdB that are secreted upon *CDiff* outgrowth (Just et al., 1995a, 1995b). In 2016 the anti-TcdB antibody Bezlotoxumab was approved for prevention of CDI recurrence by the FDA. The co-developed anti TcdA antibody Actoxumab did not show clinical efficacy and failed in clinical phase 3 (Merck Newsroom Home, 2015). Bezlotoxumab reduced the CDI recurrence from 26% to 16% in the clinical phase 3 study (MODIFY II) (Wilcox et al., 2017). Because of this limited efficacy, the increasing number of *CDiff* toxinotypes and the fact, that currently three different TcdB receptors and a potential carbohydrate structure are described, new studies to describe neutralizing and non-neutralizing epitopes are necessary, for further rational development of antibody combinations that potentially improve clinical outcome and/ or vaccine design (Greco et al., 2006; Gupta et al., 2017; LaFrance et al., 2015; Rupnik and Janezic, 2016; Tao et al., 2016; Yuan et al., 2015).

For this reason, antibodies were generated against TcdB, which were characterized in respect of antigen binding, domain specificity and TcdB neutralization in an *in vitro* assay. Furthermore, two different approaches were used for epitope mapping to identify vulnerable epitopes on TcdB.

4.1 Antibody phage display led to generation of a diverse antibody repertoire

To generate novel human monoclonal antibodies targeting TcdB, a phage display approach was chosen. Phage display had already been successfully used previously to isolate neutralizing single-domain antibodies against TcdA from an llama immune V(H)H library (Hussack et al., 2011). However, aim of this study was to generate fully human antibodies, which are better developable for possible future clinical use, since antibodies derived from other species require chimerization or humanization to reduce immunogenicity but still have lower percentual human content compared to fully human antibodies (Almagro et al., 2018). Thus, the large naïve human scFv libraries HAL9 and HAL10 were used in a pooled approach for antibody generation (Kügler et al., 2015). To generate more diverse antibodies that bind to different regions of TcdB, six antibody selections were performed on either $TcdB_{FL}$ $TcdB_{1-1852}$ or $TcdB_{CROPs}$. The panning strategies differed in regards of the TcdB fragments used, the negative selection strategy and/or the temperature. All six panning strategies led to the identification of unique and specific antibodies, therefore enrichment of specific antibody phage directed against the different TcdB variants was successful either way. Nevertheless, the two pannings at 37 °C against $TcdB_{1-1852}$ resulted in a very low number of unique scFvs (1+2), therefore the panning against the CROPs and $TcdB_{FL}$ was only performed at ambient temperature.

Sequencing with subsequent CDR analysis revealed the isolation of a total of 36 unique antibodies. The usage of HAL9 and HAL10 library in a pooled approach led to an enhanced but not exclusive selection of lambda antibodies (80%). This result is in accordance to previous studies (Kügler et al., 2015) and also in humans the majority of the antibodies are λ-antibodies (ratio λ: κ = 2:1) (Murphy and Weaver, 2018). Furthermore, antibodies of four different IGH V genes were isolated with the majority of IGHV1 and IGHV3 and lower numbers of IGHV5 and IGHV6. IGHV2, IGHV4 or IGHV7 antibodies were not selected. Presence of IGHV2 and IGHV7 is very rare in HAL9 and HAL10 libraries as well as in humans and IGHV4 antibodies are often lost during the panning procedure with a ten- fold decrease in frequency from 18,3% to 1,8%. Taken together the V gene distribution of antibodies generated in this study resembles the distribution already described for antibody selections using HAL9 and HAL10 and by large also the distribution in humans (Kügler et al., 2015).

4.2 Validation of antibody- antigen binding after format change

For further validation and characterization, the antibody candidates were converted into the bivalent scFv-Fc format. Due to a fast cloning and better production rates, this format is preferred over the full IgG format for the rapid screening of a higher number of candidate antibodies (Bujak et al., 2014). Furthermore, due to the dimerization facilitated by the Fc part and the presence of the Fc part itself it has IgG-like properties which makes it well suitable for preclinical characterization (Frenzel et al., 2016).

After subcloning and successful production in mammalian cell culture, thirty-one antibodies were tested for antigen binding and domain specificity in an antigen ELISA on four different TcdB variants ($TcdB_{FL}$, $TcdB_{1\text{-}1852}$, $TcdB_{CROPs}$ and $TcdB_{GTD}$). By antigen ELISA on the respective panning antigen, it was validated that the antibody- antigen interaction was not impaired by the format change from scFv to scFv-Fc and switch of the production system, since all antibodies bound to their respective antigen, albeit 2 out of 31 only weakly. Nevertheless, these two antibodies were not excluded from further assays and neutralization tests. It had been shown in another study aiming at generation of diphtheria toxin neutralizing antibodies, that there is no (good) correlation between binding to immobilized antigen on an ELISA plate and neutralization efficacy (Esther Wenzel, unpublished data).

4.3 Folding or epitope shielding influences binding to $TcdB_{FL}$

Even though all antibodies bound to their respective panning TcdB variant, almost no binding to $TcdB_{FL}$ was detected for five antibodies and for further seven antibodies the binding to $TcdB_{FL}$ was drastically reduced compared to the respective panning antigen.

All these antibodies have in common that they were generated on fragments of TcdB, instead of $TcdB_{FL.}$ Since equal amounts (100 ng) of all variants have been used for coating of the microtiter plates and $TcdB_{FL}$ has a higher molecular weight compared to its fragments, one easy explanation would be that there were less molecules of $TcdB_{FL}$ available for antibody binding, thus resulting in a lower signal. However, most antibodies did not show a decreased binding therefore this theory is less likely. Also coating of the same molarity of each TcdB variant is difficult to realize, since coating efficacy may vary from protein to protein depending on ionic groups and hydrophobic regions. A second possible reason is that the epitopes or binding regions of some antibodies might not be accessible in the tertiary structure of the full-length TcdB. For TcdA, a homologues toxin, a 3D model of the holotoxin is available that was generated on the basis of electron micrographs by Pruitt and coworkers. This model nicely reveals the complex domain organization of the toxin. One feature that might help understanding the different binding of TcdB fragments and $TcdB_{FL}$ is that the C-terminal CROPs form a long tail that lays back onto the N-terminal portion of the toxin (Pruitt et al., 2010). And even though the CROPs domain of TcdB is considerably smaller, electron micrographs of TcdB suggest a similar domain organization (Pruitt et al., 2010). Epitope regions that are located at the interface between CROPs and the N-terminal portion of the toxin might be less accessible in the full-length toxin due to steric hindrance, which would explain reduced antibody binding on full-length TcdB. Different antibody binding on TcdB fragments and full-length TcdB with antibodies derived from this study was also shown by Chung et al (paper submitted). To circumvent the generation of antibodies which do not bind the full-length toxin, antibody generation strategies with alternating panning rounds on full-length TcdB and TcdB fragments could be applied. Alternating panning strategies have already successfully been used to generate antibodies against complex target structures like membrane proteins (Jones et al., 2016).

4.4 Panning against $TcdB_{FL}$ preferentially led to isolation of antibodies binding the CROPs

The next question to address was the domain specificity of the generated antibodies. By performing six pannings with different TcdB variants and different panning strategies a broad variety of different antibodies with different antigen binding profiles should be generated.

In an antigen ELISA seventeen of the 31 antibodies bind to $TcdB_{1-1852.}$ These antibodies mainly originate from the four pannings against $TcdB_{1-1852;}$ only one derives from the panning on full-length TcdB. Just four of these mAbs also bind to $TcdB_{GTD}$ which indicates that preclearance of the library by incubation on immobilized $TcdB_{1-1128}$ prior to the panning in cases of panning ViF087 and ViF090 was successful, but not complete. If a stricter selection strategy is needed, the preclearance step should be combined with soluble competition during the panning as already described earlier (Stausbøl-Grøn et al., 1996). Here a broader domain specificity was aimed for, therefore soluble competition was omitted.

Worthy of mention is that in this domain mapping ELISA, an enzymatically inactive GTD mutant (D286/288N) was used. Even though the amino acid sequences differ in only two amino acids, the overall structure of the domain might be slightly changed. Therefore, epitopes might not be accessible or conformational epitopes might be destroyed. Loss of antibody binding after mutation of single amino acids had already been described for antibodies targeting the diphtheria DT toxin (Bigio et al., 1987). Due to this reason and possible different folding of the various TcdB variants epitopes within the GTD must not be excluded for the antibodies binding to $TcdB_{1-1852}$ but not to $TcdB_{GTD}$ in this assay.

Almost half (14 /31) of the antibodies characterized in this study bind to $TcdB_{CROPs,}$ even though this domain has only been present in two out of the six panning strategies (Panning on $TcdB_{FL}$ and on $TcdB_{CROPs}$). Most interestingly, the panning on $TcdB_{FL}$ almost exclusively resulted in the generation of mAbs directed against the CROPs. In *in vivo* studies it had already been shown, that the CROPs elicit strong antibody responses (Yang et al., 2014). One possible reason might be the repetitive structure of the CROPs. Due to this feature, structural elements present in the CROPs are overrepresented in the panning. Furthermore, as already mentioned above, the CROPs could shield epitopes on the other domains, thereby inhibiting generation of antibodies against these structures.

4.5 A cell-based assay revealed generation of neutralizing antibodies

To evaluate if antibodies have been generated that might be suitable for further preclinical development an *in vitro* neutralization assay of TcdB was performed.

Since the CROPs, the GTD and also the TLD of TcdB all harbor epitopes that can be targeted for neutralization with antibodies (Anosova et al., 2015; Babcock et al., 2006; Marozsan et al., 2012; Maynard-Smith et al., 2014; Wang et al., 2012) all 31 mAbs were subsequently tested in an *in vitro* TcdB neutralization assay which is based on cell rounding of Vero cells.

All 31 mAbs reduced the percentage of round cells after TcdB treatment to some extent and therefore had slight neutralizing effects. Best neutralization was achieved using ViF087_A10 or SH1429_B1, two antibodies that both bind to $TcdB_{1\text{-}1852}$ with almost complete inhibition of cell rounding which was also confirmed in a second assay using serial dilutions of these antibodies. Unfortunately, comparison of the *in vitro* neutralization efficacy of the antibodies obtained in this study with antibodies from other studies is not possible, since there is no common standard protocol for the *in vitro* neutralization assays. Therefore the assays differ in regards of amounts and productions of TcdB used, incubation/ intoxication times and in cell lines used (Anosova et al., 2015; Babcock et al., 2006; Kroh et al., 2018; Marozsan et al., 2012; Schmidt et al., 2016).

However, of the 14 antibodies directed against the CROPs domain, only two (ViF137_E7 and SH1429_H7) had neutralization efficacies of more than 50%. Maynard-Smith and coworkers have previously shown that in contrast to TcdA, generation of neutralizing antibodies against the CROPs of TcdB is difficult even *in vivo* by immunization (Maynard-Smith et al., 2014).

Deduced from the homologue TcdA, the CROPs of TcdB harbor 4 putative carbohydrate binding sites (Greco et al., 2006; Orth et al., 2014). These multiple sites might contribute avidity effects upon cell binding. Therefore, neutralization via the CROPs might be difficult.

Furthermore, these binding sites share structural similarity (repetitive elements) but differ in respect to their amino acid sequence, making it difficult to develop a single antibody that completely blocks all interactions between the CROPs and the carbohydrate structures.

Nevertheless, the approval of Bezlotoxumab for therapy of recurrent CDAD explicitly proves that neutralization via this C-terminal domain is possible (Babcock et al., 2006; Wilcox et al., 2017).

Crystal structure analysis has shown that the already approved therapeutic antibody Bezlotoxumab binds to two epitopes within the CROPs, therefore it was suggested that this

antibody blocks interaction of the CROPs with carbohydrate structures on the cell surface (Orth et al., 2014). Nevertheless, binding of Bezlotoxumab to aa 1878-1961 also inhibits interaction with CSPG4 receptor (Gupta et al., 2017) which would be a second possible mode of neutralization. Finally, due to the existence of two epitopes within the CROP domain also aggregation of the toxin as neutralization mechanism cannot be excluded. Today, it is not clear which of the above mentioned is the major neutralization mechanism.

However, due to the three receptor binding sites that are located at the border, or outside of the CROPs (Chen et al., 2018; Gupta et al., 2017; LaFrance et al., 2015; Tao et al., 2016) possible neutralization of TcdB by inhibition of CROPs binding to their target carbohydrate structures might be hidden due to uninterrupted binding to the other receptors. To test whether the anti-CROPs mAbs might lead to an increased neutralization when applied together with neutralizing mAbs directed against the N-terminal fraction of TcdB (aa 1-1852) a combinatory neutralization assay was performed where each of the anti- CROPs mAbs was tested for *in vitro* neutralization of TcdB in combination with ViF087_A10 and SH1429_B1, respectively.

Even though there was a slight increase in neutralization when antibodies were applied in combinations compared with neutralization mediated by the single antibodies ViF087_A10 and SH1429_B1 these effects were rather just additive than synergistic.

4.6 Discovery of a novel neutralizing epitope within the GTD

For future development of novel therapeutic antibodies against TcdB as well as for a rational vaccine design a deeper understanding of the molecular actions of TcdB is required, especially about potentially vulnerable regions or epitopes that can be targeted with antibodies or used as a vaccine to evoke a potent neutralizing antibody response. With the broad panel of antibodies generated in this study valuable information can be generated by correlating the neutralization efficacies of the respective antibodies to their epitopes or epitope regions. With the antigen ELISA already a rough domain mapping was performed, but resolution was very low with the few antigen fragments used in this assay. To narrow down the binding regions of the antibodies an epitope mapping was performed. Until now gold standard for epitope mapping is still X-ray crystallography, which provides profound information of antibody antigen interaction on nearly atomic resolution (Toride King and Brooks, 2018). This method has also been applied to elucidate the epitopes bound by Bezlotoxumab (Orth et al., 2014). Nevertheless, this method is very laborious and therefore not applicable for a larger set of antibodies. Furthermore TcdB is not easy to crystallize: up to date there are only structures of fragments or domains of TcdB solved (Alvin and Lacy, 2017; Orth et al., 2014; Shen et al., 2011).

Therefore, as a first approach a peptide array was chosen. This method is feasible for screening higher numbers of antibodies in parallel and is comparably uncomplicated. A prerequisite for binding of antibodies to peptides immobilized on the array surface is, that the antibodies bind to continuous epitopes, not including complex folding (Abbott et al., 2014). Due to the peptide length of 15 aa the presence of conformational epitopes is limited to alpha helical epitopes, which represent an interim stage between a linear and a conformational-discontinuous epitope. To compensate the lack of complex epitopes in the peptide array, a phage display approach that also allows the identification of conformational epitopes was used (Cariccio et al., 2016; Moreira et al., 2018). Highest resolution, down to single amino acid level, is achieved with mutagenesis libraries (Rojas et al., 2014). However, due to its size of 270 kDa this is not feasible for full-length TcdB and most likely not even all of its domains. Therefore, a TcdB-fragment library was used instead.

In both assays all antibodies were included, since also information about epitopes that don’t convey neutralization is important.

Unfortunately, but not unexpectedly, epitope mapping by peptide array was not successful for the majority of the tested antibodies. By testing the antibodies for binding to SDS and

ß-Mercaptoethanol treated TcdB variants in an immunoblot, it had been demonstrated that most antibodies, binding to the N-terminal portion of TcdB, do not bind to the linearized antigen, whereas most antibodies directed against the CROPs do. Generally, antibodies that don't bind to SDS and ß-Mercaptoethanol treated proteins are likely to bind to discontinuous or conformational epitopes; but even antibodies that do bind to SDS and ß-Mercaptoethanol treated proteins must not necessarily bind to linear epitopes, because there might be a certain degree of backfolding of the protein during the assay, as had been indicated by Park and coworkers (Park et al., 2007).

Nevertheless, even though ViF087_A10 does not bind to denatured TcdB in immunoblot and SH1429_B1 only very weakly, binding to 15 mer peptides on the peptide array was detected.

Core of their epitope is a continuous amino acid stretch within the GTD (aa 423-433 and 423-432, respectively). This epitope, primarily found by peptide array, was also confirmed by antigen fragment phage display. Remarkably, both neutralizing antibodies bind to the same epitope region: a surface exposed α- helix that is located in direct proximity to the residues involved in substrate recognition (aa 436-456) (Swett et al., 2012) (Figure 5b). Additionally, ViF087_A10 also reacted with two peptides in the peptide array that correspond to a neighboring α- helix located N-terminal of the alpha helix found by both methods. Folding of the alpha helix and the orientation of the two neighboring helices towards each other is probably mostly destroyed by SDS and ß-Mercaptoethanol treatment, which would explain the abolished binding in immunoblot.

Due to the localization of this neutralizing epitopes at least two neutralization mechanisms are possible for ViF087_A10 and SH1429_B1: i) inhibition of substrate binding or ii) sterical hindrance of $TcdB_{GTD}$ translocation through the pore. The latter mode of action has recently been described for the humanized monoclonal antibody PA41 that binds to aa 290-360 (Kroh et al., 2018).

For ViF090_A6 and ViF088_H10 both epitope mapping was only successful with the phage display approach, these antibodies bound to a bundle of alpha helices at the very N-terminus of TcdB which is conserved among large clostridial toxins and is described to guide the GTD towards the cell membrane after release into the cytosol (Geissler et al., 2010)

For one antibody, ViF137_C3, an epitope (aa 1860-1992) was found, that includes one of the epitopes described for Bezlotoxumab [aa 1902-1907 are partially protection from H/D exchange by bezlotoxumab (Orth et al., 2014)]. Nevertheless, TcdB neutralization achieved with this antibody in cell rounding assays was only less than 50%. Unfortunately, *in vitro*

neutralization efficacies of these two antibodies are not comparable, due to variations in the assay (Babcock et al., 2006). Moreover, the resolution of epitope mapping by phage display was not high enough for this antibody to determine whether these antibodies interact with the same amino acids of TcdB or not.

For most antibodies that exclusively bind to $TcdB_{1-1852}$ and $TcdB_{FL}$ in antigen ELISA it was not possible to determine the epitope by neither of the methods tested. As shown by immunoblot assay, these mAbs most likely bind to complex discontinuous epitopes, including amino acids that are located far apart on the primary structure of TcdB and only come into close proximity upon folding of the polypeptide chain. Such epitopes cannot be identified using peptide arrays and might also be hard to display on phage.

The latter is due to several possible reasons. Firstly, there is a selection pressure towards smaller antigen fragments during library cloning and packaging (Faix et al., 2004). When amino acids contributing to the epitope are too far apart on the primary structure, the corresponding TcdB-fragment phage will be underrepresented during the panning. Secondly, the TcdB fragments corresponding to the epitopes could be toxic for *E. coli*, which would lead to a loss of clones producing these fragments during library packaging; indeed, the quality control of the library, which included sequencing of 92 clones, could not prove complete coverage of the TcdB sequence, (which could of cause also be due to the number of clones sequenced which was ~0,001% of the library). Thirdly, especially TcdB fragments that have higher hydrophobicity might missfold or aggregate and finally, some peptides might not be efficiently secreted via the sec pathway. To overcome this possible limitation, Kügler et al. already suggested the use of a combination of phage vectors using the sec pathway, the twin-arginin translocation system (Paschke and Höhne, 2005) and the signal recognition particle pathway (Valent, 2001) for translocation into the periplasm (Kügler et al., 2008).

For 18 of the 31 antibodies minimal epitope regions were identified. For 13 antibodies, including the two most potent neutralizing antibodies generated in this study, results of TcdB-fragment phage display and peptide array were consistent and mutually supportive, providing profound information about neutralizing and non- neutralizing epitopes of TcdB. These new findings might be of great value for future development of therapeutic antibodies targeting TcdB and TcdB fragment or - epitope based vaccines.

4.7 Conclusion and outlook

In this study, phage display technology was used to generate a broad panel of fully human monoclonal antibodies that target TcdB, one of the main virulence factors of *Clostridioides difficile* and target of new therapeutic approaches.

ELISA and Immunoblot analysis proved TcdB binding and domain specificity of 31 analyzed antibodies and confirmed the selection of antibodies with diverse binding characteristics.

Using a cell-based *in vitro* assay, it was shown that especially two antibodies efficiently neutralize TcdB induced cell rounding. These two antibodies might be candidates for further preclinical development. Also, future therapeutic use of these antibodies, preferably as antibody combination with antibodies targeting different domains or epitopes, is easily conceivable due to the human origin of these antibodies.

By correlating the epitopes identified via TcdB-fragment phage display and peptide array with *in vitro* neutralization efficacy, a new epitope within the glucosyltransferase domain of TcdB, which conveys neutralization was identified. Summing up the results of this study as well as of anti TcdB-antibody studies published by others the following regions may be addressed in future development of neutralizing antibodies or TcdB based vaccines:

i) aa 290-360 (Kroh et al., 2018),
ii) aa 423- 432 (epitope of the two best neutralizers generated in this study),
iii) aa 1372- 1493, involved in binding to poliovirus receptor- like protein-3 (LaFrance et al., 2015; Manse and Baldwin, 2015),
iv) aa 1810-1850, involved in CSPG4 binding (Gupta et al., 2017)
v) aa 1430-1600 containing the FZD- cysteine rich domain binding region (Chen et al., 2018);

whereas the following regions should be omitted:

i) the N- and C-terminus of the GTD, since antibodies against these regions generated in this study did not show significant neutralization,
ii) the C-terminus of the CROPs [antibodies generated in this study as well as by others were poor neutralizers (Gupta et al., 2017; Maynard-Smith et al., 2014)]

Taken together, this study delivers valuable information for further development of new therapeutics against TcdB, as well as for a more rational, epitope based, vaccine design.

5 Acknowledgements

The last years were a time of up and downs, of enthusiasm, frustration and sometimes almost resignation. I am very pleased that I found so many colleagues and friends who supported me throughout this time and thus contributed to this work in one way or the other. I want to take this opportunity to express my honest gratefulness.

First of all, my profound gratitude goes to the first examiner of this thesis, my doctoral supervisor and mentor **Prof. Dr. Michael Hust**. Thank you for the scientific guidance, for sharing the frustration when things did not work as hoped for, thanks for giving me the freedom for own little side projects and thank you for the trust you have in me.

Also, I am very thankful to **Prof. Dr. Stefan Dübel** for being second examiner of this thesis, but, more important, for always friendly scientific and practical advice. You also gave me the opportunity of joining numerous exciting conferences, which I really appreciated.

My gratitude also goes to **Prof. Dr. Andreas Pich** for being part of the thesis committee and joining the oral defense of this thesis.

During the last years I also experienced valuable support from several collaboration partners. Without them this project would not have come so far.

First of all, my gratefulness goes to the **Team of the Institute of Toxicology at Hannover Medical school**, especially, to **Prof. Dr. Ralf Gerhard** for constant support during the last years. Thank you for sharing your expertise in the toxicology field, for scientific discussions and for your contribution in the Toxobuddy project. I am also very thankful to **Dr. Sebastian Goy**, who taught me how to intoxicate cells and spent some days with me pipetting antibody and TcdB dilutions and counting cells. Thanks a lot for the warm welcome in your institute. Also, I want to thank **Helma Tagte** for producing the TcdB variants.

My gratitude also goes to **Dr. Felix Löffler** and **Jasmin Heidepriem** from the **Max Planck Institute of Colloids and Interfaces** who helped me with the conduction and evaluation of the peptide arrays. I enjoyed the short stay in Potsdam and the collaboration with you, and that is not only because of the exciting results from the peptide array. Thank you for your support and thorough discussions of the results.

Another valuable collaboration partner was the **Institute of Infection Immunology, Twincore Centre, Hannover.** Here my special thanks go to **Dr. Matthias Lochner** and **Friederike Kruse,** thank you for all the efforts on establishing the *in vivo* model.

During my time as a PhD student I also supervised a number of master students on various projects. Even when they sometimes made me swear, it was a great pleasure to accompany them during these intense times. Thank you to the chipmunks **Birte Ackenhausen**, **Verena Boysen** and **Tatjana Wegner** for supporting each other as far as possible and thank you for a very special time in the 'estrogen' lab. Thank you to **Kristian Roth** for paving the way for epitope mapping by phage display. Thank you, **Maximilian Ruschig**, for your excitement on the Toxobuddy project and for bravely bearing the good cop / bad cop game. And, not less important, thank you **Philip Heine** for your support with the epitope mapping and your tackling attitude. I know I sometimes had to put a lot of pressure on to you but I hope in the end you appreciate where it led us as much as I do.

Being surrounded by helpful and caring people made it so much easier for me to overcome lasting frustrating periods and, of cause, does not harm any other time. Therefore, I want to express my profound gratitude to **all members of the Department of Biotechnology** for the great working atmosphere, for all the support in all different kind of ways and also for refreshing coffee breaks or Friday afternoon off work beers with creative discussions. Especially, I want to thank Saskia Helmsing, for generating SH1429_B1, the most potent of all antibodies analyzed in this study and also **Marie Kastull, Doris Meier and Marlies Becker** for taking care of the cell culture and always providing cells right ready for transfection for everyone.

My gratefulness also goes to **Esther Wenzel** for always open and active communication and for your support, especially during the last week. I know you were under hard pressure, but it never effected your helpfulness. I really appreciate that.

Special thanks also go to **Giulio Russo**. The time, sweat and excitement we shared on the Toxobuddy- as well as the epitope mapping project was a real pleasure. Thank you for all the intensive and deep discussion and for letting me see things from another perspective.

Thank you to **Jörn Josewski**, for always motivating and inciting me and for the nice and nevertheless productive time in Neßmersiel.

Not only in my working- but also in my private environment I received a lot of support, which is just as important.

Therefore, I want thank my **study mates, the Biotechs** for unforgettable reunions during Whitsunday holiday and occasional spontaneous, meetings. I enjoy every hour we spend together. Thank you for keeping in contact.

Also, I would like to take the opportunity to thank my **Boulder-Buddies** for our sometimes more, sometimes less intense boulder sessions which make me forget about occasional work frustration.

I also want to thank my Family, my parents **Rudi** and **Veronika** as well as my siblings **Corinna, Lisa** and **Gunnar** for consistent support throughout all my years of study, and for not taking this whole project too serious. Whenever I come home, the work related problems and troubles suddenly count less.

Last but not least, my deep gratitude goes to my fiancé **Jörn**. Thank you for your unlimited support ever since, for cheering me up and bearing my moods. From the first to the last minute I could always count and rely on you and I experienced the best encouragement I could imagine. Thank you.

6 References

Abbott, W. M., Damschroder, M. M., and Lowe, D. C. (2014). Current approaches to fine mapping of antigen–antibody interactions. *Immunology* 142, 526–535. doi:10.1111/imm.12284.

al Saif, N., and Brazier, J. S. (1996). The distribution of Clostridium difficile in the environment of South Wales. *J. Med. Microbiol.* 45, 133–137. doi:10.1099/00222615-45-2-133.

Almagro, J. C., Daniels-Wells, T. R., Perez-Tapia, S. M., and Penichet, M. L. (2018). Progress and Challenges in the Design and Clinical Development of Antibodies for Cancer Therapy. *Front. Immunol.* 8. doi:10.3389/fimmu.2017.01751.

Alvin, J. W., and Lacy, D. B. (2017). Clostridium difficile toxin glucosyltransferase domains in complex with a non-hydrolyzable UDP-glucose analogue. *J Struct Biol* 198, 203–209. doi:10.1016/j.jsb.2017.04.006.

Anosova, N. G., Cole, L. E., Li, L., Zhang, J., Brown, A. M., Mundle, S., et al. (2015). A Combination of Three Fully Human Toxin A- and Toxin B-Specific Monoclonal Antibodies Protects against Challenge with Highly Virulent Epidemic Strains of Clostridium difficile in the Hamster Model. *Clin Vaccine Immunol* 22, 711–725. doi:10.1128/CVI.00763-14.

Babcock, G. J., Broering, T. J., Hernandez, H. J., Mandell, R. B., Donahue, K., Boatright, N., et al. (2006). Human monoclonal antibodies directed against toxins A and B prevent Clostridium difficile-induced mortality in hamsters. *Infect. Immun.* 74, 6339–6347. doi:10.1128/IAI.00982-06.

Barbas, C. F., Kang, A. S., Lerner, R. A., and Benkovic, S. J. (1991). Assembly of combinatorial antibody libraries on phage surfaces: the gene III site. *Proc. Natl. Acad. Sci. U.S.A.* 88, 7978–7982.

Barlow, G. M., Yu, A., and Mathur, R. (2015). Role of the Gut Microbiome in Obesity and Diabetes Mellitus. *Nutr Clin Pract* 30, 787–797. doi:10.1177/0884533615609896.

Bartlett, J. G., Chang, T. W., Gurwith, M., Gorbach, S. L., and Onderdonk, A. B. (1978). Antibiotic-associated pseudomembranous colitis due to toxin-producing clostridia. *N. Engl. J. Med.* 298, 531–534. doi:10.1056/NEJM197803092981003.

Becker, M., Felsberger, A., Frenzel, A., Shattuck, W. M. C., Dyer, M., Kügler, J., et al. (2015). Application of M13 phage display for identifying immunogenic proteins from tick (Ixodes scapularis) saliva. *BMC Biotechnology* 15. doi:10.1186/s12896-015-0167-3.

Beer, L.-A., Tatge, H., Schneider, C., Ruschig, M., Hust, M., Barton, J., et al. (2018). The Binary Toxin CDT of Clostridium difficile as a Tool for Intracellular Delivery of Bacterial Glucosyltransferase Domains. *Toxins* 10, 225. doi:10.3390/toxins10060225.

Bigio, M., Rossi, R., Nucci, D., Antoni, G., Rappuoli, R., and Ratti, G. (1987). Conformational changes in diphtheria toxoids: Analysis with monoclonal antibodies. *FEBS Letters* 218, 271–276. doi:10.1016/0014-5793(87)81060-8.

Bird, R. E., Hardman, K. D., Jacobson, J. W., Johnson, S., Kaufman, B. M., Lee, S. M., et al. (1988). Single-chain antigen-binding proteins. *Science* 242, 423–426.

Bolton, R. P., and Culshaw, M. A. (1986). Faecal metronidazole concentrations during oral and intravenous therapy for antibiotic associated colitis due to Clostridium difficile. *Gut* 27, 1169–1172.

Bradbury, A. R. M., Trinklein, N. D., Thie, H., Wilkinson, I. C., Tandon, A. K., Anderson, S., et al. (2018). When monoclonal antibodies are not monospecific: Hybridomas frequently express additional functional variable regions. *mAbs* 10, 539–546. doi:10.1080/19420862.2018.1445456.

Breitling, F., Dübel, S., Seehaus, T., Klewinghaus, I., and Little, M. (1991). A surface expression vector for antibody screening. *Gene* 104, 147–153.

Brinkmann, U., and Kontermann, R. E. (2017). The making of bispecific antibodies. *MAbs* 9, 182–212. doi:10.1080/19420862.2016.1268307.

Bujak, E., Matasci, M., Neri, D., and Wulhfard, S. (2014). Reformatting of scFv antibodies into the scFv-Fc format and their downstream purification. *Methods Mol. Biol.* 1131, 315–334. doi:10.1007/978-1-62703-992-5_20.

Burckhardt, F., Friedrich, A., Beier, D., and Eckmanns, T. (2008). Clostridium difficile surveillance trends, Saxony, Germany. *Emerging Infect. Dis.* 14, 691–692. doi:10.3201/eid1404.071023.

Busch, C., Hofmann, F., Selzer, J., Munro, S., Jeckel, D., and Aktories, K. (1998). A common motif of eukaryotic glycosyltransferases is essential for the enzyme activity of large clostridial cytotoxins. *J. Biol. Chem.* 273, 19566–19572.

Cariccio, V. L., Domina, M., Benfatto, S., Venza, M., Venza, I., Faleri, A., et al. (2016). Phage display revisited: Epitope mapping of a monoclonal antibody directed against *Neisseria meningitidis* adhesin A using the PROFILER technology. *mAbs* 8, 741–750. doi:10.1080/19420862.2016.1158371.

Carter, P. J. (2006). Potent antibody therapeutics by design. *Nature Reviews Immunology* 6, 343–357. doi:10.1038/nri1837.

Centers of Disease Control and Prevention (2013). Antibiotic Resistance Threats in the United States, 2013 | Antibiotic/Antimicrobial Resistance | CDC. *Antibiotic Resistance Threats in the United States, 2013 | Antibiotic/Antimicrobial Resistance | CDC*. Available at: https://www.cdc.gov/drugresistance/threat-report-2013/ [Accessed April 6, 2018].

Chandrasekaran, R., and Lacy, D. B. (2017). The role of toxins in Clostridium difficile infection. *FEMS Microbiol. Rev.* 41, 723–750. doi:10.1093/femsre/fux048.

Chen, P., Tao, L., Wang, T., Zhang, J., He, A., Lam, K., et al. (2018). Structural basis for recognition of frizzled proteins by Clostridium difficile toxin B. 7.

Clostridium Difficile Vaccine Efficacy Trial - ClinicalTrials.gov Available at: https://clinicaltrials.gov/ct2/show/NCT03090191 [Accessed July 25, 2018].

Collini, P. J., Bauer, M., Kuijper, E., and Dockrell, D. H. (2012). Clostridium difficile infection in HIV-seropositive individuals and transplant recipients. *J. Infect.* 64, 131–147. doi:10.1016/j.jinf.2011.12.003.

DePestel, D. D., and Aronoff, D. M. (2013). Epidemiology of Clostridium difficile Infection. *J Pharm Pract* 26, 464–475. doi:10.1177/0897190013499521.

Durocher, Y., Perret, S., and Kamen, A. (2002). High-level and high-throughput recombinant protein production by transient transfection of suspension-growing human 293-EBNA1 cells. *Nucleic Acids Res.* 30, E9.

Edelman, G. M., Cunningham, B. A., Gall, W. E., Gottlieb, P. D., Rutishauser, U., and Waxdal, M. J. (1969). THE COVALENT STRUCTURE OF AN ENTIRE γG IMMUNOGLOBULIN MOLECULE*. *Proc Natl Acad Sci U S A* 63, 78–85.

Egerer, M., Giesemann, T., Herrmann, C., and Aktories, K. (2009). Autocatalytic Processing of Clostridium difficile Toxin B BINDING OF INOSITOL HEXAKISPHOSPHATE. *J. Biol. Chem.* 284, 3389–3395. doi:10.1074/jbc.M806002200.

Egerer, M., Giesemann, T., Jank, T., Satchell, K. J. F., and Aktories, K. (2007). Auto-catalytic cleavage of Clostridium difficile toxins A and B depends on cysteine protease activity. *J. Biol. Chem.* 282, 25314–25321. doi:10.1074/jbc.M703062200.

Elliott, B., Chang, B. J., Golledge, C. L., and Riley, T. V. (2007). Clostridium difficile-associated diarrhoea. *Intern Med J* 37, 561–568. doi:10.1111/j.1445-5994.2007.01403.x.

Faix, P. H., Burg, M. A., Gonzales, M., Ravey, E. P., Baird, A., and Larocca, D. (2004). Phage display of cDNA libraries: enrichment of cDNA expression using open reading frame selection. *BioTechniques* 36, 1018–1029. doi:10.2144/04366RR03.

Frenzel, A., Hust, M., and Schirrmann, T. (2013). Expression of Recombinant Antibodies. *Front Immunol* 4. doi:10.3389/fimmu.2013.00217.

Frenzel, A., Schirrmann, T., and Hust, M. (2016). Phage display-derived human antibodies in clinical development and therapy. *mAbs* 8, 1177–1194. doi:10.1080/19420862.2016.1212149.

Frisch, C., Gerhard, R., Aktories, K., Hofmann, F., and Just, I. (2003). The complete receptor-binding domain of Clostridium difficile toxin A is required for endocytosis. *Biochemical and Biophysical Research Communications* 300, 706–711. doi:10.1016/S0006-291X(02)02919-4.

Gao, C., Mao, S., Kaufmann, G., Wirsching, P., Lerner, R. A., and Janda, K. D. (2002). A method for the generation of combinatorial antibody libraries using pIX phage

display. *Proc. Natl. Acad. Sci. U.S.A.* 99, 12612–12616. doi:10.1073/pnas.192467999.

Gao, Q., and Huang, H. (2015). Update on antimicrobial resistance in Clostridium difficile. *Yi Chuan* 37, 458–464. doi:10.16288/j.yczz.15-131.

Geissler, B., Tungekar, R., and Satchell, K. J. F. (2010). Identification of a conserved membrane localization domain within numerous large bacterial protein toxins. *Proc Natl Acad Sci U S A* 107, 5581–5586. doi:10.1073/pnas.0908700107.

Genisyuerek, S., Papatheodorou, P., Guttenberg, G., Schubert, R., Benz, R., and Aktories, K. (2011). Structural determinants for membrane insertion, pore formation and translocation of Clostridium difficile toxin B. *Mol. Microbiol.* 79, 1643–1654. doi:10.1111/j.1365-2958.2011.07549.x.

Gerding, D. N., Johnson, S., Rupnik, M., and Aktories, K. (2014). Clostridium difficile binary toxin CDT: mechanism, epidemiology, and potential clinical importance. *Gut Microbes* 5, 15–27. doi:10.4161/gmic.26854.

Gitlin, D., and Merler, E. (1961). A COMPARISON OF THE PEPTIDES RELEASED FROM RELATED RABBIT ANTIBODIES BY ENZYMATIC HYDROLYSIS. *J Exp Med* 114, 217–230.

Goldstein, E. J. C., Babakhani, F., and Citron, D. M. (2012). Antimicrobial activities of fidaxomicin. *Clin. Infect. Dis.* 55 Suppl 2, S143-148. doi:10.1093/cid/cis339.

Greco, A., Ho, J. G. S., Lin, S.-J., Palcic, M. M., Rupnik, M., and Ng, K. K.-S. (2006). Carbohydrate recognition by Clostridium difficile toxin A. *Nat. Struct. Mol. Biol.* 13, 460–461. doi:10.1038/nsmb1084.

Gupta, P., Zhang, Z., Sugiman-Marangos, S. N., Tam, J., Raman, S., Julien, J.-P., et al. (2017). Functional defects inClostridium difficileTcdB toxin uptake identify CSPG4 receptor-binding determinants. *J. Biol. Chem.* 292, 17290–17301. doi:10.1074/jbc.M117.806687.

Hall, I. C., and O'Toole, E. (1935). INTESTINAL FLORA IN NEW-BORN INFANTS: WITH A DESCRIPTION OF A NEW PATHOGENIC ANAEROBE, BACILLUS DIFFICILIS. *Am J Dis Child* 49, 390–402. doi:10.1001/archpedi.1935.01970020105010.

Hong, P.-Y., Lee, B. W., Aw, M., Shek, L. P. C., Yap, G. C., Chua, K. Y., et al. (2010). Comparative Analysis of Fecal Microbiota in Infants with and without Eczema. *PLOS ONE* 5, e9964. doi:10.1371/journal.pone.0009964.

Hussack, G., Arbabi-Ghahroudi, M., van Faassen, H., Songer, J. G., Ng, K. K.-S., MacKenzie, R., et al. (2011). Neutralization of Clostridium difficile toxin A with single-domain antibodies targeting the cell receptor binding domain. *J. Biol. Chem.* 286, 8961–8976. doi:10.1074/jbc.M110.198754.

Huston, J. S., Levinson, D., Mudgett-Hunter, M., Tai, M. S., Novotný, J., Margolies, M. N., et al. (1988). Protein engineering of antibody binding sites: recovery of specific

activity in an anti-digoxin single-chain Fv analogue produced in Escherichia coli. *Proc. Natl. Acad. Sci. U.S.A.* 85, 5879–5883.

Johnson, S., Louie, T. J., Gerding, D. N., Cornely, O. A., Chasan-Taber, S., Fitts, D., et al. (2014). Vancomycin, Metronidazole, or Tolevamer for Clostridium difficile Infection: Results From Two Multinational, Randomized, Controlled Trials. *Clin Infect Dis* 59, 345–354. doi:10.1093/cid/ciu313.

Jones, M. L., Alfaleh, M. A., Kumble, S., Zhang, S., Osborne, G. W., Yeh, M., et al. (2016). Targeting membrane proteins for antibody discovery using phage display. *Sci Rep* 6, 26240. doi:10.1038/srep26240.

Joost, I., Speck, K., Herrmann, M., and von Müller, L. (2009). Characterisation of Clostridium difficile isolates by slpA and tcdC gene sequencing. *Int. J. Antimicrob. Agents* 33 Suppl 1, S13-18. doi:10.1016/S0924-8579(09)70010-X.

Just, I., Selzer, J., Wilm, M., von Eichel-Streiber, C., Mann, M., and Aktories, K. (1995a). Glucosylation of Rho proteins by Clostridium difficile toxin B. *Nature* 375, 500–503. doi:10.1038/375500a0.

Just, I., Wilm, M., Selzer, J., Rex, G., von Eichel-Streiber, C., Mann, M., et al. (1995b). The enterotoxin from Clostridium difficile (ToxA) monoglucosylates the Rho proteins. *J. Biol. Chem.* 270, 13932–13936.

Kapur, R., Einarsdottir, H. K., and Vidarsson, G. (2014). IgG-effector functions: "the good, the bad and the ugly." *Immunol. Lett.* 160, 139–144. doi:10.1016/j.imlet.2014.01.015.

Karczewski, J., Poniedziałek, B., Adamski, Z., and Rzymski, P. (2014). The effects of the microbiota on the host immune system. *Autoimmunity* 47, 494–504. doi:10.3109/08916934.2014.938322.

Kim, P. H., Iaconis, J. P., and Rolfe, R. D. (1987). Immunization of adult hamsters against Clostridium difficile-associated ileocecitis and transfer of protection to infant hamsters. *Infect. Immun.* 55, 2984–2992.

Köhler, G., and Milstein, C. (1975). Continuous cultures of fused cells secreting antibody of predefined specificity. *Nature* 256, 495–497.

Kotloff, K. L., Wasserman, S. S., Losonsky, G. A., Thomas, W., Nichols, R., Edelman, R., et al. (2001). Safety and immunogenicity of increasing doses of a Clostridium difficile toxoid vaccine administered to healthy adults. *Infect. Immun.* 69, 988–995. doi:10.1128/IAI.69.2.988-995.2001.

Kroh, H. K., Chandrasekaran, R., Zhang, Z., Rosenthal, K., Woods, R., Jin, X., et al. (2018). A neutralizing antibody that blocks delivery of the enzymatic cargo ofClostridium difficiletoxin TcdB into host cells. *J. Biol. Chem.* 293, 941–952. doi:10.1074/jbc.M117.813428.

Kromenaker, S. J., and Srienc, F. (1994). Stability of producer hybridoma cell lines after cell sorting: a case study. *Biotechnol. Prog.* 10, 299–307. doi:10.1021/bp00027a010.

Kügler, J., Nieswandt, S., Gerlach, G. F., Meens, J., Schirrmann, T., and Hust, M. (2008). Identification of immunogenic polypeptides from a Mycoplasma hyopneumoniae genome library by phage display. *Applied Microbiology and Biotechnology* 80, 447–458. doi:10.1007/s00253-008-1576-1.

Kügler, J., Wilke, S., Meier, D., Tomszak, F., Frenzel, A., Schirrmann, T., et al. (2015). Generation and analysis of the improved human HAL9/10 antibody phage display libraries. *BMC Biotechnol.* 15, 10. doi:10.1186/s12896-015-0125-0.

Kuijper, E. J., and van Dissel, J. T. (2008). Spectrum of Clostridium difficile infections outside health care facilities. *CMAJ* 179, 747–748. doi:10.1503/cmaj.081211.

Kurtz, C. B., Cannon, E. P., Brezzani, A., Pitruzzello, M., Dinardo, C., Rinard, E., et al. (2001). GT160-246, a Toxin Binding Polymer for Treatment of Clostridium difficile Colitis. *Antimicrob Agents Chemother* 45, 2340–2347. doi:10.1128/AAC.45.8.2340-2347.2001.

Kwaśnikowski, P., Kristensen, P., and Markiewicz, W. T. (2005). Multivalent display system on filamentous bacteriophage pVII minor coat protein. *J. Immunol. Methods* 307, 135–143. doi:10.1016/j.jim.2005.10.002.

Laemmli, U. K. (1970). Cleavage of structural proteins during the assembly of the head of bacteriophage T4. *Nature* 227, 680–685.

LaFrance, M. E., Farrow, M. A., Chandrasekaran, R., Sheng, J., Rubin, D. H., and Lacy, D. B. (2015). Identification of an epithelial cell receptor responsible for Clostridium difficile TcdB-induced cytotoxicity. *Proc. Natl. Acad. Sci. U.S.A.* 112, 7073–7078. doi:10.1073/pnas.1500791112.

Leuzzi, R., Spencer, J., Buckley, A., Brettoni, C., Martinelli, M., Tulli, L., et al. (2013). Protective Efficacy Induced by Recombinant Clostridium difficile Toxin Fragments. *Infect Immun* 81, 2851–2860. doi:10.1128/IAI.01341-12.

Lübbert, C., Johann, C., Kekulé, A. S., Worlitzsch, D., Weis, S., Mössner, J., et al. (2013). Immunosuppressive treatment as a risk factor for the occurrence of clostridium difficile infection (CDI). *Z Gastroenterol* 51, 1251–1258. doi:10.1055/s-0033-1335505.

Lübbert, C., John, E., and von Müller, L. (2014). Clostridium Difficile Infection. *Dtsch Arztebl Int* 111, 723–731. doi:10.3238/arztebl.2014.0723.

Manse, J. S., and Baldwin, M. R. (2015). Binding and entry of Clostridium difficile toxin B is mediated by multiple domains. *FEBS Letters* 589, 3945–3951. doi:10.1016/j.febslet.2015.11.017.

Marozsan, A. J., Ma, D., Nagashima, K. A., Kennedy, B. J., Kang, Y. (Kenneth), Arrigale, R. R., et al. (2012). Protection Against Clostridium difficile Infection With Broadly Neutralizing Antitoxin Monoclonal Antibodies. *J Infect Dis* 206, 706–713. doi:10.1093/infdis/jis416.

Maynard-Smith, M., Ahern, H., McGlashan, J., Nugent, P., Ling, R., Denton, H., et al. (2014). Recombinant antigens based on toxins A and B of Clostridium difficile that

evoke a potent toxin-neutralising immune response. *Vaccine* 32, 700–705. doi:10.1016/j.vaccine.2013.11.099.

McCafferty, J., Griffiths, A. D., Winter, G., and Chiswell, D. J. (1990). Phage antibodies: filamentous phage displaying antibody variable domains. *Nature* 348, 552–554. doi:10.1038/348552a0.

Merck Newsroom Home (2015). Available at: https://www.mrknewsroom.com/ [Accessed September 26, 2018].

Mkaddem, S. B., Christou, I., Rossato, E., Berthelot, L., Lehuen, A., and Monteiro, R. C. (2014). IgA, IgA receptors, and their anti-inflammatory properties. *Curr. Top. Microbiol. Immunol.* 382, 221–235. doi:10.1007/978-3-319-07911-0_10.

Mollova, S., Retter, I., Hust, M., and Müller, W. (2010). "Analysis of single chain antibody sequences using the VBASE2 Fab Analysis Tool," in *Antibody engineering Vol 2*, eds. R. Kontermann and S. Dübel (Berlin Heidelberg: Springer-Verlag), 3–10.

Moreira, G. M. S. G., Fühner, V., and Hust, M. (2018). Epitope Mapping by Phage Display. *Methods Mol. Biol.* 1701, 497–518. doi:10.1007/978-1-4939-7447-4_28.

Murphy, K., and Weaver, C. (2018). *Janeway Immunologie*. 9. Auflage 2018. Berlin: Springer Berlin.

Natarajan, M., Walk, S. T., Young, V. B., and Aronoff, D. M. (2013). A Clinical and Epidemiological Review of Non-toxigenic Clostridium difficile. *Anaerobe* 22, 1–5. doi:10.1016/j.anaerobe.2013.05.005.

Natvig, J. B., and Kunkel, H. G. (1973). "Human Immunoglobulins: Classes, Subclasses, Genetic Variants, and Idiotypes," in *Advances in Immunology*, eds. F. J. Dixon and H. G. Kunkel (Academic Press), 1–59. doi:10.1016/S0065-2776(08)60295-3.

Navalkele, B. D., and Chopra, T. (2018). Bezlotoxumab: an emerging monoclonal antibody therapy for prevention of recurrent Clostridium difficile infection. *Biologics* 12, 11–21. doi:10.2147/BTT.S127099.

Olling, A., Goy, S., Hoffmann, F., Tatge, H., Just, I., and Gerhard, R. (2011). The repetitive oligopeptide sequences modulate cytopathic potency but are not crucial for cellular uptake of Clostridium difficile toxin A. *PLoS ONE* 6, e17623. doi:10.1371/journal.pone.0017623.

Olling, A., Hüls, C., Goy, S., Müller, M., Krooss, S., Rudolf, I., et al. (2014). The combined repetitive oligopeptides of clostridium difficile toxin A counteract premature cleavage of the glucosyl-transferase domain by stabilizing protein conformation. *Toxins (Basel)* 6, 2162–2176. doi:10.3390/toxins6072162.

Orth, P., Xiao, L., Hernandez, L. D., Reichert, P., Sheth, P. R., Beaumont, M., et al. (2014). Mechanism of action and epitopes of Clostridium difficile toxin B-neutralizing antibody bezlotoxumab revealed by X-ray crystallography. *J. Biol. Chem.* 289, 18008–18021. doi:10.1074/jbc.M114.560748.

Park, H.-J., Jeon, J. H., Kang, S. G., Lee, J.-H., Lee, S.-A., and Kim, H.-K. (2007). Functional expression and refolding of new alkaline esterase, EM2L8 from deep-sea sediment metagenome. *Protein Expr. Purif.* 52, 340–347. doi:10.1016/j.pep.2006.10.010.

Paschke, M., and Höhne, W. (2005). A twin-arginine translocation (Tat)-mediated phage display system. *Gene* 350, 79–88. doi:10.1016/j.gene.2005.02.005.

Pépin, J., Routhier, S., Gagnon, S., and Brazeau, I. (2006). Management and outcomes of a first recurrence of Clostridium difficile-associated disease in Quebec, Canada. *Clin. Infect. Dis.* 42, 758–764. doi:10.1086/501126.

Pépin, J., Valiquette, L., and Cossette, B. (2005). Mortality attributable to nosocomial Clostridium difficile-associated disease during an epidemic caused by a hypervirulent strain in Quebec. *CMAJ* 173, 1037–1042. doi:10.1503/cmaj.050978.

Pera, A., Campos, C., López, N., Hassouneh, F., Alonso, C., Tarazona, R., et al. (2015). Immunosenescence: Implications for response to infection and vaccination in older people. *Maturitas* 82, 50–55. doi:10.1016/j.maturitas.2015.05.004.

Permpalung, N., Upala, S., Sanguankeo, A., and Sornprom, S. (2016). Association between NSAIDs and Clostridium difficile-Associated Diarrhea: A Systematic Review and Meta-Analysis. *Can J Gastroenterol Hepatol* 2016. doi:10.1155/2016/7431838.

Pirquet, C. von (1905). *Die Serumkrankheit von C. von Pirquet und B. Schick: Aus der K. K. Universitäts-Kinder-Klinik in Wien. (Vorstand Prof. Escherich)*. Franz Deuticke.

Porter, R. R. (1959). The hydrolysis of rabbit γ-globulin and antibodies with crystalline papain. *Biochem J* 73, 119–127.

Powers, D. B., Amersdorfer, P., Poul, M., Nielsen, U. B., Shalaby, M. R., Adams, G. P., et al. (2001). Expression of single-chain Fv-Fc fusions in Pichia pastoris. *J. Immunol. Methods* 251, 123–135.

Pruitt, R. N., Chambers, M. G., Ng, K. K.-S., Ohi, M. D., and Lacy, D. B. (2010). Structural organization of the functional domains of Clostridium difficile toxins A and B. *Proceedings of the National Academy of Sciences* 107, 13467–13472. doi:10.1073/pnas.1002199107.

Razavi, B., Apisarnthanarak, A., and Mundy, L. M. (2007). Clostridium difficile: emergence of hypervirulence and fluoroquinolone resistance. *Infection* 35, 300–307. doi:10.1007/s15010-007-6113-0.

Rebar, E. J., Greisman, H. A., and Pabo, C. O. (1996). "[8] Phage display methods for selecting zinc finger proteins with novel DNA-binding specificities," in *Methods in Enzymology* Combinatorial Chemistry. (Academic Press), 129–149. doi:10.1016/S0076-6879(96)67010-4.

Rineh, A., Kelso, M. J., Vatansever, F., Tegos, G. P., and Hamblin, M. R. (2014). Clostridium difficile infection: molecular pathogenesis and novel therapeutics. *Expert Rev Anti Infect Ther* 12, 131–150. doi:10.1586/14787210.2014.866515.

Robert Koch-Institut ed. (2009). Epidemiologisches Bulletin 24/2009. 10.

Rogers, G. B. (2015). Germs and joints: the contribution of the human microbiome to rheumatoid arthritis. *Nature Medicine* 21, 839–841. doi:10.1038/nm.3916.

Rojas, G., Tundidor, Y., and Infante, Y. C. (2014). High throughput functional epitope mapping: revisiting phage display platform to scan target antigen surface. *MAbs* 6, 1368–1376. doi:10.4161/mabs.36144.

Rondot, S., Koch, J., Breitling, F., and Dübel, S. (2001). A helper phage to improve single-chain antibody presentation in phage display. *Nat. Biotechnol.* 19, 75–78. doi:10.1038/83567.

Röthlisberger, D., Honegger, A., and Plückthun, A. (2005). Domain interactions in the Fab fragment: a comparative evaluation of the single-chain Fv and Fab format engineered with variable domains of different stability. *J. Mol. Biol.* 347, 773–789. doi:10.1016/j.jmb.2005.01.053.

Rupnik, M., and Janezic, S. (2016). An Update on Clostridium difficile Toxinotyping. *J Clin Microbiol* 54, 13–18. doi:10.1128/JCM.02083-15.

Rupnik, M., Wilcox, M. H., and Gerding, D. N. (2009). Clostridium difficile infection: new developments in epidemiology and pathogenesis. *Nat. Rev. Microbiol.* 7, 526–536. doi:10.1038/nrmicro2164.

Russo, G., Meier, D., Helmsing, S., Wenzel, E., Oberle, F., Frenzel, A., et al. (2018a). Parallelized Antibody Selection in Microtiter Plates. *Methods Mol. Biol.* 1701, 273–284. doi:10.1007/978-1-4939-7447-4_14.

Russo, G., Theisen, U., Fahr, W., Helmsing, S., Hust, M., Köster, R. W., et al. (2018b). Sequence defined antibodies improve the detection of cadherin 2 (N-cadherin) during zebrafish development. *New Biotechnology* 45, 98–112. doi:10.1016/j.nbt.2017.12.008.

Schmidt, D. J., Beamer, G., Tremblay, J. M., Steele, J. A., Kim, H. B., Wang, Y., et al. (2016). A Tetraspecific VHH-Based Neutralizing Antibody Modifies Disease Outcome in Three Animal Models of Clostridium difficile Infection. *Clin. Vaccine Immunol.* 23, 774–784. doi:10.1128/CVI.00730-15.

Scott, J. K., and Smith, G. P. (1990). Searching for peptide ligands with an epitope library. *Science* 249, 386–390. doi:10.1126/science.1696028.

Sela-Culang, I., Kunik, V., and Ofran, Y. (2013). The Structural Basis of Antibody-Antigen Recognition. *Front Immunol* 4. doi:10.3389/fimmu.2013.00302.

Shen, A., Lupardus, P. J., Puri, A. W., Albrow, V. E., Gersch, M. M., Garcia, K. C., et al. (2011). Defining an allosteric circuit in the cysteine protease domain of Clostridium difficile toxins. *Nat Struct Mol Biol* 18, 364–371. doi:10.1038/nsmb.1990.

Smith, G. P. (1985). Filamentous fusion phage: novel expression vectors that display cloned antigens on the virion surface. *Science* 228, 1315–1317.

Sougioultzis, S., Kyne, L., Drudy, D., Keates, S., Maroo, S., Pothoulakis, C., et al. (2005). Clostridium difficile toxoid vaccine in recurrent C. difficile-associated diarrhea. *Gastroenterology* 128, 764–770. doi:10.1053/j.gastro.2004.11.004.

Spiess, C., Zhai, Q., and Carter, P. J. (2015). Alternative molecular formats and therapeutic applications for bispecific antibodies. *Molecular Immunology* 67, 95–106. doi:10.1016/j.molimm.2015.01.003.

Stausbøl-Grøn, B., Wind, T., Kjaer, S., Kahns, L., Hansen, N. J. V., Kristensen, P., et al. (1996). A model phage display subtraction method with potential for analysis of differential gene expression. *FEBS Letters* 391, 71–75. doi:10.1016/0014-5793(96)00703-X.

Sun, P. (2014). "Structural Recognition of Immunoglobulins by Fcγ Receptors," in *Antibody Fc* (Elsevier), 131–144. doi:10.1016/B978-0-12-394802-1.00007-8.

Sutton, B. J., and Davies, A. M. (2015). Structure and dynamics of IgE-receptor interactions: FcεRI and CD23/FcεRII. *Immunol. Rev.* 268, 222–235. doi:10.1111/imr.12340.

Swett, R., Cisneros, G. A., and Feig, A. L. (2012). Conformational Analysis of Clostridium difficile Toxin B and Its Implications for Substrate Recognition. *PLoS One* 7. doi:10.1371/journal.pone.0041518.

Tao, L., Zhang, J., Meraner, P., Tovaglieri, A., Wu, X., Gerhard, R., et al. (2016). Frizzled proteins are colonic epithelial receptors for C. difficile toxin B. *Nature* 538, 350–355. doi:10.1038/nature19799.

Tedesco, F., Markham, R., Gurwith, M., Christie, D., and Bartlett, J. G. (1978). Oral vancomycin for antibiotic-associated pseudomembranous colitis. *Lancet* 2, 226–228.

Thiel, M. A., Coster, D. J., Standfield, S. D., Brereton, H. M., Mavrangelos, C., Zola, H., et al. (2002). Penetration of engineered antibody fragments into the eye. *Clin. Exp. Immunol.* 128, 67–74.

Toride King, M., and Brooks, C. L. (2018). Epitope Mapping of Antibody-Antigen Interactions with X-Ray Crystallography. *Methods Mol. Biol.* 1785, 13–27. doi:10.1007/978-1-4939-7841-0_2.

Unverdorben, F., Richter, F., Hutt, M., Seifert, O., Malinge, P., Fischer, N., et al. (2015). Pharmacokinetic properties of IgG and various Fc fusion proteins in mice. *MAbs* 8, 120–128. doi:10.1080/19420862.2015.1113360.

Valent, Q. A. (2001). Signal recognition particle mediated protein targeting in Escherichia coli. *Antonie Van Leeuwenhoek* 79, 17–31.

Vieira, J., and Messing, J. (1987). "[1] Production of single-stranded plasmid DNA," in *Methods in Enzymology* (Elsevier), 3–11. doi:10.1016/0076-6879(87)53044-0.

von Behring, E., and Kitasato, S. (1890). Ueber das Zustandekommen der Diphtherie-Immunität und der Tetanus-Immunität bei Thieren. *Dtsch med Wochenschr* 16, 1113–1114. doi:10.1055/s-0029-1207589.

Wang, H., Sun, X., Zhang, Y., Li, S., Chen, K., Shi, L., et al. (2012). A Chimeric Toxin Vaccine Protects against Primary and Recurrent Clostridium difficile Infection. *Infect Immun* 80, 2678–2688. doi:10.1128/IAI.00215-12.

Waterhouse, A., Bertoni, M., Bienert, S., Studer, G., Tauriello, G., Gumienny, R., et al. (2018). SWISS-MODEL: homology modelling of protein structures and complexes. *Nucleic Acids Research* 46, W296–W303. doi:10.1093/nar/gky427.

Wilcox, M. H., Gerding, D. N., Poxton, I. R., Kelly, C., Nathan, R., Birch, T., et al. (2017). Bezlotoxumab for Prevention of Recurrent Clostridium difficile Infection. *N. Engl. J. Med.* 376, 305–317. doi:10.1056/NEJMoa1602615.

Woof, J. M., and Kerr, M. A. (2006). The function of immunoglobulin A in immunity. *J. Pathol.* 208, 270–282. doi:10.1002/path.1877.

Woof, J. M., and Russell, M. W. (2011). Structure and function relationships in IgA. *Mucosal Immunol* 4, 590–597. doi:10.1038/mi.2011.39.

Yang, Z., Schmidt, D., Liu, W., Li, S., Shi, L., Sheng, J., et al. (2014). A novel multivalent, single-domain antibody targeting TcdA and TcdB prevents fulminant Clostridium difficile infection in mice. *J. Infect. Dis.* 210, 964–972. doi:10.1093/infdis/jiu196.

Yearsley, K. A., Gilby, L. J., Ramadas, A. V., Kubiak, E. M., Fone, D. L., and Allison, M. C. (2006). Proton pump inhibitor therapy is a risk factor for Clostridium difficile-associated diarrhoea. *Aliment. Pharmacol. Ther.* 24, 613–619. doi:10.1111/j.1365-2036.2006.03015.x.

Yuan, P., Zhang, H., Cai, C., Zhu, S., Zhou, Y., Yang, X., et al. (2015). Chondroitin sulfate proteoglycan 4 functions as the cellular receptor for Clostridium difficile toxin B. *Cell Res.* 25, 157–168. doi:10.1038/cr.2014.169.

Zantow, J., Just, S., Lagkouvardos, I., Kisling, S., Dübel, S., Lepage, P., et al. (2016). Mining gut microbiome oligopeptides by functional metaproteome display. *Scientific Reports* 6. doi:10.1038/srep34337.

7 Supplemental information

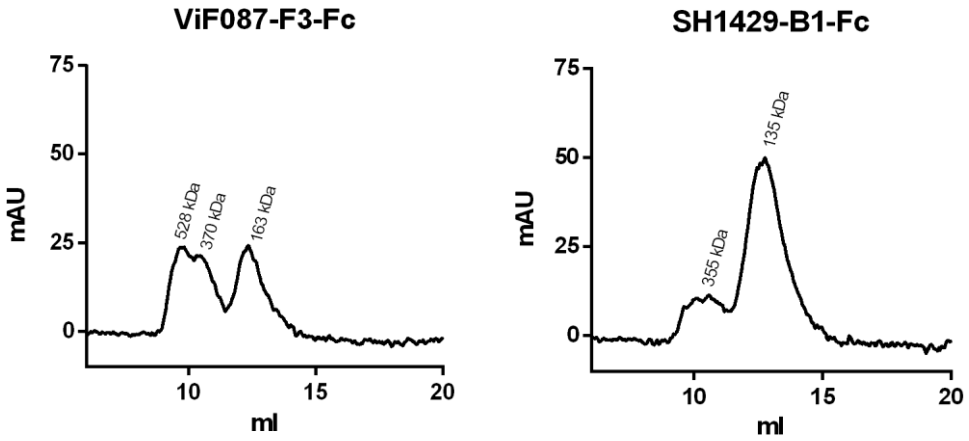

Supplementary Figure 7-1: Size exclusion chromatography

100 µg scFv-Fc were loaded onto a Superdex 200 10_300 GL column. Retention of the protein in the column was detected via UV absorption. Plotted are milli-absorbance-units against retention volume. For ViF087_F3 > 50% of the protein were in higher molecular state or aggregates. For SH1429_B1 most protein detected was bivalent scFv-Fc

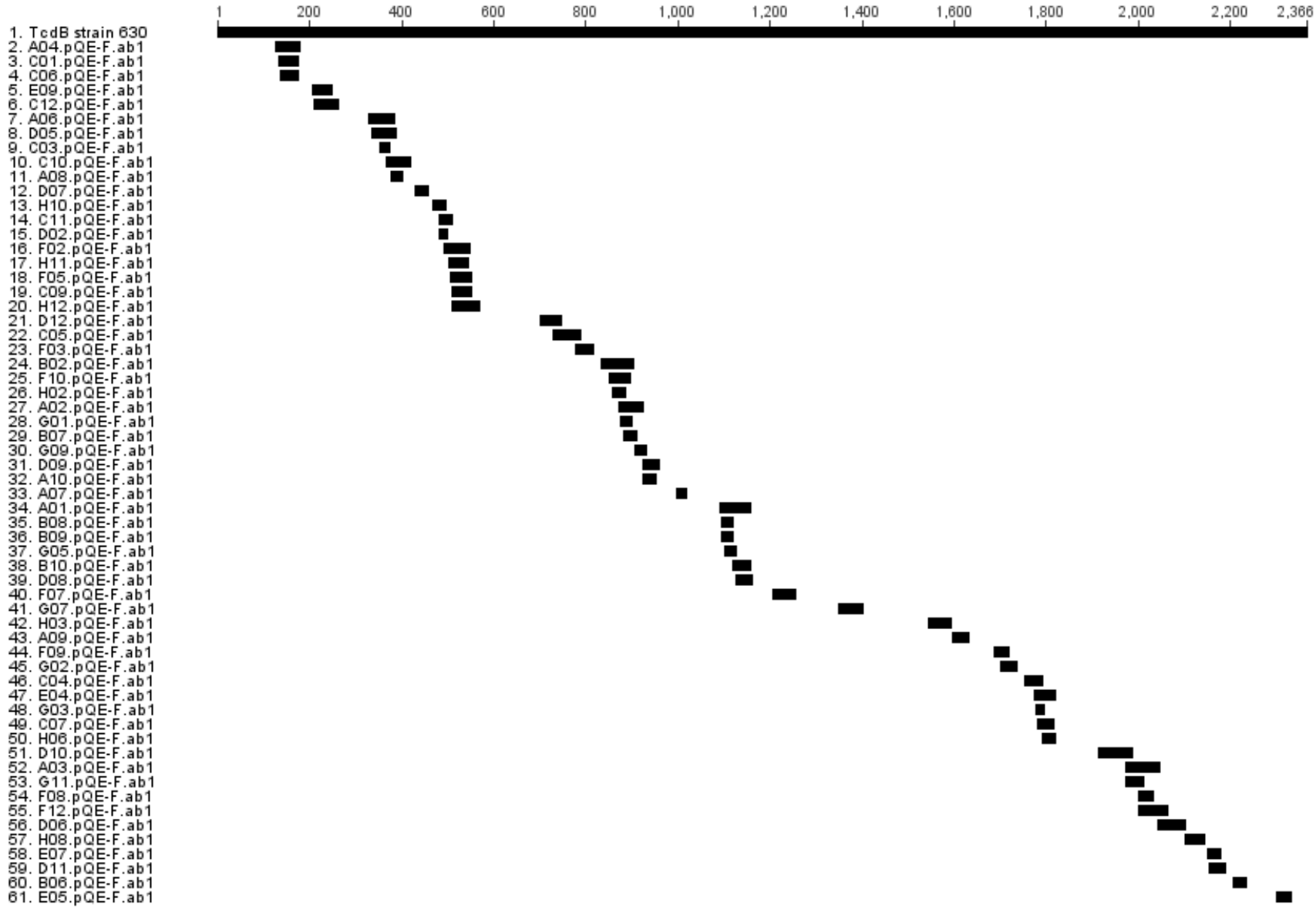

Supplementary Figure 7-2: TcdB coverage

TcdB coverage was assesd by sequencing of 92 clones. 60 among them had correct TcdB-pIII fusions and were aligned to the TcdB-Protein sequence

Extract from the result of epitope mapping by peptide array. For antibodies where specific binding to peptides was detected, the 15 strongest signals are given with signal intensity, position of first amino acid of the peptide and peptide sequence.

Supplementary Table 7-1: Results of peptide array a)

ViF087_B10			**ViF087_A10**			**SH1429_B1**		
Peptide	Pos	Signal*	Peptide	Pos	Signal*	Peptide	Pos	Signal*
YETNNTYPEVIVLDA	1708	2111	LNPAISEDNDFNTTT	414	5131	LNPAISEDNDFNTTT	414	2675
SFTAVVGWKDLEDGS	2072	1166	PAISEDNDFNTTTNT	416	3929	PAISEDNDFNTTTNT	416	1919
DMLPGIQPDLFESIE	288	1116	ISEDNDFNTTTNTFI	418	2555	ISEDNDFNTTTNTFI	418	1587
ISKVYMDDSKPSFGY	1494	816	QIENRYKILNNSLNP	402	2448	KSKNLPELSTLLQEI	790	1199
LPGIQPDLFESIEKP	290	618	LNFNNKIYYFDDSFT	2060	1752	EDNDFNTTTNTFIDS	420	1085
KDKTLANKLSFNFSD	1772	599	EDNDFNTTTNTFIDS	420	1615	NDFNTTTNTFIDSIM	422	938
AHHNEDLGNEEGEEI	2040	490	ENRYKILNNSLNPAI	404	1050	DDLVISEIDFNNNSI	1148	290
ATGSVIIDGEEYYFD	2342	450	NDFNTTTNTFIDSIM	422	785	YKRNYFEGSLGEDDN	534	235
GWLDLDEKRYYFTDE	2324	353	DDLVISEIDFNNNSI	1148	661	FNTTTNTFIDSIMAE	424	222
RYKILNNSLNPAISE	406	347	NSLNPAISEDNDFNT	412	245	DPDTAQLVISEGSGS	2356	169
IIYDKQKNFINYYKA	178	341	KTPYDSVLFQKNIED	600	180	TYKKSGRNKALKKFK	62	71
IDTYKKSGRNKALKK	60	334	YSGLVRVGEDVYYFG	2188	71	HTVTDDIDHFFSAPS	1178	65
TGKLIIDENIYYFDD	1926	324	LSESDVWIIDVDNVV	1338	70	SYYEDGLIGYDLGLV	1802	62
QPDLFESIEKPSSVT	294	320	VQLQGDKISYEAACN	582	65	HLDESGVAEILKFMN	1556	60
GIQPDLFESIEKPSS	292	315	GEDDNLDFSQNIVVD	544	65	NTSDSLMSFLESMNI	1576	60

*= Aggregate red foreground median
hits probably corresponding to the epitope;
sticky peptides, reacting with majority of antibodies
less than 10% signal intensity compared to highest signal

Supplementary Table 7-2: Results of peptide array b)

ViF087_E1			**ViF137_A9**			**ViF137_E7**		
Peptide	Pos	Signal*	Peptide	Pos	Signal*	Peptide	Pos	Signal*
FDDARAKAQFEEYKR	522	10135	FVTVGDDKYYFNPIN	1856	7216	FVTVGDDKYYFNPIN	1856	54987
ETSDPLLRQEIEAKI	1050	8572	LEDGSKYYFDEDTAE	2082	6052	DMENESDKYYFNPET	2214	28010
GKDEFNTDIFAGFDV	654	8038	SLVETEGVFTLLDDK	1128	4090	KDLEDGSKYYFDEDT	2080	26800
ELVERWNLAAASDIL	258	4950	LGKYLRVGFFPDVKT	450	2821	LEDGSKYYFDEDTAE	2082	26780
VKDSYCSNLIVKQIE	390	4596	KDLEDGSKYYFDEDT	2080	2749	IYDMENESDKYYFNP	2212	15888
FLINTLKKTVVESAI	136	2379	DMENESDKYYFNPET	2214	2608	DGSKYYFDEDTAEAY	2084	15106
ISLSLTLQDEKTIKL	1538	1946	IYDMENESDKYYFNP	2212	2351	TGFVTVGDDKYYFNP	1854	12431
LLDRIRDNYEGEFYW	1250	1670	TGFVTVGDDKYYFNP	1854	2323	NLIDDIKYYFDEKGI	2236	10518
EKISSLARSSERGYI	564	1373	MELGKYLRVGFFPDV	448	2291	GWKDLEDGSKYYFDE	2078	10109
MANVRFRTQEDEYVA	12	1300	GINLIDDIKYYFDEK	2234	2190	GINLIDDIKYYFDEK	2234	8409
GVQNIDDNYFYIDDN	2140	1266	DGSKYYFDEDTAEAY	2084	2042	ENESDKYYFNPETKK	2216	8114
ESGVQNIDDNYFYID	2138	1251	TVGDDKYYFNPINGG	1858	1995	LITGFVTVGDDKYYF	1852	6644
DRIRDNYEGEFYWRY	1252	1172	ENESDKYYFNPETKK	2216	1922	GDDKYYFNPINGGAA	1860	6096
EGINAIIEVDLLSKS	1410	1120	SKYYFDEDTAEAYIG	2086	1733	CKGINLIDDIKYYFD	2232	5844
QFGYINIEDKMFYFG	2272	1098	DKYYFNPINGGAASI	1862	1178	TVGDDKYYFNPINGG	1858	5342

*= Aggregate red foreground median
hits probably corresponding to the epitope (s);
sticky peptides, reacting with majority of antibodies
less than 10% signal intensity compared to highest signal

Supplementary Table 7-3: Results of peptide array c)

ViF137_A3			**ViF136_A6**			**ViF137_E4**		
Peptide	Pos	Signal*	Peptide	Pos	Signal*	Peptide	Pos	Signal*
DSHFISFEDISETDE	880	3433	GSVIIDGEEYYFDPD	2344	4975	ATGSVIIDGEEYYFD	2342	10020
GWLDLDEKRYYFTDE	2324	3269	ATGSVIIDGEEYYFD	2342	3292	TGKLIIDENIYYFDD	1926	6770
GSVIIDGEEYYFDPD	2344	3247	QEDEYVAILDALEEY	20	2170	GSVIIDGEEYYFDPD	2344	5340
GWIYDMENESDKYYF	2210	3196	PEYTSEHFDMLDEEV	328	1833	GWLDLDEKRYYFTDE	2324	4345
GYINIEDKMFYFGED	2274	3004	NEYSKEIDELNTYIE	212	1447	ESGVQNIDDNYFYID	2138	4298
QEDEYVAILDALEEY	20	2969	QQNELEDSHFISFED	874	1434	LDLDEKRYYFTDEYI	2326	4075
QQNELEDSHFISFED	874	2818	DFTGKLIIDENIYYF	1924	1409	KLIIDENIYYFDDNY	1928	3414
EGESINYTGWLDLDE	2316	2629	YSKEIDELNTYIEES	214	1350	SFTPSYYEDGLIGYD	1798	3055
PEYTSEHFDMLDEEV	328	2618	ILSFTPSYYEDGLIG	1796	1243	QEDEYVAILDALEEY	20	2909
TGKLIIDENIYYFDD	1926	2514	WSFDDARAKAQFEEY	520	1228	YTGWLDLDEKRYYFT	2322	2795
LEDGSKYYFDEDTAE	2082	2451	DMLPGIQPDLFESIE	288	1155	YFGETYTIETGWIYD	2200	2664
YIPEYTSEHFDMLDE	326	2449	NELEDSHFISFEDIS	876	1135	GYINIEDKMFYFGED	2274	2650
GWKDLEDGSKYYFDE	2078	2142	HFISFEDISETDEGF	882	1128	DFTGKLIIDENIYYF	1924	2641
ATGSVIIDGEEYYFD	2342	2081	IAATGSVIIDGEEYY	2340	1094	ILSFTPSYYEDGLIG	1796	2603
VGEDVYYFGETYTIE	2194	1921	GINLIDDIKYYFDEK	2234	1052	TYREPHLSIYDVLEV	1194	2574

*= Aggregate red foreground median
hits probably corresponding to the epitope;
sticky peptides, reacting with majority of antibodies

Supplementary Table 7-4: Results of peptide array d)

SH1429_C10			**SH1429_D6**			**SH1429_G1**		
Peptide	Pos	Signal*	Peptide	Pos	Signal*	Peptide	Pos	Signal*
VYYFGETYTIETGWI	2198	697	ATGSVIIDGEEYYFD	2342	468	ESGVQNIDDNYFYID	2138	48218
IAATGSVIIDGEEYY	2340	621	FKYFAHQNTLDENFE	2302	374	EGESINYTGWLDLDE	2316	30247
YSGLVRVGEDVYYFG	2188	611	KLIIDENIYYFDDNY	1928	322	GVQNIDDNYFYIDDN	2140	22512
EYIAATGSVIIDGEE	2338	563	LLDRIRDNYEGEFYW	1250	305	GWLDLDEKRYYFTDE	2324	15276
ESDKYYFNPETKKAC	2218	530	TGKLIIDENIYYFDD	1926	301	PEYTSEHFDMLDEEV	328	12238
QAVEYSGLVRVGEDV	2184	524	NIYYFDDNYRGAVEW	1934	290	YIPEYTSEHFDMLDE	326	11412
DTAQLVISEGSGSGS	2358	517	GSVIIDGEEYYFDPD	2344	286	INIELSESDVWIIDV	1334	11018
PETKKACKGINLIDD	2226	483	YFGETYTIETGWIYD	2200	269	VELVSTALDETIDLL	1008	10522
GVQNIDDNYFYIDDN	2140	463	GWKDLEDGSKYYFDE	2078	240	GSVIIDGEEYYFDPD	2344	10021
QNIDDNYFYIDDNGI	2142	382	GWIYDMENESDKYYF	2210	229	HFDMLDEEVQSSFES	334	9448
ATGSVIIDGEEYYFD	2342	362	VEYSGLVRVGEDVYY	2186	224	ATGSVIIDGEEYYFD	2342	9392
YFSDSGIIESGVQNI	2130	310	VYYFGETYTIETGWI	2198	223	ESINYTGWLDLDEKR	2318	9350
TKKACKGINLIDDIK	2228	293	FDDNYRGAVEWKELD	1938	215	TGKLIIDENIYYFDD	1926	9078
EDVYYFGETYTIETG	2196	288	VIIDGEEYYFDPDTA	2346	206	FDDNYRGAVEWKELD	1938	7804
VEYSGLVRVGEDVYY	2186	281	DGSKYYFDEDTAEAY	2084	192	NFEGESINYTGWLDL	2314	7679

*= Aggregate red foreground median
hits probably corresponding to the epitope;
sticky peptides, reacting with majority of antibodies

Supplementary Table 7-5: Results of peptide array e)

SH1429_C10		
Peptide	Pos	Signal*
LLDRIRDNYEGEFYW	1250	791
GSVIIDGEEYYFDPD	2344	547
QEDEYVAILDALEEY	20	513
NIYYFDDNYRGAVEW	1934	508
KLIIDENIYYFDDNY†	1928	498
INYTGWLDLDEKRYY	2320	491
TGKLIIDENIYYFDD†	1926	450
DRIRDNYEGEFYWRY	1252	408
ATGSVIIDGEEYYFD	2342	403
FESIEKPSSVTVDFW	298	392
LESFRENLNDPRFDY	154	389
NFEGESINYTGWLDL	2314	381
IAATGSVIIDGEEYY	2340	378
GWKDLEDGSKYYFDE	2078	336
LDLDEKRYYFTDEYI	2326	334

*= Aggregate red foreground median
hits probably corresponding to the epitope;
† = peptides reacting with majority of antibodies
Hits from this region were enriched among the highest signals, therefore also specific binding is possible in this case